3-2005

A Redesigned Tail Rotor for Improvement of CH-53E High-Altitude Performance

James A. Pritchard

A REDESIGNED TAIL ROTOR FOR IMPROVEMENT OF CH-53E HIGH-ALTITUDE PERFORMANCE

THESIS

James A. Pritchard, Major, USMC

AFIT/GAE/ENY/05-M27

DEPARTMENT OF THE AIR FORCE
AIR UNIVERSITY

AIR FORCE INSTITUTE OF TECHNOLOGY

Wright-Patterson Air Force Base, Ohio

The views expressed in this thesis are those of the author and do not reflect the official policy or position of the United States Marine Corps, Department of Defense, or the United States Government.

AFIT/GAE/ENY/05-M27

A REDESIGNED TAIL ROTOR FOR IMPROVEMENT OF CH-53E HIGH-ALTITUDE PERFORMANCE

THESIS

Presented to the Faculty

Department of Aeronautics and Astronautics

Graduate School of Engineering and Management

Air Force Institute of Technology

Air University

Air Education and Training Command

In Partial Fulfillment of the Requirements for the

Degree of Master of Science in Aeronautical Engineering

James A. Pritchard, BS

Major, USMC

March 2005

AFIT/GAE/ENY/05-M27

A REDESIGNED TAIL ROTOR FOR IMPROVEMENT OF CH-53E HIGH-ALTITUDE PERFORMANCE

James A. Pritchard, BS
Major, USMC

Approved:

/Signed/	10 Mar 05
Dr. Donald L. Kunz (Chairman)	date
/Signed/	10 Mar 05
Dr. Mark F. Reeder (Member)	date
/Signed/	10 Mar 05
Eric J. Stephen, Lt Col, USAF (Member)	date

Abstract

The Global War on Terror with specific emphasis on the recent military operation in Afghanistan has shown the invaluable contribution that heavy lift helicopters bring to the combatant commander. However, the flight range, altitudes and lift capability required to operate effectively in such an austere environment are pushing the limits of these helicopters. In an attempt to increase the operational capability of the CH-53E, this study will investigate methods for maximizing tail rotor effectiveness at high gross weights and high altitudes. This thesis records an analytical study designed to investigate the intricacies of tail rotor design and, by the computational simulation afforded through the Rotorcraft Comprehensive Analysis System (RCAS), define a tail rotor at high altitude that will reduce the tail rotor power required in hover by 10%. The versatility required of the tail rotor is seen due to the nature of the flow regime, which requires the tail rotor to effectively operate with inflow velocity from any direction, with a spanwise distribution of flow that produces Reynolds numbers up to 5.6e7 and with pilot commanded pitch changes from -10 to 24 degrees. With little to no assistance from the vertical fin, the tail rotor is most heavily relied on for antitorque response in hover; therefore, focus will be placed on hovering efficiencies tempered by solid forward flight and hover slide performance.

Acknowledgements

"I can do all things through Him who strengthens me," Philippians 4:13. As a believer in Jesus Christ, I can live my life as one who has already been justified by my Saviors' work on the Cross. Certainly my thanks is extended to Him as I live a life of strength and humility through His example, focused on God's will. "For God has not given us a spirit of fear, but of power and love and doctrine" II Timothy 1:7.

God, in His mercy, has seen fit to allow me to live my life on this earth with a beautiful, smart, exciting woman. Thank you, for your enduring support and love that has served as a wonderful source of encouragement for me. And, thank you for bearing what you must bear as the Marine Corps sends us to every clime and place.

I also thank my Mom and Dad in bringing me up in the way of the Word. No greater gift can a parent give a child than the Mind of Christ. Patience through wisdom.

To my brother, this is the billet that you should have taken. You are eminently more qualified for this than I. You have been and continue to be a leader in ways that you will never know this side of heaven.

Finally, to my thesis advisor, Dr. Kunz, thank you for your wisdom and guidance in this endeavor. Your willingness to drop everything when I stopped by for help has not gone unnoticed, and has left me with a clear vision of how I will treat my future students. The completion of this thesis is directly related to your unselfish investment in my education. Thank you.

If I have seen further than some it is because I stand among giants and ask them what they see.

James A. Pritchard

Table of Contents

Page

List of Figures

Figure Page

List of Tables

Table Page

I. Introduction

Background

In the early morning hours of January 20, 2002 a section of two Marine Corps CH-53E Super Stallions took off from Bagram Airfield, a 3,000-foot runway 27 miles northeast of Kabul, in the mountainous Parvan Province of eastern Afghanistan. Their mission was to resupply the nearly one hundred Marines holding a forward operating base in Khowst, a small town 110 miles to their south, southwest. The two helicopters were heavily loaded that morning with nearly 10,000 pounds of cargo to provide the Marines' weekly supply of ammunition, concertina wire, food and water. The extreme heights of this mountainous region and the tactical necessity for the aircrew to maintain unpredictable flying routes forced the routing to cover significantly more than the 110 mile, straight line distance to the objective. Thus, the aircraft were given the full fuel load of 15,500 pounds in preparation for a 4 hour, round-trip mission. Though dawn was still over an hour away, the eastern sky was beginning to get lighter, making the visibility on the night vision goggles slightly less acute, as portions of the route took the section in an easterly direction. At only 30 minutes into the flight, still weighing nearly 61,000 pounds, climbing at 250 feet per minute (fpm) at 105 knots through a pass at 9900 feet pressure altitude, 100 feet above the rising terrain and into a predawn sky, Dash-two lost its number one engine. Less than 12 seconds later the Marine Super Stallion impacted the ground, sustaining loss of life and unrecoverable damage to the airframe.

From Figure 24-1 in the Naval Air Training and Operating Procedures Standardization (NATOPS) Flight Manual (1) for the CH-53E, at 61,000 pounds, outside air temperature of zero Celsius and 10,000 feet pressure altitude, the aircraft can climb at a rate of 1400 feet per minute (fpm). However, once the engine was lost, the aircraft was 4,000 pounds over its ability to climb at 250 fpm as indicated in the Dual-Engine Climb chart found in Figure 27-8. In his book, "The Foundations of Helicopter Flight", Newman states, "Small changes in total power required which could be obtained by careful attention to the tail rotor design can result in a weight saving or an increase in payload. A typical power saving of 2%, say, results in a payload gain of about 12%."(2:193) On this flight, a 12% gain in the 10,000 pound payload is equivalent to 1,200 pounds, which reduces the overweight margin by nearly one third. While small improvements in tail rotor effectiveness would most likely not have prevented the incident above, it may very well have mitigated the severity of the outcome.

Overall Tail Rotor Design

A myriad of variables must be dealt with in the design process of the tail rotor, and these same variables must be reconsidered in attempt to upgrade its performance. However, there are some variables that will not be changed. First is the overall design of the anti-torque device. Cook notes that "Aerodynamically, the tail rotor is the most efficient method of counteracting the main rotor torque and supplying yaw control as well as directional stability by comparison with many other method of torque reaction.", and it is too expensive to change the anit-torque device. (3:164) Therefore, anti-torque methods such as Fenestron and NOTAR will not be considered. Second is the direction

of rotation of the tail rotor. Cook goes on to point out that the direction of rotation has great impact on the low speed handling qualities especially when in ground effect. He states that "aft-on-top" has been shown by experimental investigation to alleviate the adverse pedal gradients associated with the "forward-on-top" rotation. The CH-53E is already a forward-on-top design; therefore, the direction of rotation does not need to be changed. Third is the pusher versus tractor design. Each has its own complication. The intake air in the pusher design becomes nonuniform as it is deflected around the tail fin, resulting in greater induced power. On the other hand, the tractor design essentially operates in a modified ground effect state, as the air is pushed against the tail fin. This results in lower induced power and greater thrust, but it also pushes the tail fin in the wrong direction. The overall reaction is one with less efficiency than the pusher design (4:226). With these three variables ruled out, an introduction to the methods of improving efficiency can be discussed.

Tail Rotor Disk Area

In its simplest terms, given a certain rotor speed, tail rotor thrust is proportional to the area of the disk, which in turn is proportional to the square of the radius. Thus, small increases in the rotor radius will have somewhat larger effects on the thrust. Having geometric limitations already in place due to the proximity of the main rotor, only very small changes are allowed. With the tail rotor diameter already at 20 feet, it requires only a 2.4-inch increase (1%) to increase the thrust by nearly 2.5%. This increase does not take into account the extra induced or profile power required for the larger diameter tail rotor, but it does indicate a method of modest increase and can serve as a point of

departure for this study. Prouty mentions several reasons to have either a large or small tail rotor. He notes that the trend in size is due mainly to the disk loading of the main rotor. As shown in the following equation, the main rotor disk loading, DL (main), is the ratio of the thrust produced by the main rotor to its area.

$$DL_m = \frac{T}{\pi R^2}$$

He goes on to say, "that small tail rotors are used with low main rotor disc loadings and big tail rotors are used with high main rotor disc loadings." (6:655) The relationship between the rotor ratio and DL follows this equation:

$$\frac{1}{7.15 - .27DL_m}$$

The CH-53E in this scenario had a maximum gross weight of 61,000 lbs, with a main rotor diameter of 79 feet, the DL is 12.44 and the ratio of the rotor diameters is .253. Figure 1 shows that the CH-53E lies slightly below the trend line, which indicates that the tail rotor is a little small for the main rotor disk loading. Note here that the trend line comes from the average of many helicopter tail-to-main rotor diameter ratios and disk loadings, and many of the samples deviate significantly from the average, leaving the CH-53E with a very close fit. Also, the trend line has no significance aside from the fact that it was produced as a compilation of manufactured designs, and that it bears out the average relationship between main and tail rotor diameters and main rotor disk loading.

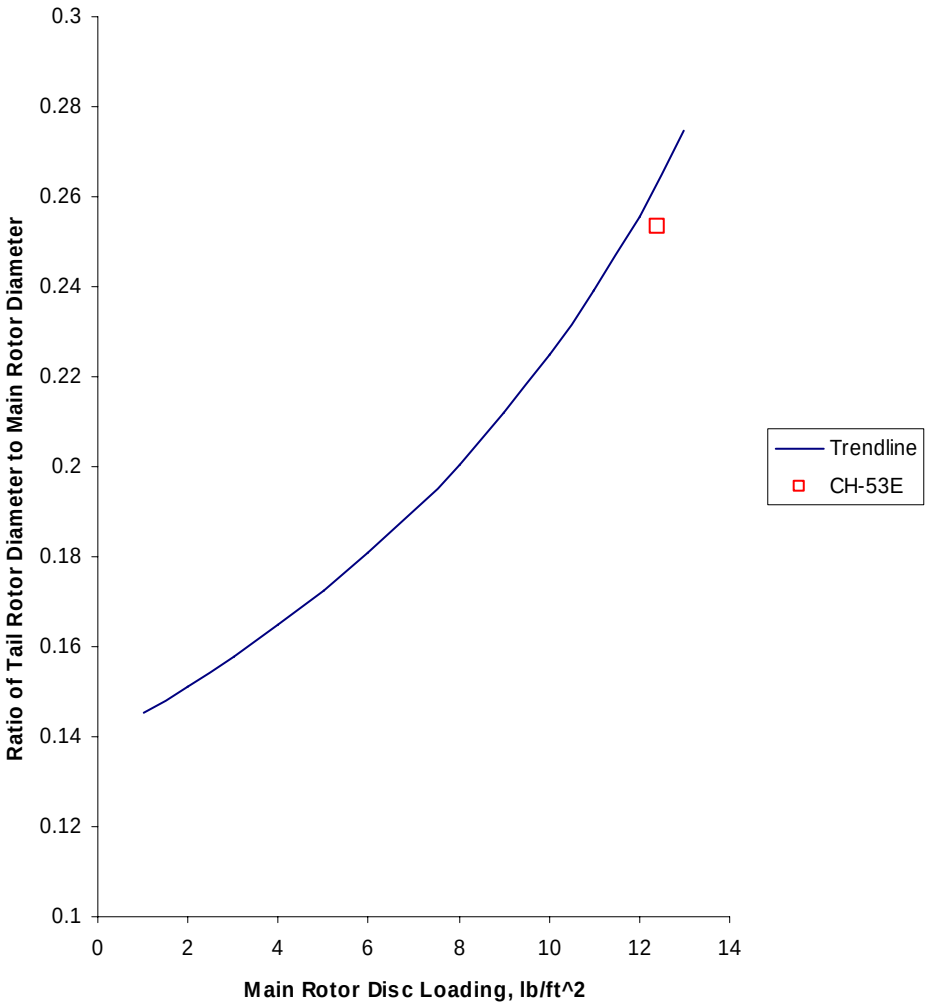

Figure 1. Tail Rotor Sizing Trend

Twist

Twist is the next method for increasing the efficiency of the tail rotor. Figure 2 shows the advantage of the twisted versus untwisted blade. It can be seen that the lift coefficient is greatest near the root and decreases towards the tip. This negative twist, also called washout, allows for a uniform inflow over the entire disk, which reduces the induced power. (4:91)

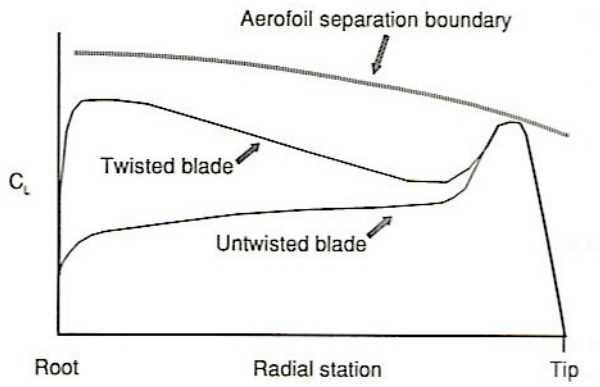

Figure 2. Lift Distribution for Twisted and Untwisted Rotor Blades (2:194)

Newman shows that on the NACA 0012 airfoil a twist with a maximum of 20 degrees will achieve a 36% increase in thrust over the untwisted airfoil. Leishman describes twist as a geometric way to decrease the induced velocity, which varies with Ωr, Ω (Omega) being the frequency of rotation in radian per second and r being the local rotor radius. Decreasing the spanwise varying induced velocity produces a nearly constant inflow velocity, which reduces the severity of the helicopter down wash. The twist distribution that results in uniform inflow across the rotor disk is called Ideal Twist, and it is calculated by the following equation, where $\theta(r)$ is the local pitch angle, θ_t is the pitch at the blade tip and r is the local radius. (4:91)

$$\theta(r) = \frac{\theta_t}{r}$$

Difficulty in manufacturing a blade with ideal twist has resulted in designers turning to various linear distributions in order to approach the uniform inflow situation. Linear twist is calculated by solving the following equation. (6:13)

$$\theta = \theta_0 + \frac{r}{R}\theta_1$$

In this equation, θ_0 is the blade twist if the blade were to extend to the center of the rotor hub rotation, and θ_1 is the total twist from the center of the hub to the tip of the blade. Linear twist is currently used most often in the range of -5 to -16 degrees. (6:13) The CH-53E uses -20 degrees for the main rotor twist and -8 degrees for the tail rotor. Prouty states that a linear distribution of -20 degrees twist is the closest to the ideal case. (6:39)

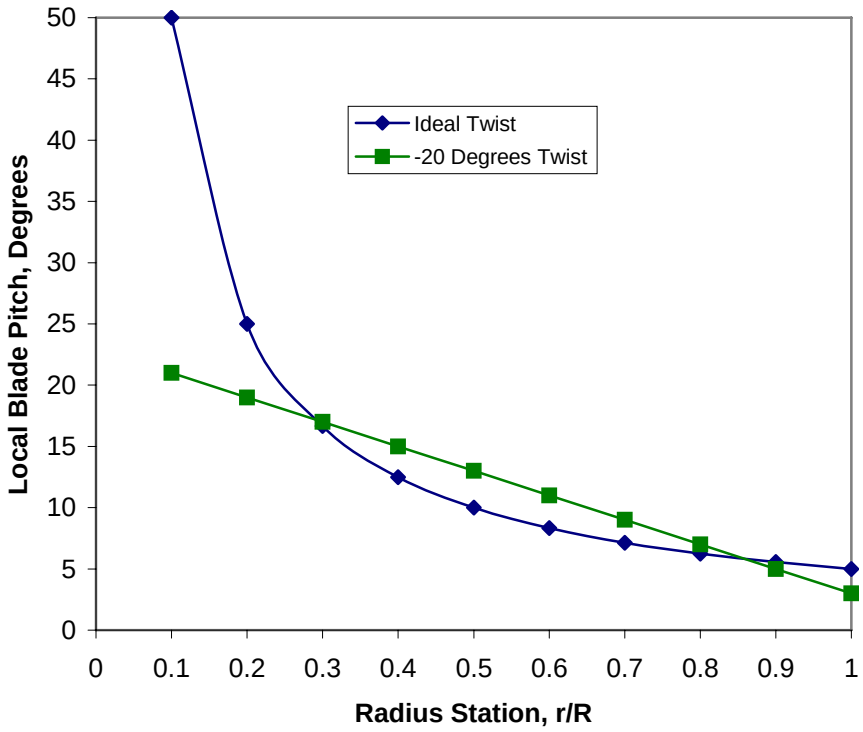

Figure 3. Comparison of Ideal Twist and -20 Degrees Linear Twist

Taper

In trying to achieve maximum efficiency, another method is to taper the blades from root to tip. Without taper the lift coefficient of an ideally twisted blade is very high

at the blade root, and as the lift coefficient increases the blade will be susceptible to stall in that region. Prouty says that the primary effect of taper is to enable each section of the rotor blade to operate at its maximum $\frac{C_l^{\frac{3}{2}}}{C_d}$, which will provide a more even distribution of lift over the whole disk. (6:46) Taper causes this effect to occur by increasing the lift coefficient at the root and decreasing it at the tip, thus making a more uniform distribution over the span of the blade, which reduces the profile power and increases the figure of merit. It can be shown that the figure of merit for an optimum rotor, where the chord varies hyperbolically with span, is between 2 and 5% higher than a rectangular rotor with ideal twist (4:97). However, a completely hyperbolic chord distribution is not physically possible for a rotor, see Figure 4; thus approximations by linear taper are used.

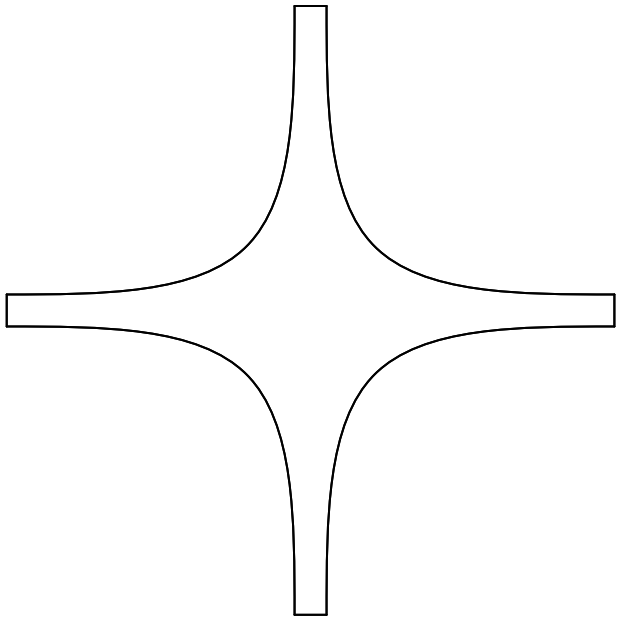

Figure 4. Rotor with Ideal Taper

The proper application of taper will result in a blade with an increase in planform surface compared to that of the original rectangular blade. If the original root chord is used and

the taper applied, then the blade tip will end up with a very small chord and subsequently low local Reynold's number. The taper is to be applied such that the tip chord is only marginally reduced, while the root chord grows to allow for overall greater surface area.

Airfoil

The CH-53E uses a NACA 0015 symmetric airfoil for its tail rotor. Figure 5 shows that greater tail rotor thrust can be achieved by a cambered airfoil compared to a symmetrical airfoil. This would seem to indicate that cambered airfoils are inherently superior to symmetric airfoils and should be used for the tail rotor. However, what it fails to indicate is that the increased pitching moments produce more control system loading, which must be overcome by the control servos [3]. Leishman [4] states, "While the higher maximum lift obtained with cambered airfoils can help reduce rotor solidity and thereby minimize tail rotor size and weight, this can be outweighed by their larger pitching moments and poorer performance when operating at negative angles of attack." It is interesting to note that Sikorsky is now using SC1095 cambered airfoils on its newer model helicopters, namely the H-60 and the S-76 [4].

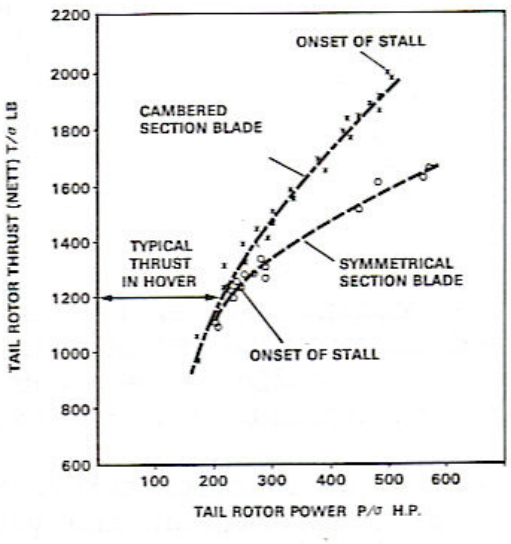

Figure 5. Comparison of Cambered and Symmetric Airfoils (5:1.10)

This study will limit the investigation to three airfoil alternatives, one symmetric and two cambered.

Number of Blades

Prouty points out that the number of blades used is driven, aside from cost, by having an aspect ratio of radius to chord between 5 and 9. (6:658) If the aspect ratio is too low, then the tip losses will counter any benefit of having a simple two blade design, as shown in Figure 6. The aspect ratio of the CH-53E tail rotor, with its four blades, is about 8, (6:699) which is well within Prouty's criteria, but there is room for improvement. Interestingly, Leishman states, "Tail rotors typically have two or four blades, with no particular aerodynamic advantage of one number over the other". (4:226) Yet it is clearly shown in Figure 6 that there is an advantage in tip loss, albeit small, but an advantage nonetheless.

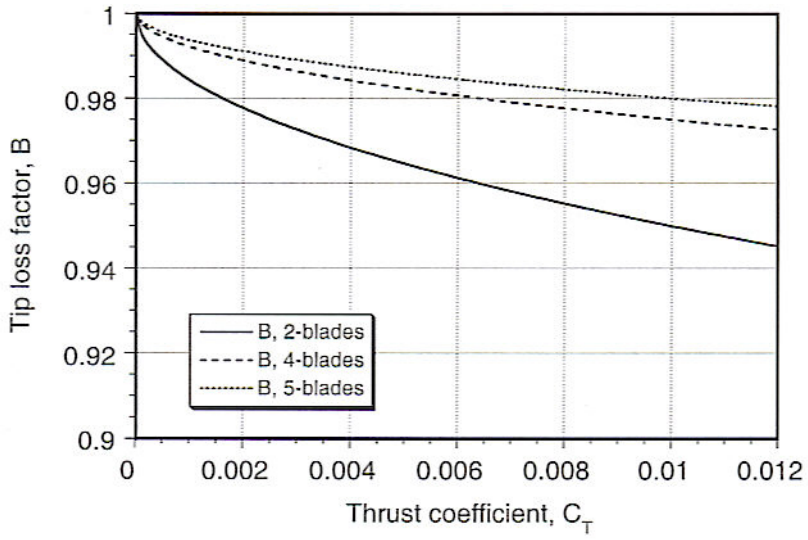

Figure 6. Tip Loss as a Function of Thrust Coefficient and Blade Number (4:49)

Problem Statement

The problem addressed in this thesis stems directly from the United States', and particularly the United States Marine Corps', involvement in the war in Afghanistan. The capability of the CH-53E as a heavy lift platform is well established in the military and aviation communities. Conducting limited operations for a short period at high altitude is a tailor-made task, suited specifically for the heavy lift strengths of this helicopter. However, sustained operations, which utilize the CH-53E at maximum gross weight and operating altitude on a day-in day-out basis, can cause these helicopters to be stressed beyond their capability. One answer to this problem is to reduce the maximum allowable payload, thereby flying well within the flight envelope and subsequently reducing the combat impact and resupply capability for this aircraft. The other answer, which is the right one, is to continually develop and upgrade the existing helicopter to be

able to accommodate the combatant commander's request for heavy lift support. This thesis will chronicle an investigation into improving CH-53E tail rotor performance at high density-altitudes, while minimizing the power impact to the main rotor and maintaining level 1 handling qualities.

Research Objectives

Due to the altitude and weight characteristics of the incident related in the first portion of this introduction, improvements relating to material and noise signature will not be investigated; rather the focus will be on upgrading power and efficiency. These upgrades will manifest themselves through the manipulation of several elements in the existing tail rotor design: camber, twist and taper, which are selected for their relative ease of integration into existing aircraft, and tail rotor diameter and number of blades, which are viable alternatives, but possess more inherent risk because of the changes required to the aircraft.

Each of the five design changes has relative advantages and disadvantages, which must be weighed in order to determine suitability of use. Increasing hover efficiency adversely affects the forward flight envelope of the helicopter, thus changes must be evaluated for all regimes associated with helicopter flight. The first objective of this research is to determine the contributions afforded by each design change when implemented as an independent change. This initial investigation will be limited to hover applications. Once the analytical results yield performance changes, selected modifications will be applied in aggregate. The second objective is to introduce a new tail rotor, which will then be compared to the original design and evaluated based upon

its total increase in efficiency. Many legitimate methods of tail rotor hover improvements have the ability to increase the hover performance, but they also reduce the forward flight envelope of the helicopter. Thus, weight must be given to each regime of flight in order to prevent the selection of a tail rotor, which performs well in one area yet poorly in another. Therefore, the third objective is to validate the new tail rotor against the existing performance criteria of the CH-53E. Here, maximum forward speed and sideward flight envelopes will be determined, ensuring the overall performance of the new tail rotor design meets or exceeds the current configuration in all aspects.

Questions

The first question that this thesis will answer is which of the selected design changes will yield the greatest tail rotor power required savings. Some of the changes, namely twist and taper, are long established as having positive impact on hover performance, yet manufacturing costs and limitations often require these two be left out of the final design. With advances in manufacturing technology come the opportunity for realizing the benefits afforded by these two changes.

The second question to be addressed is which changes can be collectively applied in order to amplify their positive impact on performance. Positive individual improvements are no guarantee of positive collective improvements; therefore, focus must be directed to the combined solution and its performance versus the original design.

Finally, the third question to be answered is whether this new tail rotor could have made a positive impact on the case study previously mentioned. This is no place to play "Monday morning quarterback", but simulating design upgrades and applying them to a

real world scenario emphasizes the need for these upgrades and validates research and development for the same.

Methodology

The analytical results collected for this thesis were obtained using a program called Rotorcraft Comprehensive Analysis System (RCAS). Once the model helicopter was developed and coded, it was run at various altitudes in order to set a base line for investigation. Five separate variations to the base model were made and run separately at the same altitudes to get the changes in performance, measured in horsepower and Figure of Merit (power efficiency). The separate variations were evaluated based on their percent decrease in power required, and then the top three performers were collected into a matrix of all possible design changes and run to convergence in a forward flight batch input. Weighting was determined for hover performance, based on figure of merit, and forward flight, based on maximum forward speed. Key portions of the design matrix were simulated while the remainder of the points were interpolated. Following the selection of the new tail rotor design came some validation of handling qualities by simulating out of ground effect, left and right slides.

Performance Measures

In determining the relative merits of each design change, several quantifiable characteristics will be evaluated. The first deals with the power required on the helicopter, which ties in closely with drag. The second is Figure of Merit, which is a method of determining hover efficiency of helicopters. The third is Handling Qualities,

which will determine the work load that that the pilot must exert during a task while keeping the helicopter under control.

Power Required

As will be seen in the Problem Statement section, this thesis will be dealing with helicopter power – more specifically, helicopter tail rotor power. In order to understand simulation results and make good decisions regarding performance upgrades, there must exist some familiarity with the different types of helicopter power; therefore, the three primary components of power will be briefly introduced and explained. The first is called induced power, and it is similar to the induced power of a wing which is a function of angle of attack, α. It is normally understood as being associated with the power that overcomes the drag that is produced by lift. As the pitch on the blades increases to produce lift, the lift vector is tilted aft; it is the horizontal component of the aft tilted lift vector that is termed induced drag. Prouty shows the relationship between induced drag and the horsepower associated with it by first defining the induced drag as the thrust, T, times angle of attack (6:125)

$$D_{induced} = T\alpha_{induced} = \frac{T^2}{2\rho AV^2}, \text{lb},$$

then defining the induced power as:

$$h.p._{induced} = \frac{D_{induced}V}{550} = \frac{T^2}{1{,}100\rho AV}$$

Figure 7 shows the three types of helicopter power and their summation as the total power. In the slow flight regime, induced power dominates but quickly drops off. This is because it is easier for the rotor to accelerate the incoming volume of air if that air

already has some velocity. Note that the advantage of forward flight in reducing the induced velocity approaches a maximum asymptotically, and its greatest effects are felt by 80 to 100 knots. Figure 7 is a representative chart and is shown for illustrative purposes only, as the curves will vary with the configuration and shape of a helicopter.

The second type of power is parasite power, and it refers to the power required to over come the drag incurred by all non-rotor parts of the helicopter. Prouty says that this power could be described in the same terms as for a fixed wing aircraft, except for the fact that the wing area, S, is difficult to quantify on the helicopter. Therefore, the best fit is to use the equivalent flat plate area, f. So the parasite drag becomes a function of drag and dynamic pressure, (6)

$$f = \frac{D}{q}, \text{ feet squared}$$

Figure 7 shows how parasite power starts at zero and makes the smallest contribution to total power in slow flight. At high airspeeds, however, it becomes the largest contribution to total power required.

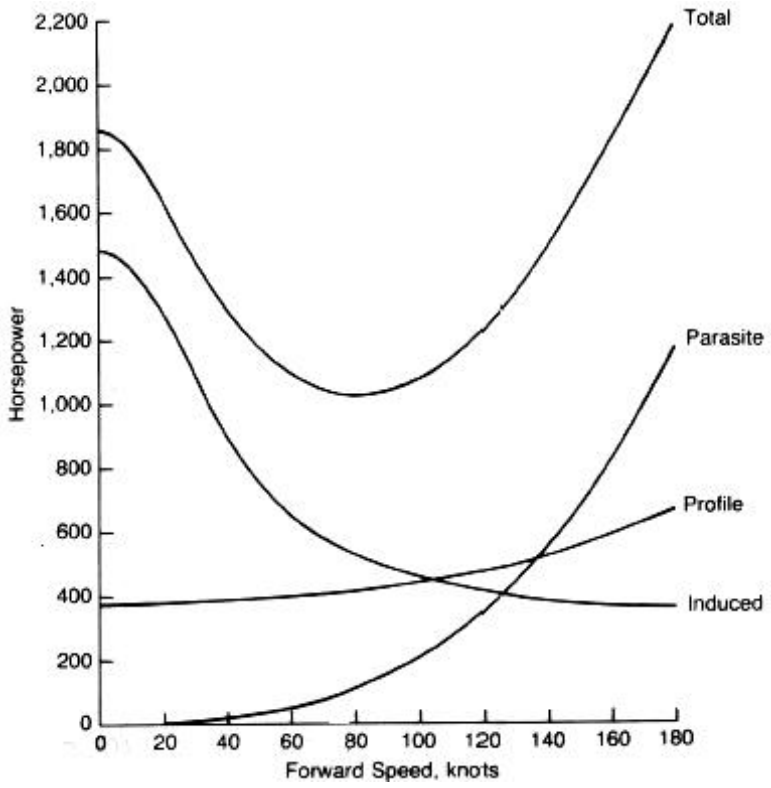

Figure 7. Helicopter Power as a Function of Forward Airspeed (6:130)

The third type of power is profile power and is the power to overcome the friction drag associated with the rotor blades in forward flight. Prouty breaks out two parts to profile power: torque and H-force, where the H-force is the friction on the blade. The combination of torque and H-force is represented in the following equation,

$$h.p._{Q+H} = \frac{\rho A_b (\Omega R)^3 c_d (1 + 3\mu^2)}{4400}$$

where A_b is the blade area, ΩR is the rotational speed in radians per second times the rotor disk radius, c_d is the drag coefficient in hover and μ is the kinematic viscosity of the air. (6:133-134)

Recall that these are helicopter power definitions used for clarification in the source of power/drag being studied. Since this study is limited to rotor blades, only induced and profile power will be discussed.

Figure of Merit

The figure of merit, FM, is a non-dimensional term that quantifies the efficiency of a hovering rotor and is defined as the ratio of ideal power to the measured or actual power. (4:46)

$$FM = \frac{P_{ideal}}{P_{measured}}$$

The ideal power is derived from the momentum equation and is expressed in terms of thrust coefficient. Since the momentum equation deals with inviscid flow, there are no frictional losses, and the power term is strictly induced power. (4:44)

$$C_{P_i} = \frac{C_T^{\frac{3}{2}}}{\sqrt{2}}$$

The measured or actual power has viscous terms so that the power coefficient includes induced and profile power. Due to aerodynamic, mechanical, electrical and hydraulic losses the ratio of ideal to measured power will always yield a fraction, and figures of merit from .7 to .8 show good hover performance. (4:47). RCAS outputs both C_P and C_T so that the FM can be calculated using the following formula.

$$FM = \frac{\frac{C_T^{\frac{3}{2}}}{\sqrt{2}}}{C_{P_{measured}}}$$

Leishman states that figures of merit for efficient rotor systems are between .7 and .8. (4) The figures of merit calculated for many of the tail rotor blades tested during this investigation range from .85 to .89, which is impractical for a physical helicopter, and several reasons for this exist. The RCAS model is coded primarily with rotor blade information for both main and tail rotors. The structural information is limited to the bare minimum for the model to work and represents no mechanical, electrical or hydraulic systems that will produce losses. Prouty discusses power required losses, and how they may be calculated. (6)

$$\text{Power loss per Gear Box} = K[\text{Design max. power} + \text{Actual power}], \text{h.p.}$$

$$\text{Generator loss} = [\text{Load in watts}]\ \frac{1}{(.75)(746)}, \text{h.p.}$$

$$\text{Hydraulic pump loss} = [(\text{Design pressure, psi})(\text{Flow rate, gpm})]\frac{1}{(.8)(1714)}, \text{h.p.}$$

The coefficient K varies from .0025 for spur and bevel gears to .00375 for planetary gears. The CH-53E has five power-train gear boxes with a total of eight bevel gears and one planetary gear, three generators, and three hydraulic pumps operating at 3000 psi. Total losses for the CH-53E are estimated to be 4%. Since the losses are the same for all models simulated in this study, they were excluded for simplicity. Note that this, along with the exclusion of tip loss effects, will inflate the figure of merit numbers; however, relative gain and loss is in view here.

Handling Qualities

High lift coefficients and low induced power requirements are of little use if the resulting configuration requires too much pilot input in order to maintain control or does

not possess enough maneuverability for the mission. In 1969, George Cooper and Robert Harper wrote a paper on the handling qualities of aircraft, and the major thrust of the paper was to quantify the stability and control aspects of an aircraft by assigning numbers to certain levels of pilot workload during tasking. Inputs to the rating scale include pilot tasking, possible failures or system degradation and environmental issues. Tasking ranges from high workload activities like aerial combat and aerial refueling, to low workload activities like cross-country flights. Failure and system degradation inputs quantify handling qualities when systems are less than 100% operational; certain systems may go unnoticed if they are inoperative, yet others will render the aircraft unflyable if they are not fully functional. Environmental inputs quantify how the aircraft handles with the occurrence of certain types of weather phenomena. (12:1-3)

Following a flight, pilots are asked to quantify each task performed by assigning it a number from one to ten, with one being the best and ten being the worst. Numbers 1, 2 and 3 are grouped into a performance level that is deemed acceptable and satisfactory. Numbers 4, 5 and 6 are grouped into a performance level deemed acceptable but unsatisfactory. Numbers 7, 8 and 9 are grouped into a performance level deemed unacceptable. Number 10 is in its own category and deemed unflyable. See Figure 8 and note the pilot rating scale on the right. This chart groups the pilot ratings into their appropriate performance level. These three performance levels make up the standard for accepting aircraft into military service. All military aircraft have to be Level 1 certified. This requirement is for overall aircraft performance; each aircraft does not have to be Level 1 in all its tasks, but the collective grading must yield Level 1. (12:4-10)

This applies to upgraded aircraft components as well as new aircraft acquisitions. Following the incorporation of certain changes, which affect the aerodynamic performance of the aircraft, test must be conducted to ensure compliance with Level 1 handling qualities

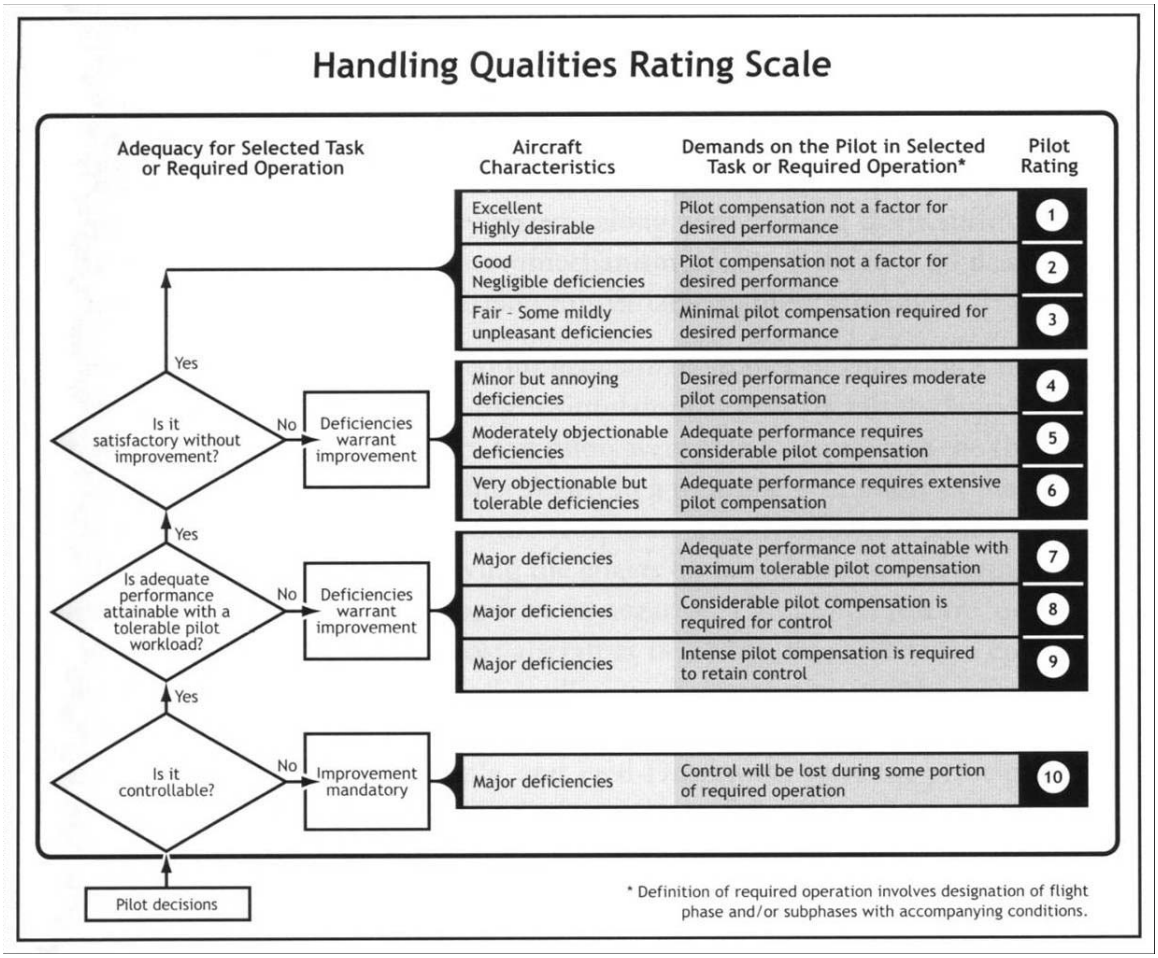

Figure 8. Cooper-Harper Handling Qualities Rating Scale (14)

Relevant Research

In 1969 at the 25th American Helicopter Society annual National Forum Lynn, Robinson, Batra and Duhon submitted a paper from the Bell Helicopter Company in Fort Worth, Texas. (8) In the introduction, the authors emphasis the preeminence of the open

tail rotor as the most efficient anti-torque device presently in use. They also point out that unlike the propeller, the tail rotor must perform with relative wind from any direction, and unlike the main rotor, the tail rotor must produce positive and negative thrust.

In the Design Criteria section the authors state that, “The first step in designing a tail rotor is to establish the required thrust and the conditions under which it must be generated.” They also state that the tail rotor is most heavily taxed in the hover and slow flight regimes. They go so far as to say, “There are no special high-speed tail rotor thrust requirements. Experience has shown that if the low-speed tail rotor thrust requirements discussed below are met, the forward flight requirements will be satisfied.” They go on to say, however, that the forward flight characteristics of the tail rotor need to be tested, especially if approaching high local Mach numbers. The two conditions that will determine maximum required tail rotor thrust are maximum sideward flight speed and directional change in hover. The combination of either of these two conditions with maximum main rotor thrust will set the upper limit on the required thrust from the tail rotor.

The final section, and the majority of the paper, is found in Principal Design Considerations, which is broken up into six categories:

1. Interference
2. Rotor Parameters
3. Control
4. Sideward Flight
5. Design Torque

6. Flapping

This thesis will deal only with the Rotor Parameters section, which is again broken down into five parts; the first of which is Diameter and Disc Loading. The authors list three considerations in tail rotor design: overall size of helicopter, ground clearance, and tail rotor power requirements and weight. A tradeoff study is suggested for the third consideration. Given the example of payload for the UH-1H, the paper states that a 2% decrease in power required can increase the useable payload by over 14%, and the authors say, “In many cases a 2% total power reduction may be obtained by careful attention to the tail rotor design.”

The second consideration is the Tip Speed and the Number of Blades. Several benefits of high tip speed are mentioned, such as: lighter, less torque, and less susceptible to blade stall and gusty conditions. However, the down side of high tip speed is increased profile power, compressibility effects and increased noise. Adding an extra blade has the benefit of reducing the noise as each blade will carry less of the overall load. The authors suggest future tail rotor designs will focus more on reducing blade noise and will probably do so by having tail rotor tip speeds around 575-650 feet per second.

Negative blade twist, the third consideration, is incorporated to improve the spanwise load distribution. Hover and low speed flight benefit most from twisting the blade, while forward flight gains nothing as the inflow air comes from either side of the rotor disk.

“A primary parameter in tail rotor design is the blade airfoil section,” which is the fourth consideration. The authors state that airfoil selection is one of three ways the helicopter designer can compensate for a tail rotor that is intended for high thrust, “The

other two means available to the designer are to make the blade as light as possible (delays precessional stall) and to increase the tip speed." Next a list of prioritized features for the tail rotor is given: high maximum lift coefficient, low drag coefficient, low pitching moments and compressibility effects. The authors suggest that future tail rotor design will depend largely upon airfoil selection, especially cambered airfoils.

Blade chord, the fifth and final consideration, can be calculated using an equation the authors derived using linear theory. The equation works for design ambient conditions given yaw rate and yaw acceleration, and is applicable as an initial guess for the design.

In January of 1974 Wayne Wiesner and Gary Kohler published a study for the U.S. Army Air Mobility Research and Development Laboratory in Fort Eustis, VA. (9) The document was written in response to the previous decade's single-rotor helicopter performance shortcomings, called, "directional control irregularities," by the authors. As an appendix, Wiesner and Kohler catalog eight specific reports from 1962 through 1971 which detail the apparent inadequacies of tail rotor design. These reports cite problems such as inadequate directional control, yaw oscillations in side-winds and tail shudder. Their work proposes 23 specific criteria, which need to be addressed by the helicopter designer in order to ensure adequate performance. They are:

1. Placement of tail rotor with respect to main rotor
2. Placement of tail rotor with respect to fin
3. Direction of rotation
4. Critical thrust and power azimuths
5. Critical wind velocity

6. Critical IGE hover height
7. Selection of optimum tail rotor disc loading and diameter
8. Determination of shaft thrust to net thrust ratio (fin loss)
9. Airfoil selection
10. Blade twist
11. Main rotor power
12. Selection of tip speed and number of blades
13. Design net thrust required
14. Selection of solidity and maximum blade incidence
15. Right pedal blade pitch limit
16. Design power
17. Pitch-flap coupling
18. Tail rotor shaft sweep
19. Directional control rate limiting
20. Blade flapping limit
21. Critical loads azimuth
22. Full-scale design thrust versus blade incidence
23. Horizontal stabilizer loads

The paper can be broken down into three general parts. The first part comprises the introduction and necessary background information dealing with the airflow around the tail rotor. The second part is the body of the work and is comprised of 23 sections, each dealing with one of the design aspects. Each of the sections is further broken down into three parts: discussion of the pertinent theory and equations, guidelines regarding the

particular design aspect, and several charts that provide a significant amount of information with which design decisions are made. The final part of the paper has an example with specified customer requirements. Wiesner and Kohler walk through the design process by explaining how they arrived at a design for each of the 23 aspects. Since this thesis is interested in upgrading an existing design by changing five selected aspects, only those pertinent portions of Wiesner and Kohler's Tail Rotor Design Guide, which deal with the selected aspects, will be noted here.

Section 7 of Tail Rotor Design Guide deals with optimum tail rotor disc loading and diameter. "This guideline presents a method to determine the optimum tail rotor disc loading, defined as that which requires minimum power and permits smooth, approximately linear pedal changes of minimum magnitude with changes of sideward flight velocity." In the discussion section, the relative merits of "bottom-aft rotation" and "top-aft-rotation" are discussed with reference to tail rotor collective inputs. Most helicopters, including the CH-53E have top-aft-rotation. Wiesner and Kohler state, "For bottom aft rotation in left sideward flight, the collective pitch increases as the rotor enters the vortex ring state." But, in the same flight regime, for bottom forward rotation, the vortex ring state is impeded by the influence of the main rotor wake, resulting in, "collective pitch required is approximately constant until the windmill brake state is reached, at which point the collective required decreases rapidly." The remainder of the discussion section notes takes the reader through the charts, explaining how to extrapolate information based on the size of the helicopter in question. In the guideline section, Weisner and Kohler detail specific instructions regarding helicopter size. Large helicopters with disc loading above 8 pounds per square foot are to be designed with tail

rotors to achieve the full 35 knots left sideward flight; whereas, smaller helicopters with disc loading less than 6 pounds per square foot are to make design tradeoffs between left sideward speed and weight. For the 35 knot sideward flight expect the disc loading to be approximately 14 pounds per square foot; for smaller helicopters with, perhaps, 20 knots sideward flight, expect the disc loading to be around 12 pounds per square foot. The section is concluded with short remarks about sizing, "The diameter should be selected on the basis of tail rotor shaft thrust required at the design right sideward flight velocity and the selected disc loading."

Section 9, Airfoil Selection, starts out with one of the biggest problems in helicopter design; the incompatibility of hover and forward flight. "Because of the complex nature of the flow environment in which a tail rotor operates, optimizing the sectional requirements separately for each of the three flight regimes listed would lead to two or even three different and incompatible sets of airfoil sections. Therefore, the selection of the best section or sections for a tail rotor will require a careful compromise of mutually exclusive aerodynamic characteristics, and the final choice should be made only after careful examination of both flight requirements and structural constraints as discussed in the following paragraphs." The discussion section then lists and describes five sectional characteristics which need to be addressed:

1. Maximum-lift coefficient
2. Pitching-moment coefficient (and center of pressure)
3. Type of stall
4. Profile drag

5. Compressibility effects on drag and pitching moments at Mach numbers above the critical Mach number

Weisner and Kohler state that the maximum-lift coefficient is the most important aspect of tail rotor airfoil design. They caution, however, that it is not the only aspect to consider, but if the maximum-lift coefficient is not adequate then even the best of the other categories will not make up for the lack of lift. The lift coefficients must be evaluated in light of the section pitching-moment coefficients. The NACA 0012, as a symmetrical airfoil, has zero pitching-moment coefficients, but its maximum lift-coefficient is relatively low compared to some of the cambered airfoils. Since all cambered airfoils exhibit some degree of pitching-moment, it is up to the designers to find the right balance between high lift and low pitching-moments. Some of the airfoils noted have trim tabs, which, while slightly reducing the lift coefficient, will significantly reduce the pitching-moments. Weisner and Kohler next state that the least desirable stall condition is leading edge stall, which is a prerequisite to the onset of stall flutter. Luckily, the authors say, most blunt-nosed airfoils exhibit trailing edge stall. Unlike the importance of high lift, low drag is not as critical a requirement in tail rotor design; however, it is noted that some airfoil designs do in fact possess both high lift and low drag. The last consideration takes into account two adverse effects of compressibility: drag divergence and pitching-moment break. The authors define drag divergence as, "characterized by a rapid growth of drag with increasing Mach number for a given incidence [and] is associated with the occurrence of supercritical flow conditions." They go on to define pitching-moment break as, "a function of the shift of the center of pressure toward the trailing edge with increasing freestream Mach number." Fortunately,

these two adverse effects can be mitigated using the same techniques. Also noted is that this situation emphasizes the need for tapering the blade tips in the case of high thrust and high local Mach numbers. In this section the guideline quickly reiterates what was presented in the discussion; namely, "The airfoil to be selected for a tail rotor should have high lift, near-zero pitching moment, low drag, and trailing-edge stall characteristics similar to those of the VR-7."

Section 10 deals with blade twist and starts out with, "Because vehicle sensitivity to twist is small, the final decision will be based on a qualitative judgement. The important considerations are hovering efficiency, directional control capability, and blade loads. Weisner and Kohler present a concise discussion of the merits of blade twist, noting the necessity for a triangular airload distribution and constant inflow for greatest hover efficiency. The problem with twisting the blades is that the negative thrust requirements will have to be met with more pedal throw since the angle of attack has been lessened by the twist. In the guideline section, it is recommended to conduct a trade study regarding blade twist and payload. "A value of –9 degrees of blade twist represents a good compromise."

The final section this study will note is Section 12, selection of tip speed and number of blades. Much of the information in this section is based on the noise signature of the aircraft and deals with main rotor blade numbers and tip speeds. It is suggested that for large helicopters the main rotor tip speed will be between 700 feet per second and 750 feet per second; it is also suggested that the designers use that same tip speed for the tail rotor. Several reasons are presented for keeping high tip speed on the tail rotor: lower pitch link loads, lessen effects of blade stall in critical portions of flight, lower tail rotor

system weight, and less susceptibility to gusts. The guideline section states that the acceptable noise signature, as an operational requirement, is the driving factor; then pick the blade number based on tip speed and gross weight.

Written in 1978, C.V. Cook's "A Review of Tail Rotor Design and Performance" (3) discusses some of the improvements in tail rotor design during the 1970s and outlines some improvements for future design. Cook begins by stating a fundamental truism in helicopter production, namely that as the production cycle is underway, the helicopter will receive upgraded components, which invariably make it heavier than the original design weight, yet no compensation is made for the increased demands on the tail rotor. Increasing the, "all-up-weight" as Cook terms it, will adversely affect handling qualities in the hover and slow flight regimes more so than in forward flight. This is due to the fact that only the tail rotor alleviates the demands on directional control in the hover and slow flight; conversely, in forward flight, both the tail rotor and the vertical fin achieve the directional control needed.

In developing the second section of the paper, Cook writes, "Aerodynamically, the tail rotor is the most efficient method of counteracting the main rotor torque and supplying yaw control as well as directional stability by comparison with many other methods of torque reaction." He reiterates that the demands on the tail rotor are levied most heavily during times of slow flight and heavy weight, and points out those are the situations during which directional control will potentially suffer the most. After a considerable amount of development, Cook explains why the forward-on-top direction of tail rotor rotation is ill-advised by saying, "a ground 'horse-shoe' vortex can be created which engulf the tail rotor producing adverse pedal gradients with the tail rotor rotation in

the same sense as the ground vortex, i.e. forward at the top." Cook then uses the NACA 0012 as a baseline and discusses how to improve performance by using other airfoils. He illustrates that while the load distribution on the blade increases towards the tip, the lift coefficient decreases due to the increasing Mach numbers; as stated, these conditions reduce the effectiveness of the NACA 0012 or any other symmetrical airfoil. Due to extensive research on the part of US and European manufacturers in exploiting the advantages of the cambered airfoil, significant improvements can be made in tail rotor efficiencies. The most notable drawback of the cambered airfoil is the inevitable pitching moment produced. Making a larger and heavier tail rotor control servo, which is detrimental to the overall aircraft design, can compensate for these moments. Cook suggests another way to compensate for the moments is by using preponderance weights. "The weights are rigidly mounted on the feathering cuff and can be positioned to react to both the "propeller moment" (sometimes referred to as the tennis racket effect) and the mean aerodynamic pitching moment." In addition to cambered airfoils, Cook states that blade twist is another technique that will beneficially affect tail rotor thrust and power. The higher disc loading of the tail rotor over the main rotor allows the tail rotor to accept greater twist than does the main rotor. While Cook suggests that twist values as high as 16 degrees may be achievable, he recognizes the adverse effects of forward flight and concedes a lesser twist may be more reasonable. Cook concludes that compared to an untwisted, symmetrical airfoil, the properly twisted and cambered airfoil may achieve as much as a 50% increase in thrust.

The next section of the paper deals with rotor dynamics, in which Cook discusses both the dynamic response (flapping and feathering motions, articulated and semi-rigid

rotors) and the dynamic stability (symmetric and anti-symmetric instability) of the tail rotor. While discussing flapping frequencies and problems related thereto, he makes an interesting comment regarding camber and twist, "The introduction of cambered airfoil sections and blade twist requiring greater pitch angles is going to aggravate further these problems."

The fourth section discusses the problem of tail rotor noise. "The noise is particularly noticeable during the aircraft approach and at certain azimuth positions in hover, where its characteristic annoying "whine" leads to increased detectability in the military situation and a community nuisance in the civil application." Cook notes that if the rotational direction of the helicopter is aft-on-top it will cut the noise signature in half when compared to the forward-on-top direction of rotation. He finishes the section by stating that the tail rotor tip speed is a causal factor in the high noise, but that noise can be significantly reduced by a slight reduction in tip speed. He suggests that a main rotor tip speed of 700 feet per second should be complimented by a tail rotor tip speed of 650-660 feet per second.

The design portion of the paper deals with the materials of construction and is of little concern to this thesis. In his conclusion, Cook sums up his main points and makes the prediction that military applications will soon drive the 35 knot sideward flight requirement up to 60 knots, so that helicopter designers will be placing even greater demands on the tail rotor.

G.M. Byham, chief engineer of Westland Helicopters, submitted "An Overview of Conventional Tail Rotors" (10) at a two day conference of the Royal Aeronautical Society in 1990. Byham begins with the basic notion that the job of the tail rotor is

broken down into separate parts as: Torque Reaction, Control and Yaw Stabilization. Byham deals with each part in a simple, overarching manner. The purpose of this section is to orient the reader on the specific tasks and difficulties of those tasks faced by the conventional tail rotor.

Next Byham describes the flow conditions around the tail rotor and details the complexity of having to operate at both hover and forward flight. He sets up the problem by stating that tail rotor placement is determined by ground clearance, drive train requirements and weight considerations, which normally places the tail rotor near the main gearbox height and on the helicopter centerline. The problem with this placement comes in with forward flight as the air entering the tail rotor has already been disturbed by moved around the main rotor and the majority of the helicopter body. The result of this disturbance is seen as a loss in dynamic pressure particularly across the lower half of the tail rotor disc. Byham also develops the problem of the hovering helicopter experiencing the horseshoe vortex off the main rotor. In this situation the air coming off the back end of the main rotor down wash mixes with the tail rotor causing reduced tail rotor performance. Both these conditions, disturbed air off the main rotor disc and horseshoe vortex development from the main rotor downwash, lend to the realization that the direction of rotation for the tail rotor needs to be aft-on-top.

Tail rotor sizing is dealt with next as Byham begins with the premise that sizing depends upon maximum required tail rotor thrust plus an error margin for stall. What needs to be remembered, Byham points out, is that the theoretical maximum thrust from a given diameter tail rotor is not nearly accurate enough to provide a workable solution. Conditions such as fin blockage, main rotor vortex interference, increased induced flow

in left sideward flight must all be taken into account. Byham suggest a that, "good margins from stall onset should be built into the design, recognizing not only the worst steady state condition but also the most adverse design temperature and altitude combination." Beyond the power required for torque reaction is the power required for producing yaw rates; yawing the helicopter produces gyroscopic flapping which in turn changes the spanwise angle of attack variation. "It is normal the yaw manoeuver cases define the most demanding tail rotor thrust conditions in relation to tip stall. Therefore the specification worst manoeuver cases tend to be associated with the onset of tip stall and are predominant in the blade area sizing process." Variation in pitch on the tail rotor can change 40 degrees from its lowest, autorotative setting to its highest, sideward flight setting. These changes come from pedal movement and depend upon the control rigging of the aircraft. Byham suggests that for Naval aircraft the break down in pedal movement percentage is as follows: pitch range for hover thrust is about 16 degrees and comprises 40% of the control range, autorotative control is about 10 degrees and is about 25% of the control range, finally, sideward flight inflow pitch range is about 14 degrees and 35% of the control range.

Next Byham deals with Dynamics and Blade Pitch and it begins with the geometry of the tail rotor hub and the necessity of the pitch bearing and the flap bearing. The lack of a lag bearing in the tail rotor is due to the "built in" nature of the hub lag compensation. "Simple coupling between blade flap motion and pitch (delta-3) offers some flap control and is the most common process employed." The complexity of fully understanding the dynamic motions of the tail rotor is partly a matter of knowing the aerodynamic flow field and partly a matter of knowing the material response to load;

Byham offers this explanation: “The difficulty of the problem is in the very large variety of fundamental rotor modes that must be considered, combined with a very significant number of potential forcing frequencies created by the tail rotor’s self generated time dependant loading, the family of frequencies that arise from the tail rotor working in the wake of the main rotor and the interaction of the major fuselage structural frequencies.”

Byham then discusses the mechanical design of the tail rotor, which has made few but significant changes over the past 25 years. The conventional bearing has had problems with cost, service life and maintainability, and has therefore undergone some renovation. Two new tail rotor designs have emerged: the elastomeric bearing and the bearingless head, both of which have served to decrease the maintenance requirements of the tail rotor.

Finally, Byham makes some general observations on tail rotors. He notices that tail rotor ground clearance is one difficulty that must be addressed by the designer, and some solutions (namely the Fenestron) have achieved a high degree of success. Helicopters heavier than 10,000 pounds are more easily designed to have no tail rotor ground clearance problems, therefore the designers spend more time in trying to achieve better yaw control. Byham notes some interesting trends:

1. The ratio of main rotor to tail rotor thrust is basically constant at .1 for any size helicopter.
2. Dimensional growth of helicopters generally falls between approximately weight raised to the 1/3 power and weight raised to the 1/2 power.
3. Tail rotor diameter verses main rotor diameter slowly increases with gross weight, ranging from 1/6 to 1/4.

Lieutenant A.D.S. Ellin, Royal Navy, wrote a paper called “Flight Measurement Illustrating Key Features of Tail Rotor Loading Distribution” (11) about an experiment with pressure sensors on a Puma tail rotor. Ellin had four goals associated with the experiment: design equipment which would record pressure distributions on a tail rotor in flight, perform flight tests to evaluate low speed performance, further fight tests around deficiencies found from the first series of flights, finally determine tail rotor blade loading and flow patterns. The pressure indicator was placed at the 2% chord, to record incidence for up to .85 Mach, and 95% chord, to record the sudden rise in pressure associated with flow separation. Ellin used two different approaches during analysis in order to uncover more information from the acquired data. First he studied a six second period (about 125 revolutions) in its entirety at a sample rate of 4096 Hz, and then he studied each individual rotation separately. While the individual rotation study provided more detail, the nature of the flow was often unclear because of the significant changes from one rotation to the next. However, the six second period provided a broader look at the flow environment revealing how it changed, which gave significance to the higher fidelity, single rotation study.

Flight testing was conducted in slow flight both in and out of ground effect including moderate sideslip left and right. Ellin stated that the flight test phase effectively demonstrated, “the extent of the non-uniformity in the flow over the tail rotor in what are steady flight conditions. This reinforces the argument that any attempt to analyse tail rotor loadings by averaging the effects of a series of revolutions would produce results of very questionable accuracy.” In his conclusions he states that the

single revolution study could identify several separate influences on the tail rotor: the effects of the wake from the preceding tail rotor blade, the main rotor wake, and fin interference. Finally, Ellin states the complexity of understanding the nature of the flow around the tail rotor, "Consideration of the airflow within a main rotor tip vortex and specifically the changes in spanwise flow it can induce on the tail rotor blade has shown that a multilevel approach to the derivation of blade loading will be required."

Research Focus

This thesis is based upon the CH-53E mishap previously described. Therefore, the model produced for this paper was designed as a heavy helicopter operating in a standard atmosphere at high altitude. The heavy weight will require the main rotor and consequently the tail rotor to produce a significant percentage of their maximum power by increasing pitch on all blades. In forward flight, the main rotor will have to increase its power a disproportionately greater amount than will the tail rotor, because the tail rotor is relieved of some of its anti-torque duties by the presence of a vertical fin. However, in hover, the tail rotor must produce all the anti-torque thrust with no assistance from the vertical fin. High-altitude reduces the density of the air and requires the rotor to achieve greater pitch in order to produce the same amount of thrust. As the pitch increases the airfoil gets closer to its maximum coefficient of lift; increasing beyond this maximum will cause the airfoil to stall. Therefore hovering at high gross weight and high altitude produces a condition of limited power and decreased directional controllability. This condition places one of the most severe strains on the tail rotor and will provide a good basis for comparison of separate rotor designs. The five methods for tail rotor

improvement previously mentioned will be compared against each other in order to find the best combination of hovering efficiency and forward flight performance.

Significance

In its role as the only Marine Corps heavy lift helicopter, the CH-53E Super Stallion is very valuable to the Marine air-ground task force (MAGTF) Commander as the backbone for many MAGTF capabilities such as movement of forces into crisis areas, credible over-the-horizon combat power, sequential introduction of follow-on forces, and rapid withdrawl. No other Marine Corps aviation platform has the ability to fulfill these MAGTF capabilities, from afloat, to the same degree as the CH-53E. As with every military aviation asset, this airframe will require periodic upgrades in order to maintain its ability to perform in combat and in peacetime. Heavy lift upgrades are often conveniently bundled into the arena of engine and main rotor performance, while the tail rotor is left out, being accepted as adequate. The significance of this paper is to express the importance of tail rotor performance, to emphasize the difficulty in tail rotor aerodynamics and to show the marked improvements attainable with small changes in tail rotor design. The CH-53E will be in the Marine Corps arsenal for many years to come, as evidenced by its approval for the Service Life Extension Program (SLEP). Upgrades for the Super Stallion include improved engines, main rotor blades, tail rotor blades, cockpit, etc. It is imperative that the Marine Corps, in conjunction with Sikorsky Aircraft Corporation, a highly regarded aircraft manufacturer and builder of the CH-53E, make every effort to provide the very best tail rotor possible for use by both our current and future warfighters.

Thesis Overview

This thesis contains four chapters. Chapter 1 is the introduction and contains nine separate parts not including this overview. The Background describes the aircraft mishap, which has generally served as the scenario for this study. The Design section covers some fundamental information regarding helicopter tail rotor design by focusing on five specific aspects. Major John Amsden, USMC, from PMA-241 in Patuxtent River, Maryland, supplied the Problem Statement. The three Research Objectives and three Questions attempt to clarify the thrust of the study. A short Methodology is included in order to introduce the manner in which the information is to be obtained and condensed. Performance Measures are developed in order to appreciate the ways of evaluating the tail rotor blade options. The Relevant Research details significant ideas and changes in tail rotor technology over the past forty years. The Research Focus explains harsh conditions in which the tail rotor will be evaluated and modified. Finally, the Significance of this work is related to the individuals who are in most need of its correctness, the warfighter.

Chapter 2 contains the method of investigation and is broken down into three parts. In the first part, the Aerodynamic and Structural Models of the RCAS program are explained, to include hierarchical structure and specific inputs. Next the construction of the base model in RCAS, as referenced in Appendix A, is development and explained. Finally, the chapter ends with a description of the simulated environment and a full line-up of proposed design changes.

Chapter 3 is the data analysis and results, which contains the RCAS outputs in graphical form. The first portion of the chapter deals with how the individual design changes affect the performance in hover relative to the base model. Emphasis is placed on relative change not numerical value due to the generic form of the coded model. The next portion of the chapter deals with the new design, and how it performs in hover compared to the base model. The final portion of the chapter records the new design performance in hover, forward flight and azimuthally changing wind compared to the base model.

Chapter 4 is the final chapter, and it elucidates the concluding thoughts and recommendations for future study.

II. Methodology

RCAS

The tool used for the simulations in this thesis is the Rotorcraft Comprehensive Analysis System (RCAS). (7) Development began in 1997 by the combined efforts of the U.S. Army Aeroflightdynamics Directorate (AFDD) and Advanced Rotorcraft Technology, Inc. (ART) to upgrade the capabilities of the existing analysis system called the Second Generation Comprehensive Helicopter Analysis System (2GCHAS). The new system was designed to use the benefits of 2GCHAS while overcoming its shortcomings. "The improvements include enhanced computational efficiency, the ability to handle large motion maneuvers, a substantially improved nonlinear beam element, an interactive development environment, and an improved user interface." (pg preface) RCAS is a comprehensive and inter-disciplinary system, which is able to model a wide range of configurations while allowing for varying complexity. Analysis is compatible with changing flight regimes from hover to forward flight to complex maneuvers. This analysis covers many different engineering specialties including performance, aerodynamics, vibration, flight controls, aeroelastic stability, flight dynamics and simulation.

RCAS modeling is based on hierarchical structure that includes the Top-Level Physical Model and the Top-Level Solution Model. Under the Top-Level Physical Model are the Structural, Aerodynamic, Control System, and Engine/Drivetrain Model. (Figure 9) Of particular importance to this thesis are the Structural Model and Aerodynamic Model under the Physical Model, and they will be further reviewed here.

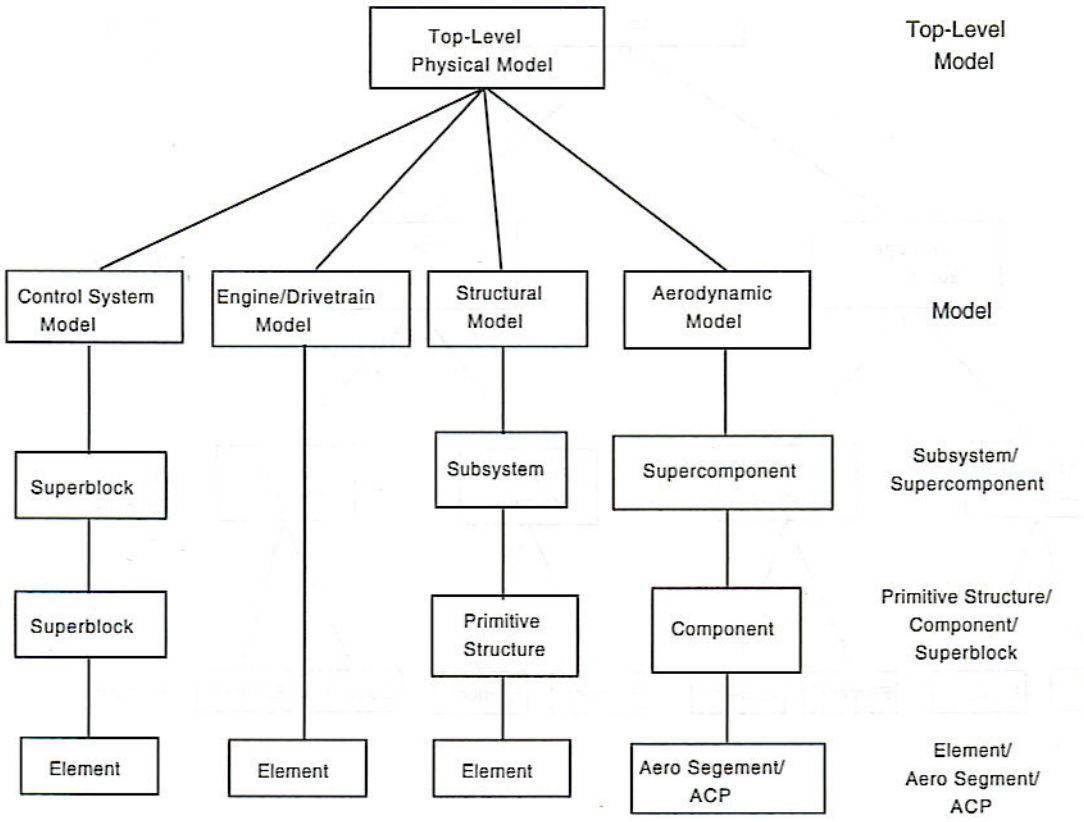

Figure 9. RCAS Top Level Hierarchy (7)

Structural Model

The RCAS Structural Model is composed of three levels of components: subsystems, primitives and elements. Subsystems, being the highest level, deal with the fuselage, rotor and control system. The subsystems are composed of any number of primitives of the designer's choosing, and the primitives are composed of any number of finite elements. The element is the fundamental building block of the Structural Model. The hierarchy of the Structural Model is shown in Figure 10

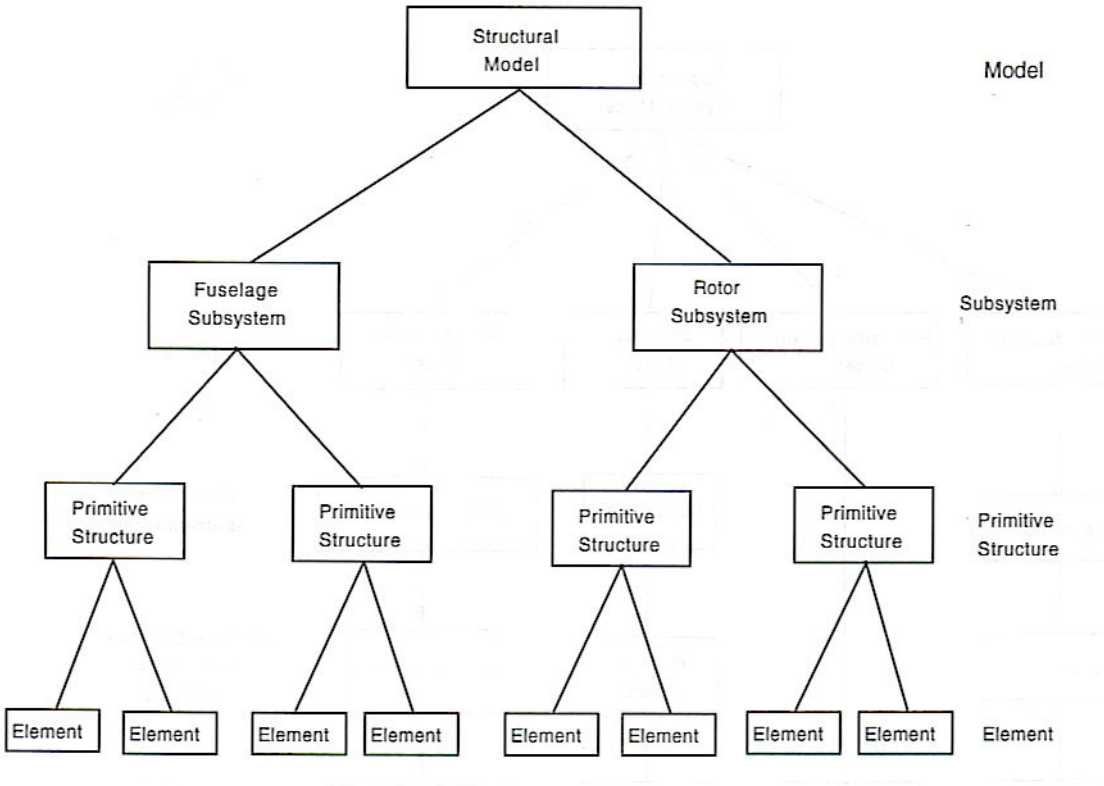

Figure 10. RCAS Structural Model Hierarchy (7)

The element, as the smallest portion of the hierarchical structure, comes in eleven different varieties that must be thoroughly understood in order to devise the most accurate model. These elements are connected together in three-dimensional space to form a primitive structure. A primitive structure is a finite element model, which stands independently, yet is part of the whole physical model. The highest level inside the structural model is the subsystem. Recall that the subsystem comes in three varieties and is named for the specific portion of the aircraft that it represents: fuselage, rotor or control system. One or more primitive structures will combine to form a subsystem, and one or more subsystems will combine to form the Structural Model, on which the RCAS

analysis is run. The recommended order of building the Structural Model is from the top down, so that the model is defined first followed by the subsystems then primitives then finally each element. Once formed, the Structural Model is an independent portion of the total input file, and it can be checked for correctness in its entirety, or each subsystem, primitive and element may be checked independently.

As per the RCAS User's Manual, "The process of creating a finite element model of a primitive structure is perhaps the most involved activity in the model definition process." The formation of the Primitive structure is accomplished by assembling multiple elements. The data, which forms the Primitive structure, comes in two forms: geometry-dependent and geometry-independent. Geometry-dependent data is governed by nodes, elements and connectivities, while geometry-independent data deals with the properties which define the element not its location and orientation. There are three distinct parts in defining the geometry of a primitive structure: basic geometrical layout, structural node placement and defining material between nodes. The nodes are placed in a coordinate system of the designer's choosing and are given a node point identifier and three coordinates unique to that coordinate system.

Once the structural nodes have been established and are placed to define the geometry of the primitive structure, the elements that connect the nodes may be defined. The four separate items defining each element are an identifier, nodal connectivity, element properties and the selection of option. The two nodes it connects define the orientation of the element; the orientation takes on the following description:

1. "The x axis is along a straight line connection the first node to the second node.

2. The y axis is orthogonal to the x axis and is parallel to the xy plane.
3. The z axis is orthogonal to both the x and y planes."

The connection of those elements at the nodes is the formation of the Primitive structure. Once the Primitive structure is completed, the Subsystems may be formed. A Subsystem is limited to one of the following components: rotor, fuselage, drivetrain or control system. In the formation of the Structural Subsystem only one airframe, drivetrain and control system is allowed, however this does not limit the number of rotors used. Each subsystem must have a name, which will distinguish it from the other subsystems. Next is selecting the type of subsystem. Any subsystem that has rotating primitive structures is to be called a rotor, and any subsystem that is comprised of a fixed structure is to be called a fuselage. The rotor and fuselage will be linked at a single point called the hub node. Each Primitive structure has a parent coordinate system that must be related to the Subsystem coordinate system.

The Structural Model is the top level of the Structural hierarchy and is comprised of a number of subsystems described by the user. The reference frame of each subsystem must be defined with respect to the frame of the model and is done by means of origin coordinates and the orientation of the coordinates. In marrying up the rotor with the fuselage, RCAS uses a connectivity called a rotating-to-nonrotating transformation, and it is located at the hub, which is the origin of the rotor subsystem. The location of the global coordinate frame (G-frame) is arbitrarily chosen by the user, but it should be oriented for ease of analyzing the output data. The RCAS User's Manual suggests the x axis be positive forward, the y axis be positive to the pilot's right and the z axis down.

Aerodynamic Model

The Aerodynamic Model utilizes a hierarchy in much the same way as the Structural Model. From top down, it is composed of supercomponents, components and aerosegments. The supercomponent can be either a wing, aerobody or auxiliary rotor. Supercomponents are formed by components that are either lifting surfaces or bodies. Components are formed by aerosegments, which are the fundamental building block of the Aerodynamic Model. Aerodynamic forces are computed at certain points on the aerosegment; these points are called Aerodynamic Computation Points (ACPs). The following is an excerpt from the RCAS User's Manual regarding calculations performed on the Aerodynamic Model, "The aerodynamic model also specifies the airloads and induced inflow for aerodynamic surfaces and bodies. Airloads for rotor blades and other lifting surfaces are based on lifting line theory and are computed using linear coefficients or table look-up. Corrections for tip loss and yawed flow are available. Linear unsteady effects are computed using the Greenberg model. Unsteady, nonlinear airfoil dynamic stall effects are represented with the Leishman unsteady aerodynamics model. Inflow may be modeled using momentum theory, Peters-He finite state dynamic inflow, a prescribed vortex wake, or a free wake. Interference is obtained from the wake of a supercomponent or optional simplified wake interference models."

The Aerodynamic model defines the specific points upon which the aerodynamic forces and moments act; these points are the ACPs. The Aerodynamic model defines the loads at the ACPs as well as the geometry between them. Calculations for the airloads require the local flow velocity at each ACP. This flow velocity is a function of the rigid

body motion and the dynamic response. The solution producing the dynamic response model is a portion of the finite element solution. Therefore it is necessary to marry up the structural model nodes with their corresponding ACPs. This allows the aerodynamic forces and moments to be transferred to the structural model nodes for solution.

As shown in Figure 11, there are four levels in the hierarchical structure of the aerodynamic model: segments, components, supercomponents and the aerodynamic model. Segments are like the elements of the structural model and have a surface area, orientation, and aerodynamic characteristics. Each segment has an ACP associated with it so that loads can be computed at that point. From the joining of segments comes an aerodynamic component, which is like the primitive structure of the structural model. The three types of aerodynamic components are: lifting surface, body and auxiliary rotor. The following is supplied for the understanding of the lifting surface, "A lifting surface component is comprised of a continuous set of aerodynamic segments and is represented by a lifting line. The segments which comprise the lifting surface are rectangular in shape and their ACPs are located at the midpoint of the quarter-chord span line of the segment." The body component is made up of only one aerodynamic segment and its associated ACP. Collecting aerodynamic components yields an aerodynamic supercomponent, which is like the subsystem of the structural model. The supercomponent we are most interested in for this study is the tail rotor. The rotor supercomponent is comprised of at least one aerodynamic lifting-surface component, which represent rotor blades. The top of the aerodynamic hierarchy is the aerodynamic model. The purpose for defining the model is to be able to categorize the levels below it. Also, the model sets the coordinates

for the reference frame to which each sub level must be oriented. This also sets a common reference frame between the structural and aerodynamic models.

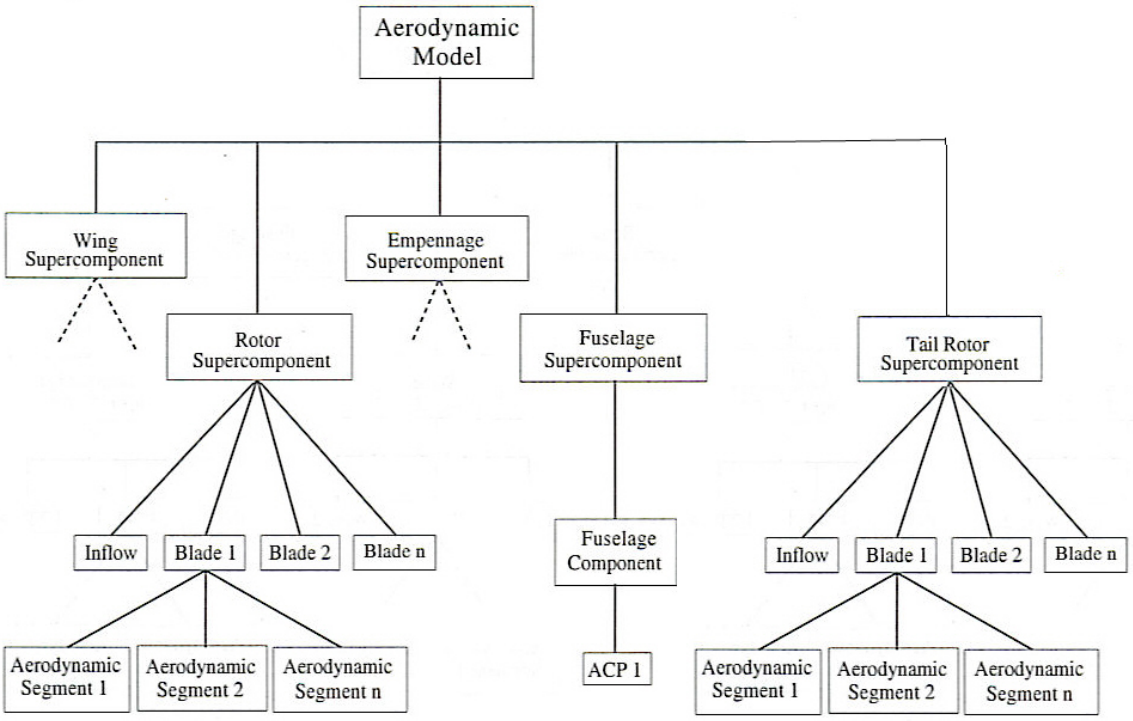

Figure 11. Aerodynamic Model Hierarchy (7)

CH-53E Model

Recall that in the Problem Statement the focus of this thesis is on upgrading the CH-53E tail rotor; however, the model has been simplified significantly, and only the basic attributes of the CH-53E have been duplicated. Seven main rotor blades, four tail rotor blades, a fuselage and a vertical fin are all that have been coded for this study. The input file for the RCAS program is comprised of screens, which are the input locations for modeling an aircraft. Screens are cued by a single "S" followed by the screen name in all capital letters, for example, SUBSYSIDS, which stands for Subsystem Identifications. The overall flow of the input file follows the hierarchical structure

presented above. The aircraft model will hereafter be called the Base Model in order to differentiate later on from the tail rotor design modifications. For the following Base Model explanation, refer to Appendix A.

At the top of the Structural Model hierarchy are screens designed to name, place and orient the subsystems. The three subsystems are FUSE, MROTOR and TROTOR representing the fuselage, main rotor and tail rotor respectively. The screen named SSORIGIN allows the placement of the three subsystems to be described with respect to the Global or G frame of reference. The FUSE subsystem is placed at the origin of the G reference frame, from which the other subsystems are measured. The MROTOR is three feet forward of the origin on the x-axis and six feet above the origin measured in the negative z-direction. Refer to Figure 12 and note that the z-axis on the G reference frame points out the bottom of the helicopter. The TROTOR is placed 44 feet aft, 10 feet above and 9 feet to the left of the origin. SSORIENT allows the orientation to be defined by rotating about the G frame axes in a user designated order. Under the SSORIENT screen the "2" axis refers to a y-axis rotation. The MROTOR is rotated 175 degrees so that the x-axis faces the tail, the y-axis is out the right side of the helicopter and the z-axis faces up. 175 degrees is used instead of 180 degrees because the CH-53E main rotor head has a forward tilt of 5 degrees. Figure 12 illustrates the relationship between the different reference frames. The screen called CONTROLMIXER sets the control interface between the pilot inputs and the control surface deflection. The .017453 is placed in each of the four control stations in order to convert from degrees to radians. This allows the user to input degrees into the program, which is more intuitive than working in RCAS required radians. The CH-53E has a very complicated control mixer, which uses five

types of mixing: collective to pitch, collective to roll, collective to yaw, yaw to pitch and yaw to roll, but these have not been incorporated into this design. (1) The information needed for connecting a rotating rotor and a fixed fuselage is in the screen called ROTNONCONST, which stands for rotating-to-non-rotating construction. The hub node is the position for the rotating-to-non-rotating transformation and is also the center of rotation for the blade subsystem. Both the rotor subsystem and the fuselage subsystem must define the position of the hub node in the ROTNONCONST screen.

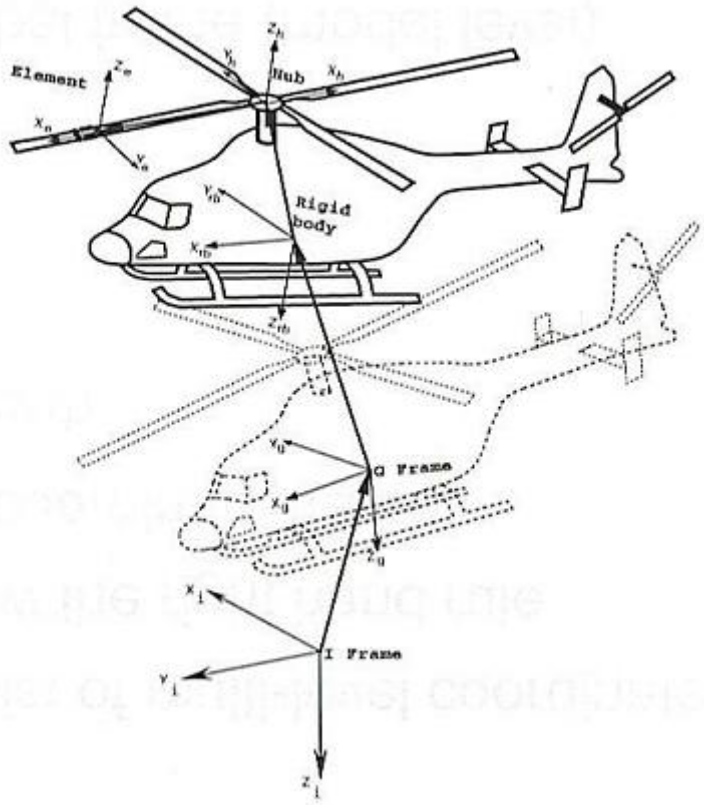

Figure 12. RCAS Orientation Frames (7)

Next, each of the three subsystems is defined in type, placement and orientation. Also the primitive structures of the FUSE are listed under the SUBSYSCOMP screen; the FUSE has two primitive structures: FUSEPS and VFINPS, which will each get their own screens in the next section. PSORIGIN and PSORIENT place and rotate the two primitive structures of the FUSE subsystem. The VFINPS was placed 39 feet behind the origin measured on the negative x-axis. The first rotation is a z-axis rotation for 90 degrees to get the y-axis facing forward, while the second rotation is on the y-axis to get the z-axis pointing normal from the vertical fin and the x-axis in line with the vertical fin. Only 70 degrees of rotation is required because the tail on the CH-53E is canted 20 degrees to the left. CONNCONST describes the connection between both of the primitive structures and the subsystem.

Primitive structure FUSEPS is then given coordinates to the other major portions of the model in the G frame. Recall that the G frame is the classical "Controls" reference frame with the x-axis out the nose, y-axis out the pilot's right side and the z-axis out the bottom of the helicopter. RIGIDBAR then defines the connective elements between the respective nodes. In the same way primitive structure VFINPS is oriented and connected in the following screens.

The second of the three structural subsystems is MROTOR, which has seven primitive structures associated with it. The origin and the orientation of those primitive structures is listed under PSORIGIN and PSORIENT. The origin of the blades is at the hub so all the values for the frame origin offset are zero. The orientation of the blades depends upon each blade. RCAS places the number one blade over the tail, as can be seen in Figure 12, then numbers the blades clockwise from the top, so the number two

blade is –51.4 degrees from blade one, and so on. The second rotation is about axis number two, the y-axis, and represents the precone angle on the rotor blade sleeve. The final screen in the MROTOR subsystem is the main rotor rotational speed called ROTORPARM, which is given in radians per second.

The main rotor blades now come into view as primitive structures, under the subsystem MROTOR, and the first is designated BLADE1. All of its properties are specified including element type, node placement and hinge sequence. For this design the rotor blades are coded to be 39.5 feet long, and the hinges operate first in lead-lag then in flap. Instead of having to repeat all of this for each of the blades, RCAS allows the user to copy the information from Blade1 to all the other blades in the PRIMIT screen. The structural properties of the blades are defined next in the RBEPRP screen, which stands for Rigid Blade Element Properties. Damping and stiffness of each hinge is set as well as the blade mass and center of gravity position. The hinge offset is the distance from the hub to the hinge pivot point and is estimated to be 2.15 feet. The stiffness of the lead-lag and flap hinges is a product of the size of the helicopter and generally differ by an order of magnitude for a fully articulated head, such as the CH-53E rotor head. The mass moment of inertia must be calculated from some other information. Prouty lists the polar moment of inertia (J) for the main rotor as 51,800 slug-ft^2. (6:699) This is useful in solving the equation below, as we know the mass, m, and the displacement from the center of the hub to the center of gravity of the rotor blade, y, and the polar moment of inertia, J.

$$J = I_{yy} + my^2$$

The mass moment of inertia comes out to be 4800 slug-ft^2.

The mass of the entire helicopter is then expressed in the RBMRP screen. For this model the gross weight of the helicopter is 61,000 lbs was used.

Back up to the subsystem level, TROTOR is defined as having four primitive structures, the four tail rotor blades, whose origins are at the subsystem TROTOR, and whose orientations are specifically defined for each blade. Note that the precone angle is zero for the tail rotor. These are the screens to modify when adjusting the number of tail rotor blades as will be done in this investigation. ROTORPARM here defines the rotational speed as before, but this time for the tail rotor. The primitive structure, TBLADE1, is defined in nodal position and elemental connection. FENODE defines the length of the blade as 10 feet. Adjusting the tail rotor diameter requires modifying this input. Each of the other tail rotor blades is then copied. The structural properties of the tail rotor blades are described in damping and stiffness, as well as mass and center of gravity. The tail rotor on the CH-53E has no lead-lag hinge, and the flap stiffness was set to zero as it is free hinge. The mass moment of inertia for the tail rotor blade was found from Equation 1 with mass and distance to the tail rotor center of gravity known, and the polar moment of inertia given by Prouty as 181 slugs-ft-squared. These screens conclude the Structural Model portion of the input file.

Next is the Aerodynamic Model with its supercomponents, components and segments. The Aerodynamic Model requires user inputs that must match the inputs given in the Structural Model. Therefore, distances and rotations will exactly coincide with the previous information. This model has four aerodynamic supercomponents: ADROTOR, TAROTOR, BODYSC and VFINSC, which stands for Aerodynamic Rotor (Main Rotor),

Tail Rotor, Body Supercomponent and Vertical Fin Supercomponent respectively. The origin and orientation of those supercomponents is defined with respect to the G Frame coordinate system. The AIRFOIL screen accepts information for the BLADEAF (blade airfoil) and TBLADEAF (tail rotor airfoil). The .C81 file following the airfoil name keys the program to find the correct airfoil data for each airfoil. FW0013 is the airfoil used for the vertical fin, and its lift, drag and moment coefficients must be provided. For this thesis the SC1095 was used for the main rotor, and NACA 0015 was used for the base model tail rotor. Other airfoils used in comparison of tail rotors are the NACA 0012, SC1095 and VR12. COMPID lists the components, their related primitive structures and the structural node to which they are tied. CPORIGIN and CPORIENT perform the same function as SSORIGIN and SSORIENT do in the structure model hierarchy; recall that these inputs must match the inputs previously given to the Structural Model. INFLOW allows the user to choose one of six different inflow regimes. All of the results collected for this paper was done so with uniform momentum inflow (half wings and rotors). AEROPTION also has six different options; a zero or one turns the option on or off, except for the Dynamic Stall, which can accept, inputs from zero to three. For this study, yawed, unsteady flow and compressibility effects were used.

Down on the component level is ADBLADE1, which is defined as a lifting body and has AERONODE data in eleven segments at user specified distances down the span of the blade. The normal lift distribution on a rotor disk has a spanwise increasing lift gradient, thus it is beneficial to place nodes more frequently on the outer portions of the blade span to allow RCAS more resolution in calculating the lift. Refer to Figure 12 and note the frame of reference used in AERONODE is the elemental frame. AEROSEG

describes the blade chord and the blade twist. The method used here for calculation the –20 degrees of twist on the CH-53E main rotor is by establishing zero twist at the 75% span location, so that 15 degrees of twist is applied inboard of that location and 5 degrees applied outboard. Note that the twist is defined in radians. Once again the copy function, AEROCO, duplicates the blades for a total of 7 main rotor blades.

TAROTOR is the corresponding supercomponent on the tail rotor, and CPORIGIN and CPORIENT describe the origin and orientation respectively. The same INFLOW and AEROPTION information is used for the tail rotor as was used for the main rotor. The component level for the tail rotor is called TABLADE1, and its nodes and segments are described in AERONODE and AEROSEG respectively. More nodes are placed on the outboard portions of the blade for greater computational resolution , and the blade twist is referenced from the 75% chord location. AEROCO makes three more identical blades to make the four bladed tail rotor. AERONODE information will change for those cases involving the increase of tail rotor diameter. Chord and twist will also change for their corresponding alterations. The base model has a constant chord, which is a taper ratio of one, and eight degrees of washout. Changes will include increasing the taper ratio and twist.

The third of four supercomponents is the BODYSC. CPORIGIN and CPORIENT place and rotate the BODYCP, which is the component making up BODYSC. The INFLOW was set to zero and the AEROPTION utilized linear coefficients. Finally the VFINSC was described and its component parts were given an origin and orientation. It also had no INFLOW and a linear airfoil coefficient. Its component, VFINCP, was given

several nodes and a 5-foot chord. That concludes the design input for the helicopter, next is the Analysis Data

The initial conditions screen, called INITCOND, holds the information for the amount of stick and pedal input for the initial conditions; all inputs on this screen are in degrees because the CONTROLMIXER screen, found in the Model, converts from radians to degrees. These initial trim settings are important in telling RCAS where to start searching for a trim solution. If the numbers are not within a reasonable proximity of the final trim values then the program will not converge, and the output data will be inaccurate. AEROSTATCONST is the screen where the altitude data is placed. The Specific Type option allows for five choices, and choice one uses the standard atmosphere, requiring only an altitude input. Trim Data and Output Data govern the convergence criteria for the program and the output file name and placement for the data once the input file has been run in RCAS. All the analytical results are stored in a file called Rscope.log. Following the completion of a run, the Rscope file must be renamed in order to maintain the output results. If the Rscope file is not renamed prior to running the next case then the old analytical results will be dumped and replaced by the new run results.

Design Changes

The RCAS program will be run at four different altitudes: 6,000, 8,000, 10,000 and 12,000 feet, for each design configuration change. Low speed information is more critical to this study than high speed, so all data will be collected for hover out of ground effect (HOGE). Once the five configuration changes have been run and the results

analyzed, they will be tested in forward flight in order to validate the usefulness of the design. Based on the combined performance of the hover and forward flight portions, a design concept for the new tail rotor will be devised. The new tail rotor will then be tested in hover to note the change in hover efficiency; it will be tested in forward flight to ensure that is at least matches the forward flight performance of the base model; finally, it will be tested in azimuthally changing winds up to 35 knots to ensure its handling qualities remained Level 1. The airfoils used for the base and the three proposed models are presented below.

Sikorsky currently uses the NACA 0015 airfoil as the tail rotor for its CH-53E.

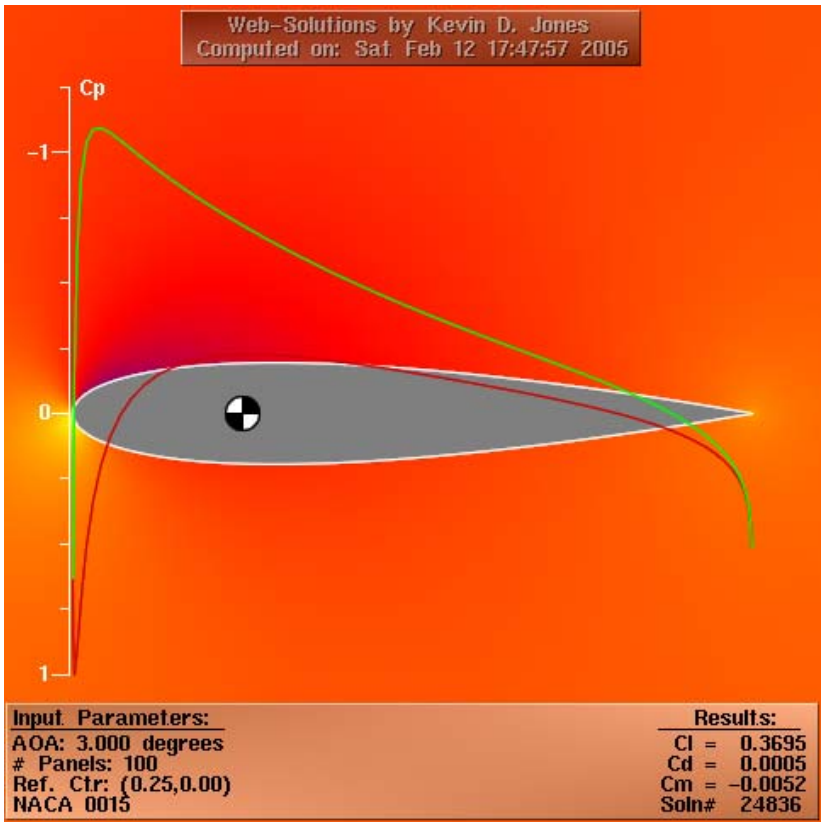

Figure 13. NACA 0015 Airfoil with Pressure Coefficient Distribution. (13)

The radius of the 4 bladed tail rotor is 10 feet, and it has 8 degrees of washout. This current configuration will be referred to as the Base throughout this thesis. Figure 13 depicts the NACA0015 at 3 degrees angle of attack (AOA). This figure and the following 3 figures are representations of airfoil calculations made by potential panel code method. The green line is the pressure coefficient (Cp) for the upper surface, and the red line is the Cp for the lower surface. The shaded black and white circle inside the airfoil indicates the reference center and is located at the quarter-chord position. Note the thickness of this airfoil. At 15%, it is the thickest of all the airfoils tested. Thick airfoils have the ability to operate at high AOA without stalling; however, their thickness incurs high drag as the Mach number increases. Notice that the results section of the illustration includes the lift, drag and moments coefficients, which will prove to be useful information when determining the comparative merits of the airfoils. With a chord length of 1.24 feet and a 10 foot span, the tail rotor on the CH-53E has an aspect ratio of nearly 8, which is nearing the high side of Prouty's suggestion between 5 and 9. The very tip of the CH-53E tail rotor blade is tapered, but for this study it is assumed to be rectangular in shape for two reasons. First, the simplicity of a rectangular model is advantageous in programming. And second, the taper configuration studied here is a full blade taper, which is not representative of the original design. Also, due to the quantitative nature of this study, only the comparative differences in blades are desired. Table 1 includes a number of helicopters using some of the airfoils studied here.

Helicopter Make and Model	Main Rotor	Tail Rotor
Aerospatiale AS 350B	NACA 0012	NACA 0012
McDonnell Douglas (Hughes) 500E	NACA 0015	
Schweizer/Hughes 300C	NACA 0015	
Sikorsky UH-60A	SC 1095	SC 1095
Sikorsky CH-53E	SC 1095	NACA 0015
Sikorsky s-76A	SC 1095	SC 1095

Table 1. Current Uses for the Blades Tested (6:684-701)

Following is the list of five changes to be compared against the base model.

Airfoil

1. NACA0012

Figure 14 shows the NACA 0012 airfoil at 3 degrees AOA. As before the upper and lower surface pressure coefficients are illustrated in green and red respectively. At 12% thickness, the NACA 0012 is considerably thinner than the base airfoil. This should lead to less profile drag and a better lift to drag (L/D) ratio, which will reduce the profile power required to operate the tail rotor. The Cl for the NACA 0012 is 2.2% less than that of the NACA 0015. However, this marginal decrease in Cl is accompanied by a large drag reduction, as the coefficient of drag is reduced by 40%. This is not to say that there will be a 40% savings in power to run this tail rotor; but since the slightly lower Cl will require a slightly larger blade pitch in order to achieve the same amount of lift, therefore the blade will not achieve the full 40% profile power savings. Also note that the lower surface Cp of the NACA 0012 does not become quite as negative as does the lower surface Cp of the NACA 0015. This is a function of the thickness of the airfoil. The

thicker the airfoil, the greater the lower surface contributes to the lift. Finally, notice the upper surface Cp passes through zero near the 90-95% chord line. Airfoil shape determines both attainable lift and resulting drag, but if the flow separates at the trailing edge then a much larger drag penalty will have to be paid. Therefore airfoil design encompasses the techniques that relieve the pressure differences between the upper and lower surface without allowing the flow to separate. (15)

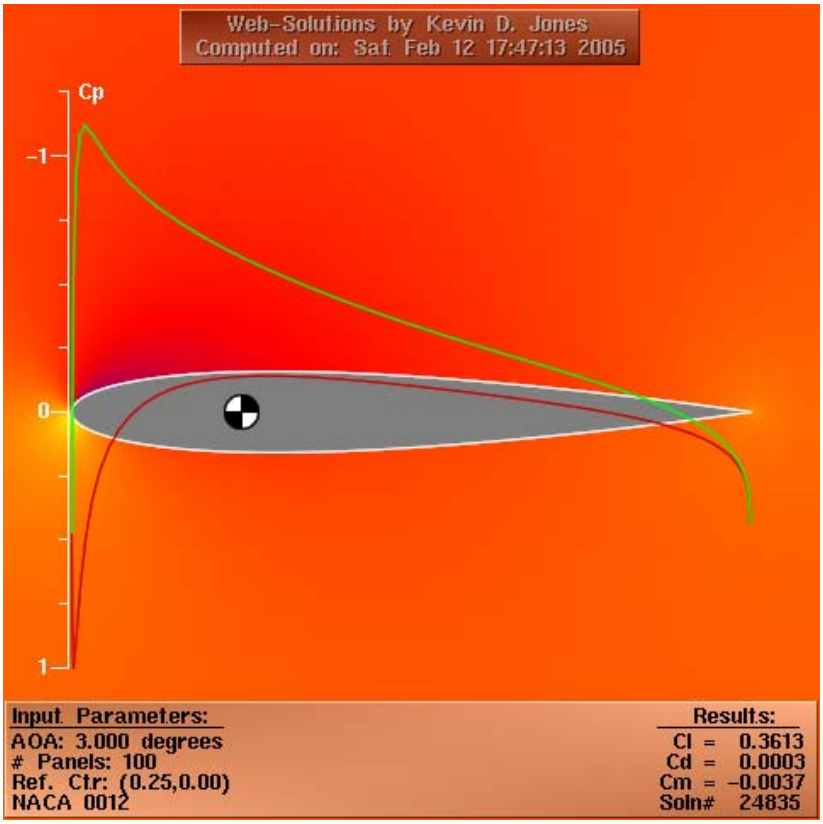

Figure 14. NACA 0012 Airfoil with Pressure Coefficient Distribution (13)

2. SC1095

The SC 1095 is an airfoil widely used by Sikorsky for both main rotors and tail rotors. The airfoil has a 9.5% thickness and is the thinnest of the four airfoils studied. It is also the first of two cambered airfoils with a 0.8% camber. The camber is determined by the displacement of the upper and lower surface mean line from the chord line. More camber generally translates into more lift but also more drag. Even though the SC 1095 is the thinnest of the airfoils it has the second highest drag coefficients of the four, but the increase in lift coefficient is nearly 18%.

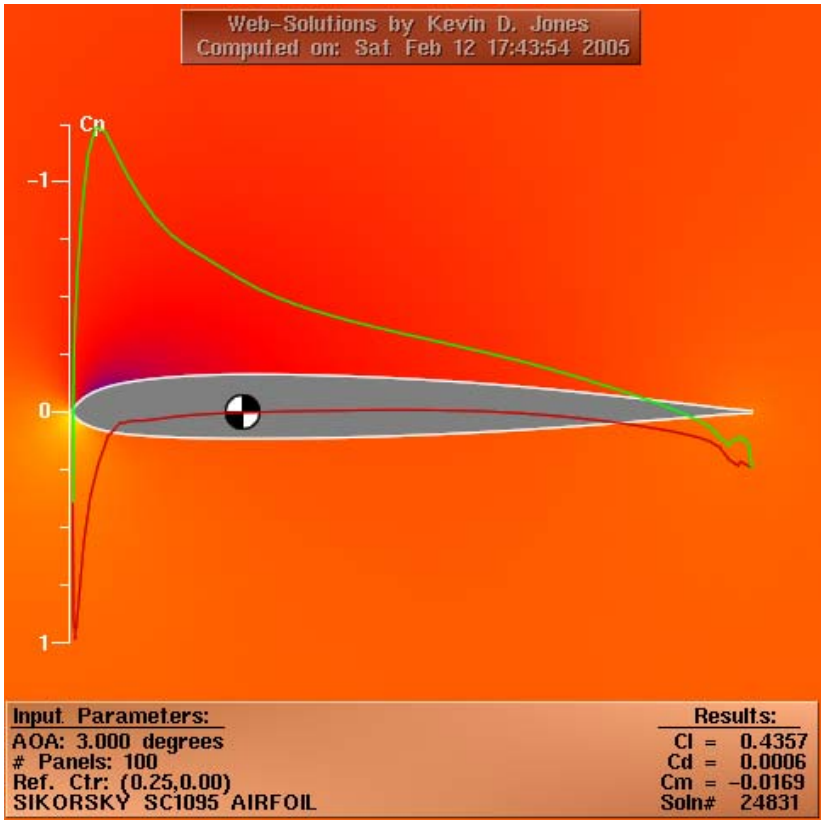

Figure 15. SC 1095 Airfoil with Pressure Coefficient Distribution (13)

3. VR-12

The Boeing (Vertol) airfoil has the benefit of being designed by numerical methods studies. Leishman notes,

> The latest airfoil sections, the VR-12 and the VR-15, represent the best compromise in terms of maximum lift capability at the lower Mach numbers typical of the retreating blade while maximizing the drag divergence Mach number and meeting hover requirements and control load limitations. (4:286)

While having the highest Cd at this AOA, it possesses other noteworthy attributes, namely it also carries the highest Cl, 20% greater than the NACA 0015. The moment coefficient is also the lowest of all the airfoils, which is unusual since the NACA symmetric airfoils are known for their low pitching moments. Note how the slope of the upper surface pressure coefficient becomes less negative over the middle portion of the chord. This leveling out delays the onset of flow separation and controls the magnitude of the pitching moments. The trailing edge is slightly turned up and produces the effect, seen here, of the upper surface Cp crossing zero prior to the lower surface.

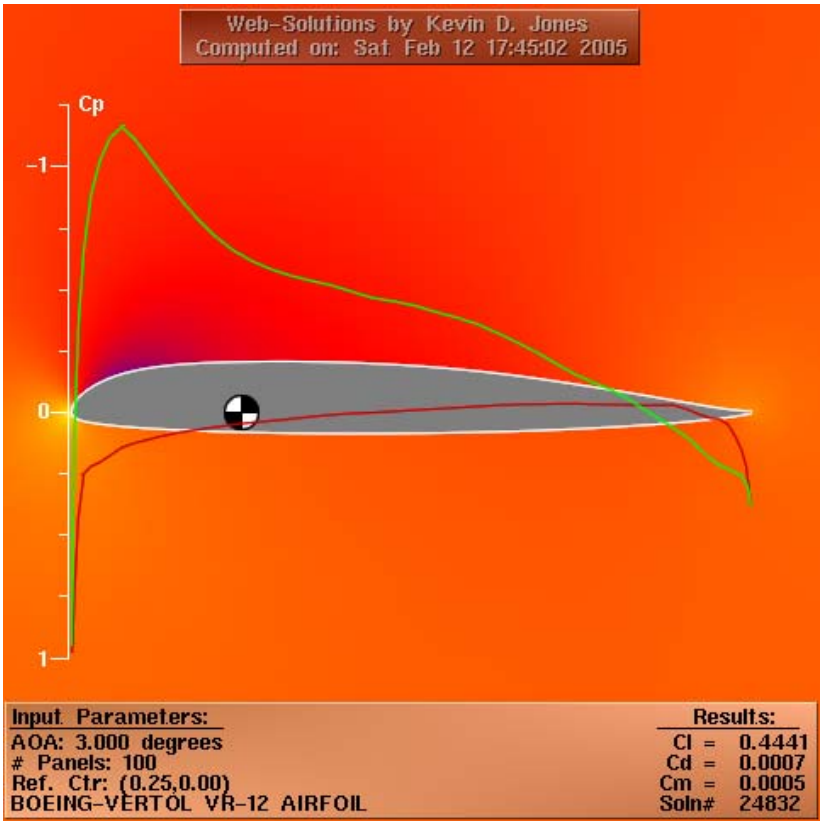

Figure 16. VR-12 Airfoil with Pressure Coefficient Distribution (13)

Radius Increase

1. 1 inch
2. 2 inch
3. 3 inch

Radial increases will have several effects on the tail rotor. First, an increase in the radius will increase the aspect ratio (AR), as the AR varies with the square of the span. A longer blade will suffer less from tip loss, but it will also see greater profile drag at the tip since the tail rotor will be turning at the same rpm. Note: there is no allowance in this study for varying the rotational speed (Omega) of the rotors. Second, the larger rotor will

be able to produce greater thrust, as the rotor thrust varies with the radius to the fourth power. However, the power required to turn the rotor varies with the radius to the fifth power. Since this rotor can produce greater thrust, it will not need as much pitch on the blades to achieve the required thrust, thus the profile power will be less. There will be a give and take between drag divergence and the reduction in pitch which will determine the overall effect of the increased span.

Twist

1. 12 degrees
2. 16 degrees
3. 20 degrees

Figure 17 illustrates a method for determining the placement of twist between the nodal framework of the tail rotor blade in RCAS. The y-axis represents the blade twist in degrees, and the x-axis represents the span of the blade in feet. The zero twist is set at 75% span and the blade is twisted on either side of that arbitrarily chosen point. RCAS will not put a value of twist on a node. It will only assign twist between nodes; therefore the twist calculations must be made so as to correspond with the center point between each node as depicted in the bottom of Figure 17. Recall that RCAS defaults to radians, so the input needs to be converted from degrees to radians.

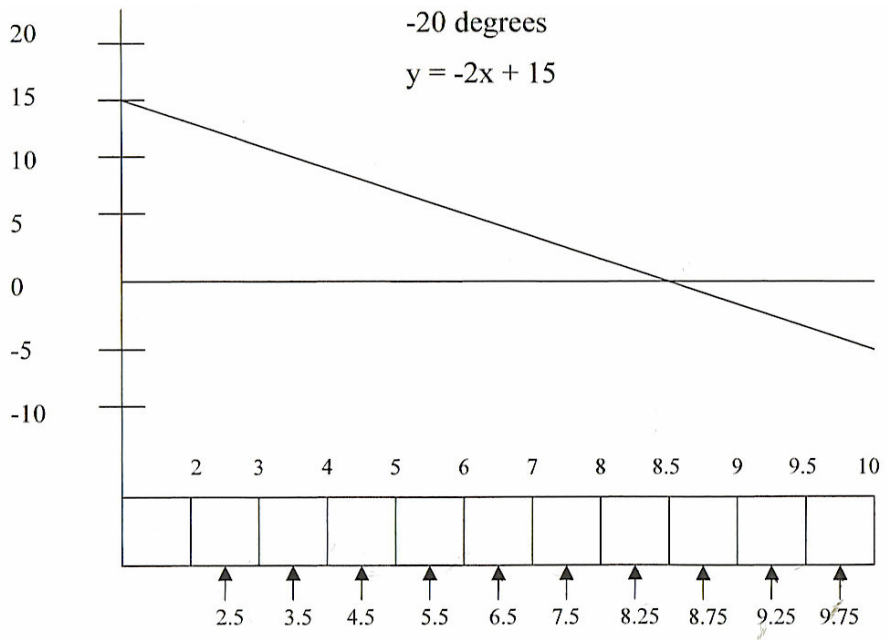

Figure 17. Method for Determining the Placement of Twist in RCAS

Linear taper

Leishman says that a hyperbolic variance of chord with span will result in the optimum lift over drag ratio (L/D). (4:97) He goes on to say that, the hyperbolic variance is impossible to manufacture, but any decrease in chord over the span will have positive effects on the hover performance. For tapering to be effective, the overall area of the blade must be increased. Reducing the outer portion of the blade, which produced the majority of the lift due to the greater dynamic pressure, places more emphasis on the performance of the inner portion of the blade. If the chord length on the inner portion is not adequately increased to compensate for the reduction in lift at the tip then the overall performance of the blade will suffer with respect to the original rectangular design. Figure 18 shows the planform for the base blade and the tapered blade. The base blade has an area of 12.4 square feet and an aspect ratio of 8, the first tapered blade has an area

of 17 square feet and an aspect ratio of 5.9, and the second tapered blade has an area of 20 square feet and an aspect ratio of 5. The taper design requires the aspect ratio to decrease over the rectangular blade. An attempt may be made to taper the blade while maintaining the aspect ratio, but this will only lead to an extremely small tip chord and significantly reduced lift.

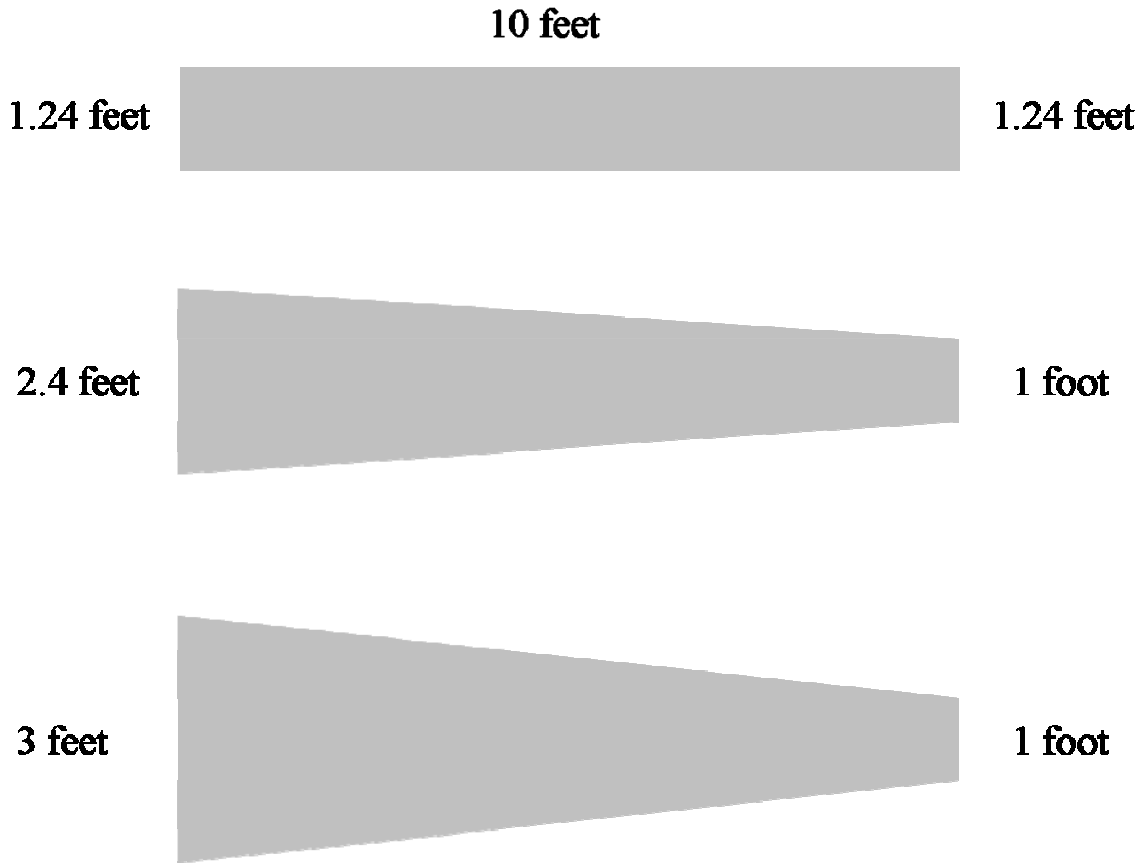

Figure 18. Comparison of Base Blade to Tapered Blades

Blade number increased to 5

1. Without maintaining rotor solidity

Rotor solidity, σ, is the ratio of blade surface area to rotor disk area, and it can be calculated by the following expression: (6:16)

$$\sigma = \frac{BladeArea}{DiskArea} = \frac{bcR}{\pi R^2} = \frac{bc}{\pi R}$$

where b is the number of blades, c is the chord length of each blade and R is the rotor radius. The first iteration of the blade increase is designed to investigate the effects of adding a geometrically identical blade to the tail rotor. The chord length of the CH-53E tail rotor blades is 1.24 feet and the rotor radius is 10 feet, and the disk solidity is .157, while the addition of the extra blade increases it to .197. In design considerations, the load factor will play a dominant role in deciding what rotor solidity to use. High load factors require more solidity, while low load factors require less. If using a cambered airfoil with a high lift coefficient then not as much solidity is needed. Two opposing issues come to the forefront. The extra blade will not only increase the weight of the tail rotor, possibly interfering with the center of gravity balance, but it will also increase the profile drag thus requiring more power. On the other hand, the increased solidity is capable of greater thrust and will require less pitch than the base design for any power setting. (6:657122)

2. Maintaining geometric solidity of rotor disk

The second iteration of the 5 bladed investigation is to maintain the base model tail rotor solidity by adding a blade and reducing the chord length. The airfoils on the 5 bladed design will have a new chord length of .986 feet, thereby matching the rotor disk solidity of .157. In reducing the chord length of each blade more pitch will be required for the production of thrust; therefore, more profile power. It is not clear which configuration will have the advantage, nor is it clear that either will provide a worthy substitute for the base model.

Analysis of Simulation Results

There are three major subsets of results that will be analyzed in order to determine rotor blade selection and performance upgrade. The first is hover performance, which is the characteristic of primary concern, and it will be represented using two charts, one of power required vs. altitude and another of figure of merit vs. altitude for each design change.

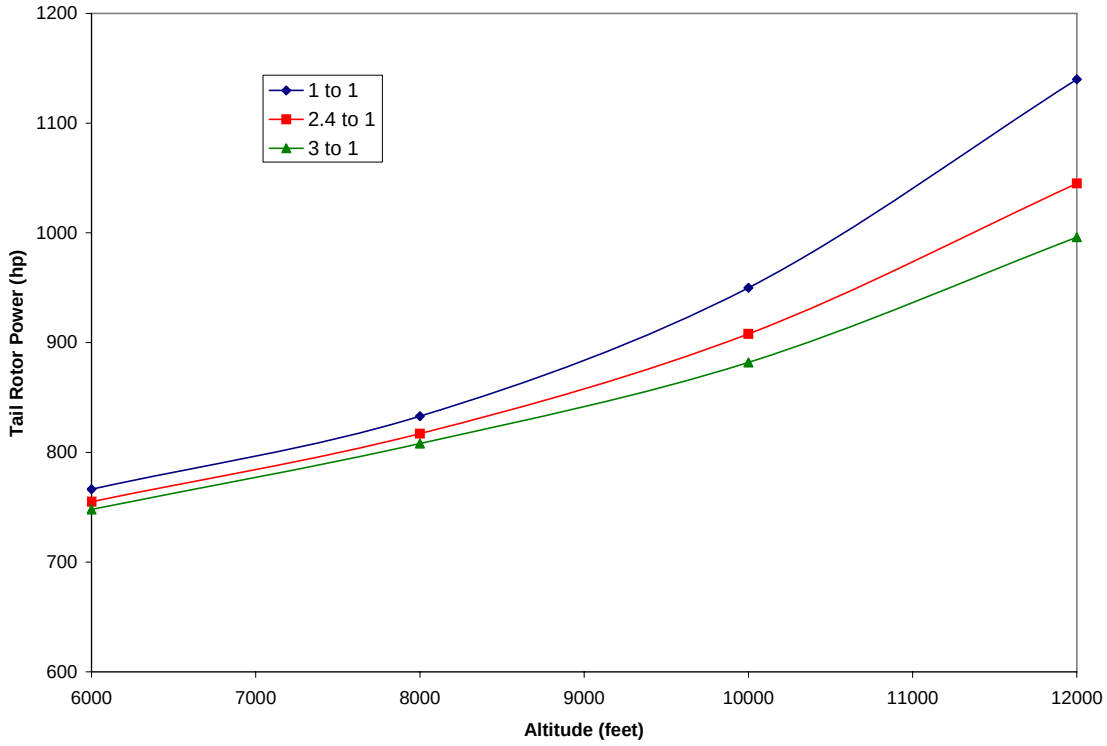

Figure 19. Example Tail Rotor Power Required Chart

Figure 19 is an example of how the analytical results for the hover portion of the investigation will be depicted. The percent savings in power and percent change in figure of merit will be calculated at the 10,000 foot mark, which is the design altitude corresponding to the mishap scenario. The second analysis is airspeed verification.

While this thesis is not primarily concerned with maximum forward airspeed, the nature of hover performance upgrades is to detract from forward flight capability. Therefore, the new tail rotor design will be chosen such that it posses the same or better forward flight performance as the base model. The tail rotor options will be run through a forward flight batch case that will step up the forward flight speed from 35 knots at 10 knot increments up to 100 knots then at 5 knot increments up to 190 knots. It is not expected that any of the options will converge at the upper limit, but it was chosen in order to get a full spread of forward airspeed maximums.

190	X	-
180	X	-
165	X	X
155	X	X
135	X	X
120	X	X
115	-	X
105	X	X
90	X	X
80	X	X
70	X	X
50	X	X
35	X	X
	1 to 1 11 deg VR12	1 to 1 8 deg Base
	21	19
	0.84	0.76

Figure 20. Example Forward Airspeed Convergence Chart

Figure 20 show an example of the airspeed study for this thesis. With airspeed on the left side and airfoil information on the bottom, convergence is indicated by an "X" and non convergence is indicated by a dash in the middle field of the chart. The "1 to 1" refers to the taper ratio and "11deg" and "8 deg" refers to the amount of washout. Next the airfoil is listed, with "base" referring to the NACA 0015 of the CH-53E current design. Below

the airfoil is the number of convergences, or "X"s, for that specific design combination. Here the chart was cut off for the sake of room, but the "21" and "19" represent what may be presented for a given blade. Under the convergence numbers is the normalized convergence number. A total of 25 iterations are run, which represent the 25 airspeeds from 35 to 190 knots. Dividing the convergence number by the total possible gives a percentage of convergence for the design, and this will be the form of comparison for the different configurations. Finally, the hover slide test will set the helicopter in a slide at 35 knots from 360 counterclockwise at 30 degree increments back to 360. This is the level one handling qualities verification. Should the new tail rotor require more power than the base model at any point in the azimuthally varying slide, it will be marked invalid, as it will be degraded in its controllability. Figure 21 shows the set up for the hover slide verification.

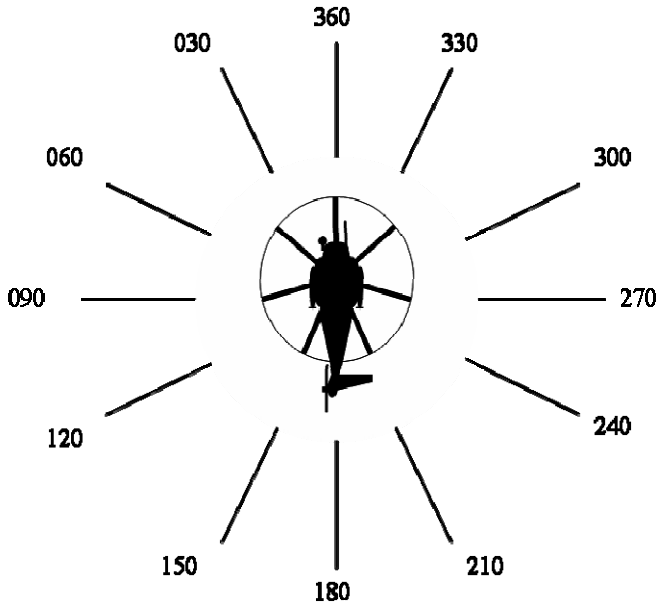

Figure 21. Azimuthally Varying Winds to Simulate Hover Slides and Verify Handling Qualities

Chapter Overview

This chapter discussed the RCAS simulation program by explaining two major portions necessary for the proper development of the input file. It also covered the information necessary for model development and explained certain fundamental aspects regarding this specific model. The five specific design changes were discussed in detail along with their appropriate modifications. Finally, the details of analyzing the simulation results were discussed, and charts were provided for orientation.

III. Data Analysis and Results

Overview

This chapter will present the output data from the RCAS simulations beginning with the individual design changes and moving to the combined changes. It should be pointed out that the investigative altitude is 10,000 feet, and all comparison in percent change is referenced at that altitude, yet all charts have at minimum a 4,000 foot range allowing trends in performance to come to light.

Individual Design Changes in Hover

Note that for the following simulations the weight of the helicopter was held constant. As the altitude increases the density of the air decreases, which decreases the profile power, but it also deceases the effectiveness of the rotor blades so that more pitch must be added in order to counter the main rotor torque. The overall effect is that power required will go up with increasing altitude.

Airfoil

Figure 22 shows the four different airfoils studied and how they vary in power required over a range of altitudes from the surface to 12,000 feet. The airfoil investigation was the only one that included altitudes below the predetermined lower boundary of 6,000 feet. This was done in order to gain an appreciation for the variations between 6,000 and 12,000 feet. The first point of concern, and perhaps the greatest, is the hover performance of the SC 1095 airfoil compared to the others. Quite surprisingly, between 6,000 and 9,000 feet it requires the most power. Above and below those

altitudes it shows a small margin of improvement over the base model with about 1/10% reduction in required power. The SC1095, as the thinnest of the airfoils tested would probably have favored a higher rotational speed for the tail rotor. Its profile drag would not have been nearly as affected by the increase in dynamic pressure as the other, thicker airfoils, and it would have needed less pitch, due to the higher flow velocity, than currently required. The NACA 0012, a great all around performer, made a good showing, but its thickness produces too much profile drag to be the most efficient airfoil; however, it reduced the power required by 3.6%. The VR-12 showed the least amount of power required to run the rotor system, and it had a power savings of 9% from the base model. While the least power required is important, an even better measure for rotor hover performance is calculating the figure of merit, FM.

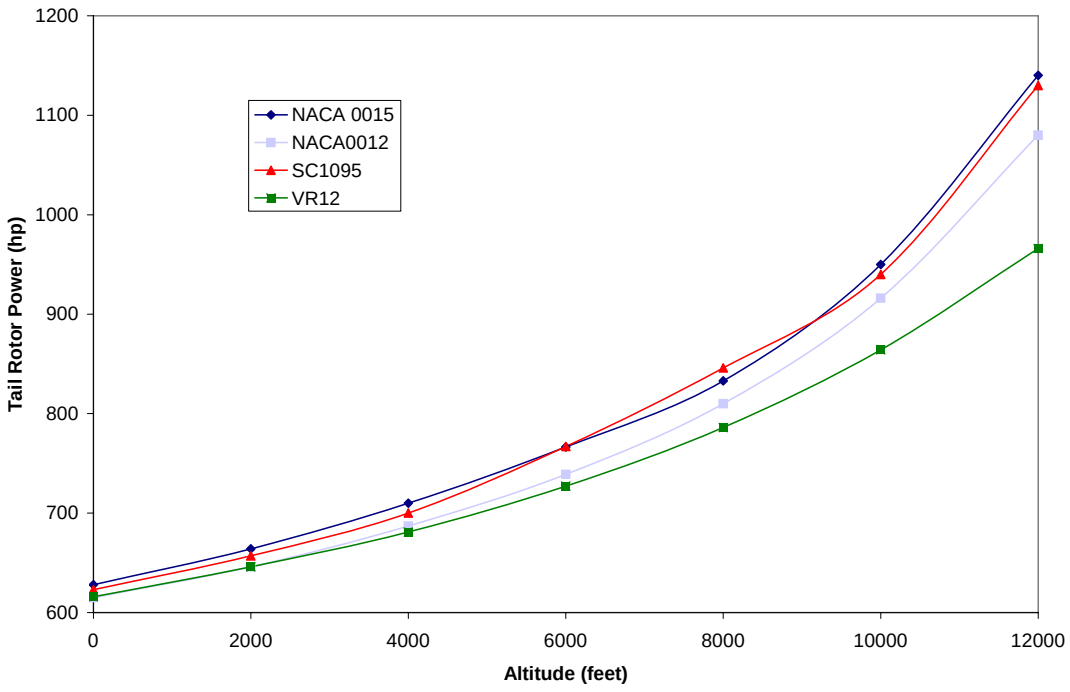

Figure 22. HOGE Performance with Different Airfoils

Figure 23 shows the FM for each airfoil from seal level to 12,000 feet. Once again, the airfoil information was run at a larger number of data points to find the trend in performance. It is clear from figure of merit results in Figure 23 that the airfoils appear to favor certain altitudes. The base airfoil (NACA 0015) favors the low altitudes, and its highest FM is at 2,000 feet. The SC 1095 peaks out at 4,000 feet, which happens to be the design altitude for US Army helicopters, then jockeys for position with the base airfoil until about 10,000 feet and above where it has a slight edge. The NACA 0012 shares the highest FM with the VR-12 from sea level to 2,000 then falls away as the VR-12 continues to increase. The VR-12 has the highest peak at 6,000 then gradually decreases on its way up to 12,000 feet. These types of changes in Figure of Merit are indicative of the design for each blade. The SC 1095 is a poor at high altitudes because the 9.5% thickness requires excessive pitch for the required lift resulting in high induced power.

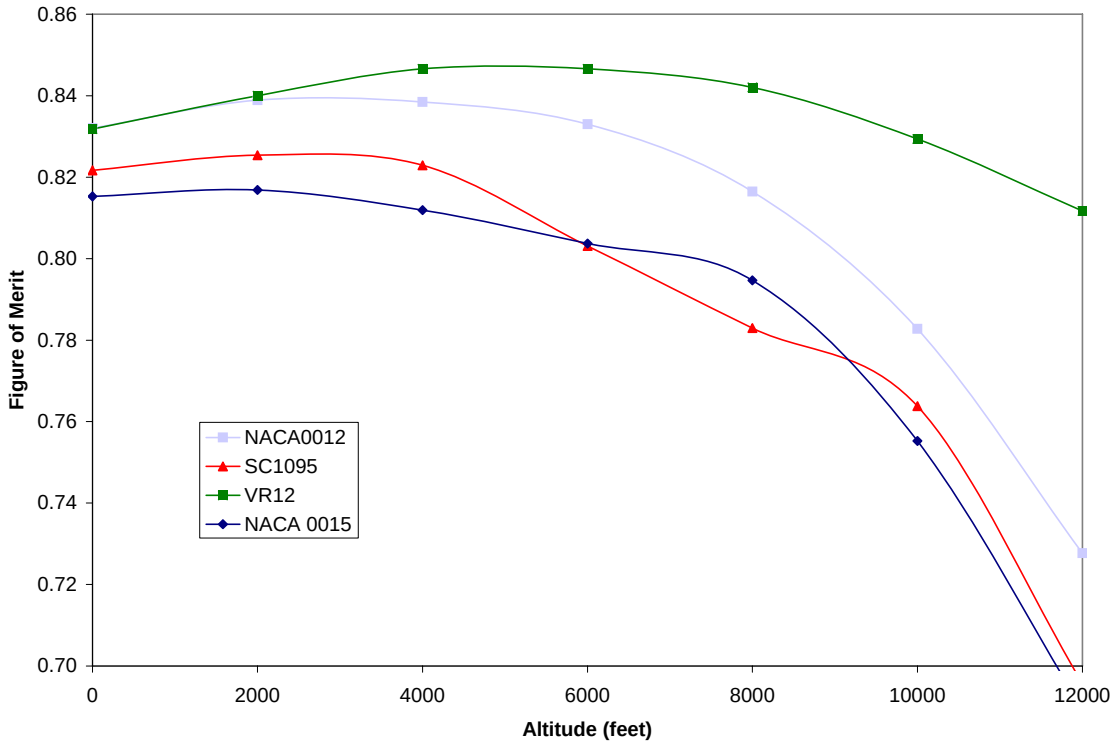

Figure 23. Figure of Merit versus Altitude for Simulated Airfoils

Twist

As seen in Figure 24, power required decreased for each incremental increase in blade twist. Twist comprised the largest power required savings of all the methods of increasing efficiency. -12 degrees produced a savings of 5.7%, -16 degrees produced 9% and -20 degrees produced the highest savings at 11.36%. Recall that twist serves to reduce the induced velocity at the blade tip so that the induced velocity over the whole rotor disk is as uniform as possible. Figure 25 shows the figure of merit for each twisted blade with diminished returns as the twist increases.

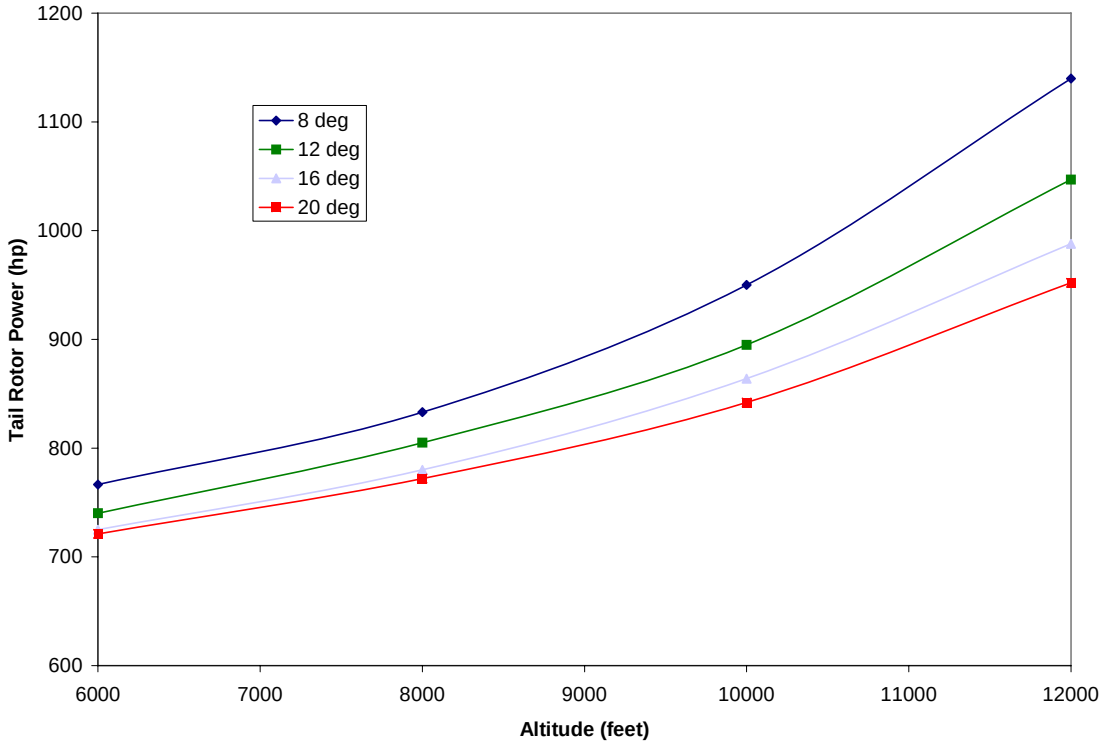

Figure 24. HOGE Performance with Increasing Twist

Even though -20 degrees of twist provides the best FM, lesser twist will most likely be used once forward flight performance is factored into the selection. Due to the positive effects that washout, or negative blade twist, have shown in these simulations, this technique will be used in the development of a new tail rotor blade.

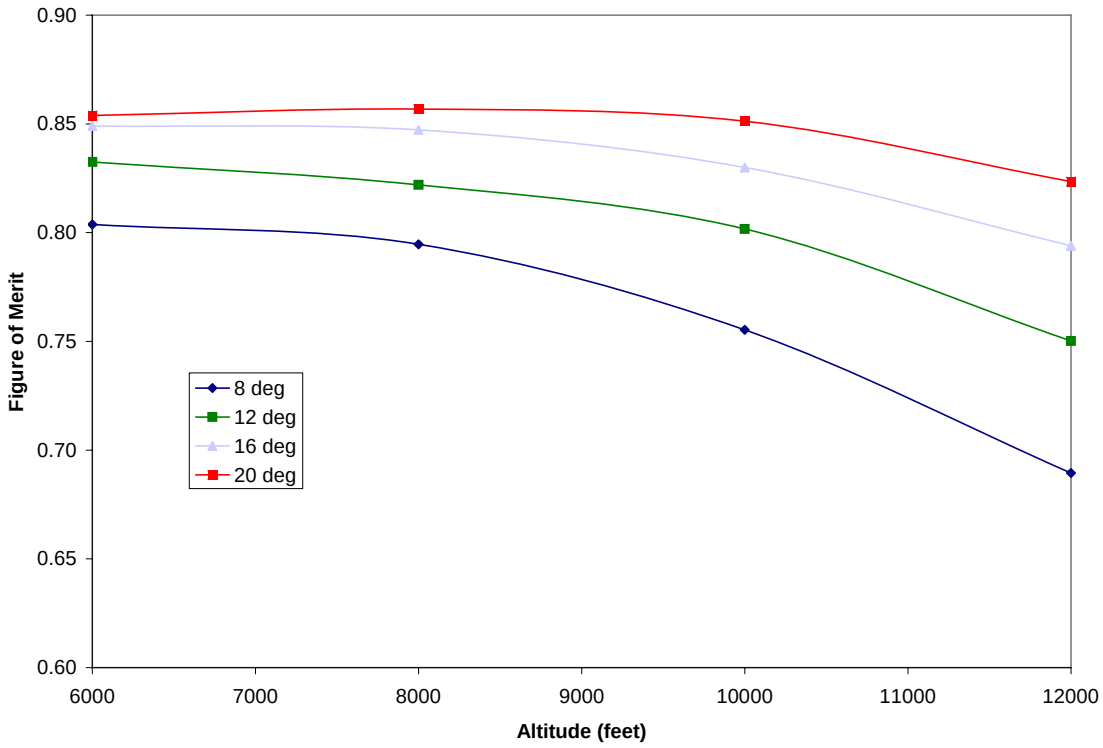

Figure 25. Figure of Merit versus Altitude for Simulated Twists

Taper

The initial investigation regarding blade taper began with a study of the hyperbolically varying blade planform. It became apparent that the linear approximation was both easier and more desirable because it had the potential to be a real, not merely theoretical, solution. Two taper ratios were used for the simulations, 2.4:1 and 3:1. As a point of note, the initial attempt at taper ratio was calculated by holding the root chord constant at 1.24 feet and tapering the remainder of the blade down to .5 feet. This resulted in the planform area being significantly less than the rectangular shape of the base model. With a reduction in blade area of 30%, the resulting blade was unable to produce enough thrust to hold the helicopter in a steady hover, and the RCAS program

was unable to converge to a trim solution. However, the program was able to output the tail rotor power required, which was approximately 50% less than that of the converging solutions. This showed that the reduction in blade area and the slight taper applied had beneficial effects on the drag, but it did so at the expense of the requisite amount of thrust. The proper method for describing the geometry of a tapered blade is to hold the .75 span constant and run the slope to intersect the y-axis and the tip at the proper x-axis distance. The two useable attempts at taper increased the area of the planform, and their performance is more commensurate with the expected performance increase of the optimum taper blade. The first taper ratio used was 2.4:1 and it represents about a 35% increase in blade area and produced a power savings of 4.4% over the base model, while the 3:1 represented about a 60% increase in blade area and 7% decrease in power required.

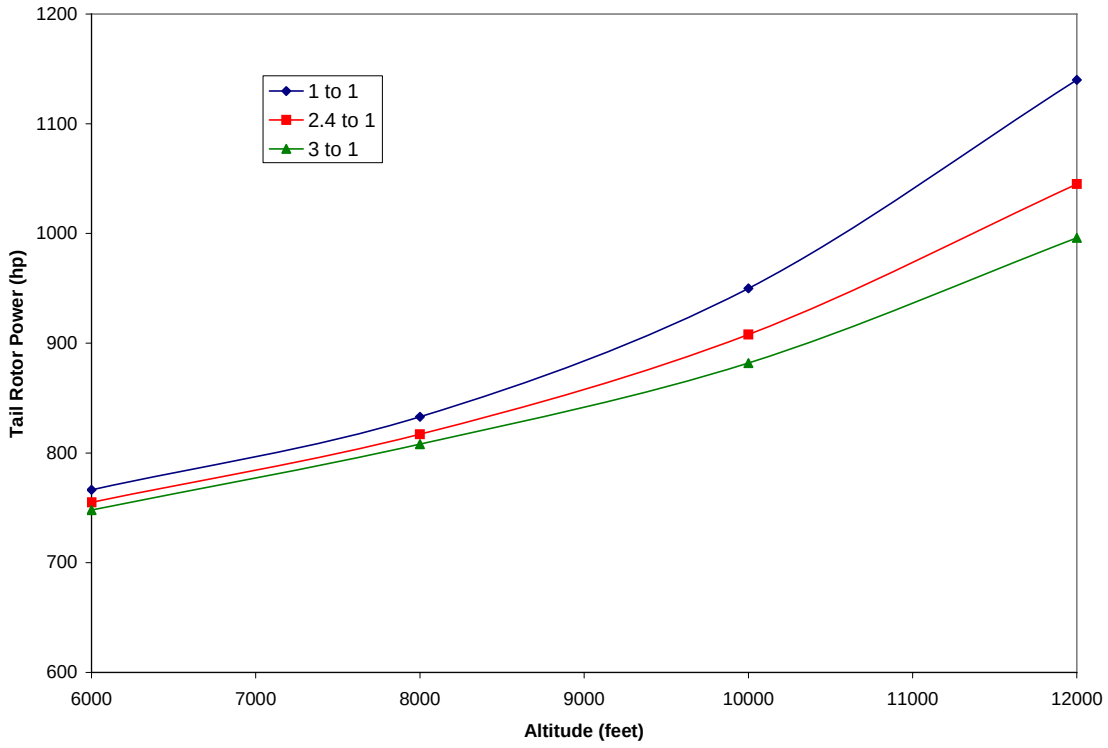

Figure 26. Effects of Less than Ideal Taper on Power Requirements

Figure 26 shows the relationship between increasing taper and decreasing power required. It indicates that the positive effect on power reduction produced by a ratio change from 1:1 to 3:1 is linear. This is different from the twist results, which produced diminishing returns with increasing twist. The effects of taper have been shown in this simulation to positively affect the FM and reduce the power required; therefore, it will be used in the development of the new tail rotor.

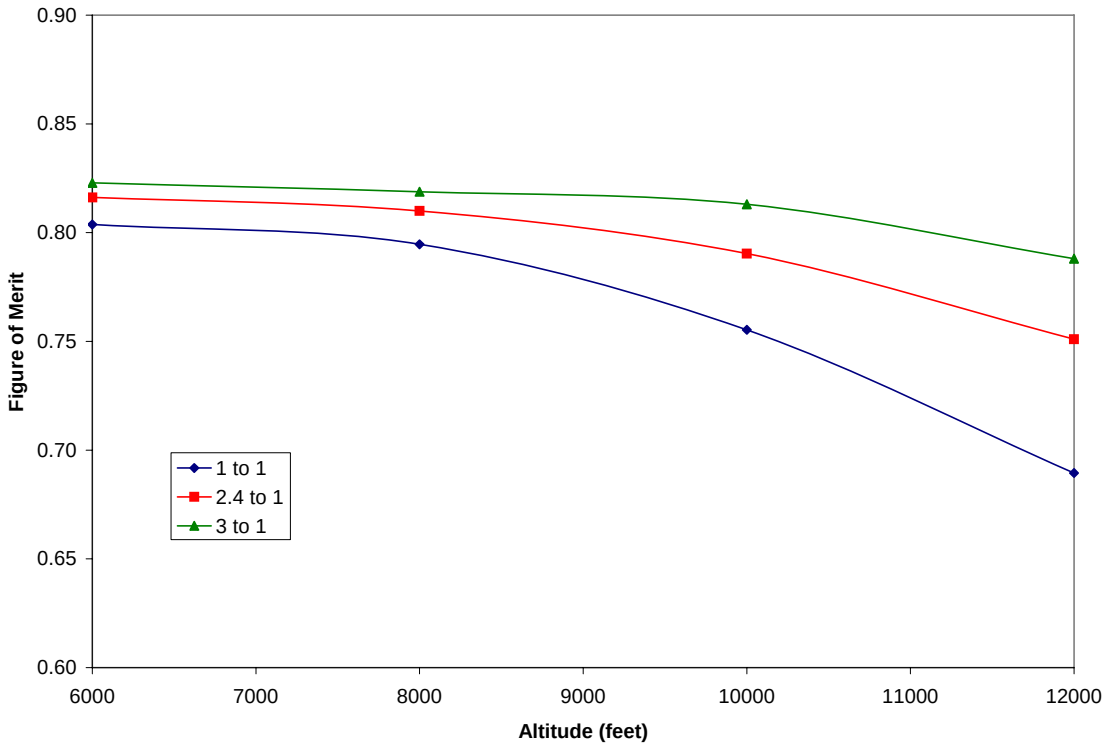

Figure 27. Figure of Merit for Taper Ratio

Radius

The small increases in radius conducted here only marginally decreased the power required, as indicated by Figure 28, while also decreasing the FM. This turned out to have the lowest return of any of the options, with the 10.25 foot radius returning a 2% savings, and the 10.5 foot radius returning 2.1%. The decrease in power required is because the larger blade is able to produce more thrust at a given pitch. However, the FM goes down with the worsening ideal to actual power ratio. It may seem backwards that the FM goes down when power required also goes down, but since the larger diameter rotor system has the potential for greater power (higher ideal power) then even a

modest decrease in actual power will not bring up the FM. Such is the case here. Recall the following relationships: (4:44,46)

$$FM = \frac{\frac{C_T^{\frac{3}{2}}}{\sqrt{2}}}{C_{P_{measured}}}$$

and,

$$C_T = \frac{T}{\rho A(\Omega R)^2}$$

and,

$$C_P = \frac{T}{\rho A(\Omega R)^3}$$

Since the thrust, T, to maintain a steady hover is constant for the tail rotor regardless of size and design, as the tail rotor disk area, A, increases then the thrust coefficient, C_T, must decrease with the cube of the radius R. The same can be said for the coefficient of power, C_P, except that it varies with the 4th power of R. In order for the larger diameter rotor to have a better FM than the base model the rotor rpm, Ω, needs to be reduced so that C_T remains constant. Then the lower C_P from the larger radius will produce a better FM. Figure 28 and Figure 29 combine to illustrate the effects of density more so than any of the other figures. At the lower altitudes, all three designs are using about the same amount of power required, but the smaller diameter of the base model gives it a higher figure of merit compared to the others as previously discussed.

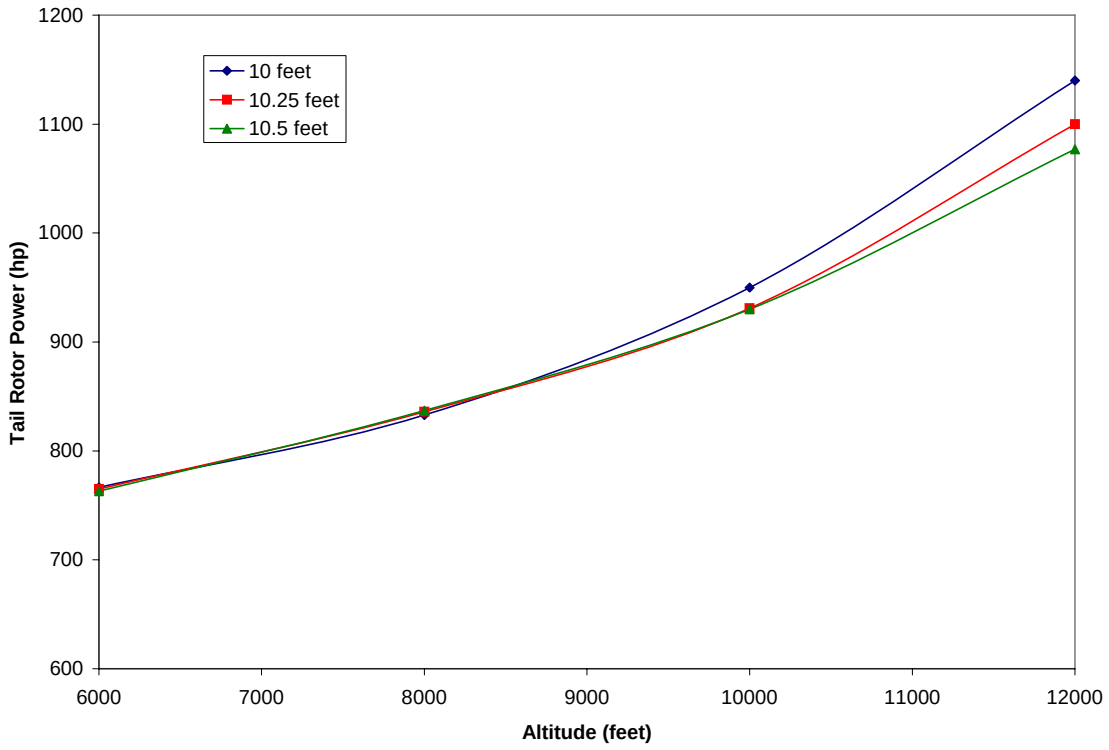

Figure 28. HOGE Performance with Increasing Radius

Decreasing density, ρ, with increasing altitude requires the smaller diameter, base rotor to pull more collective pitch for the required thrust. The larger diameter rotors also require greater collective pitch with increasing altitude but to a lesser degree due to their larger size. Above 10,000 feet the base model is unable to maintain its FM advantage due to the decreasing density and increasing power required. Note, in Figure 28, that the 10.5-foot radius rotor is on a shallower slope than the 10.25-foot radius rotor, indicating that the larger rotor will eventually have a higher FM. This shows that the effects of higher induced velocity at the blade tips is relieved by the decrease in dynamic pressure, and the rotor becomes more efficient than its smaller counterparts. Due to the adverse effect on FM, the rotor radius increase will not be used on the new tail rotor blade.

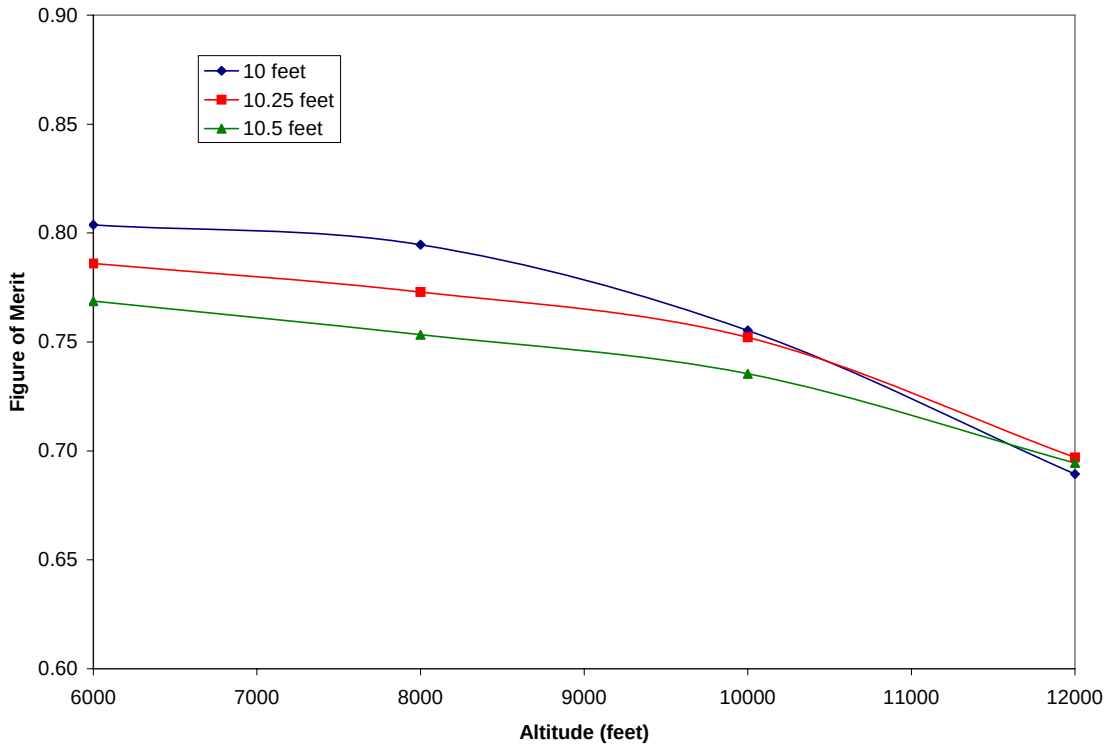

Figure 29. HOGE Figure of Merit with Increasing Radius

5 Blades

The two scenarios with the addition of a 5th blade resulted in opposite effects, making for an interesting topic of investigation. When the rotor solidity was maintained, meaning that the blade chord was reduced to accept the 5th blade without changing the rotor disk solidity, the power required was increased over the straight addition of a 5th blade. Maintaining solidity resulted in a power savings over the base model of 1.5% but a decrease in FM of .1%. This is due to the smaller blade surface and the ensuing large pitch angles reached. Not only did it require more power to run that rotor disk, it also ran it at a lowered ideal to actual power ratio, hence the FM went down. Alternatively, adding an identical 5th blade and allowing the rotor disk solidity to increase

proportionately resulted in better performance and 7.5% power savings. As discussed previously, high disk loading situations call for high rotor solidity. Thus, the extra blade overcame the added weight and profile drag by requiring a lesser pitch from each blade. Due to the complication of actually adding another blade, this study will forego further investigation of this option.

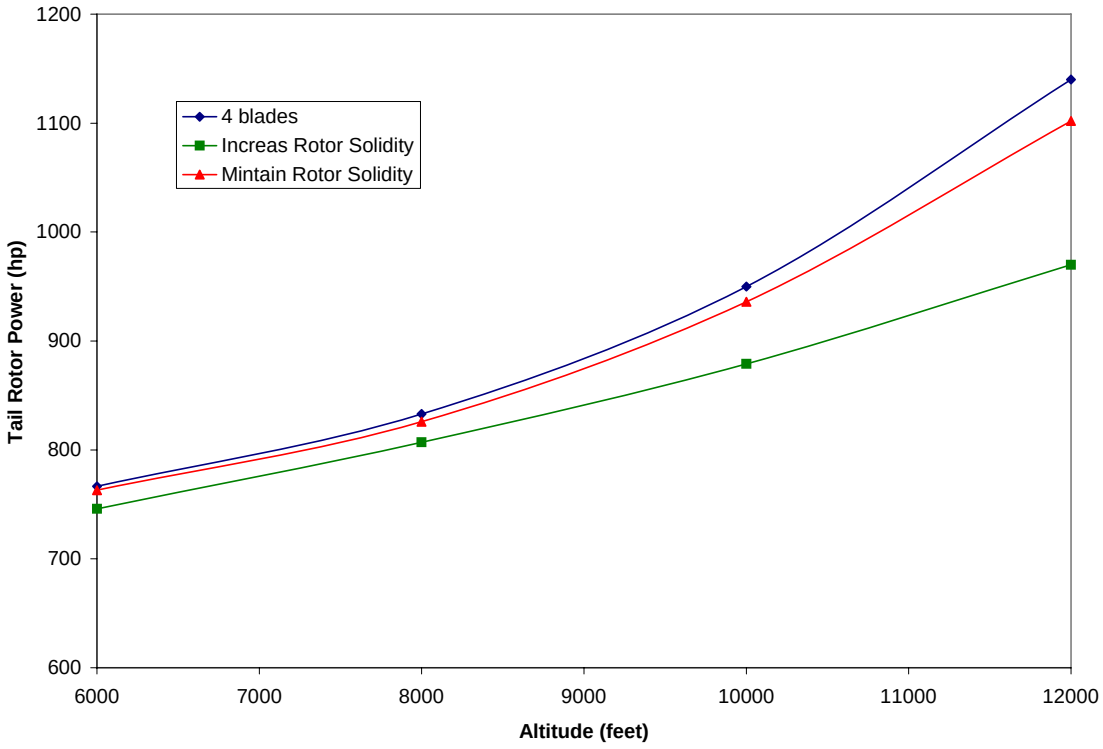

Figure 30. HOGE Performance with 5 Tail Rotor Blades

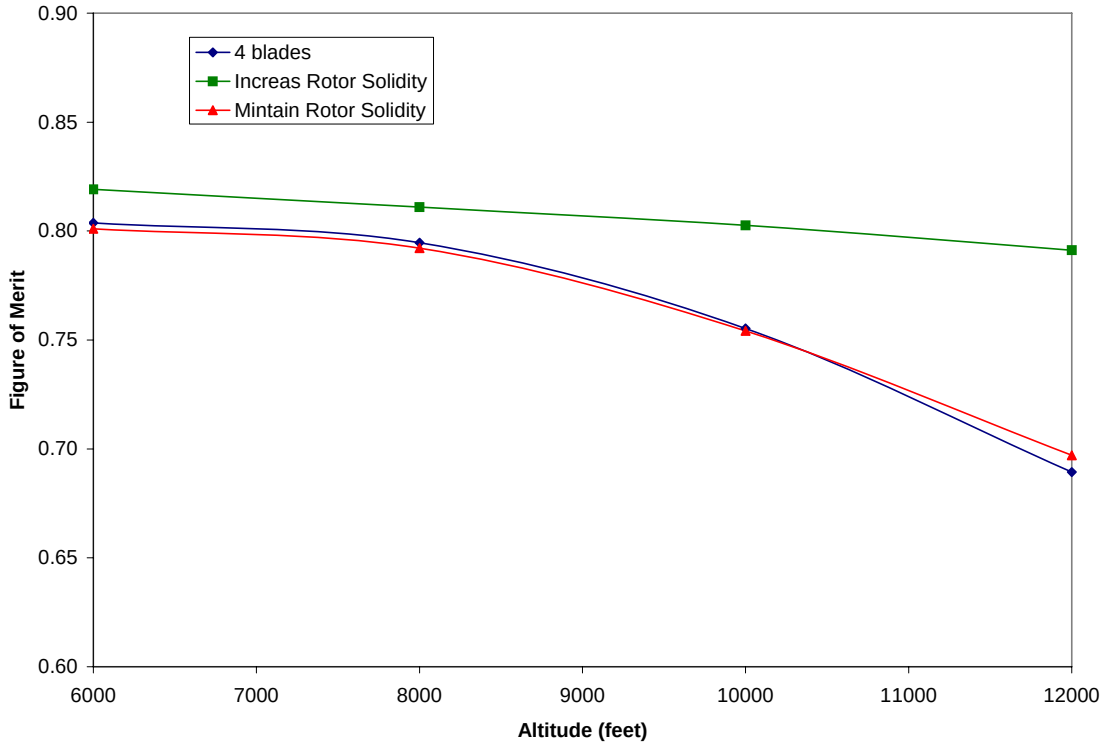

Figure 31. Figure of Merit with 5 Tail Rotor Blades

Determining the Type and Value of Changes

Airfoil

The VR-12 performed significantly better than the other airfoil options in the hover, but validation of this model must be made in forward flight to produce a valid result; therefore, forward flight simulations were conducted on each airfoil with differing taper ratios and twists. In order for maximum forward airspeed to be determined by RCAS, simulations must be run from hover to the unknown maximum in an incremental manner. This is due to the trim requirement that RCAS places on convergence. If no trim solution is found for the given configuration and airspeed then no analytical results can be obtained. Figure 32 shows the analytical results from the forward flight

simulations as they were compiled in order to make a determination on the most favorable airfoil. The O and N are different types of non-convergence and not important to this study.

190	-	-	-	-	O	-	-	-	-	-	-	-	-
185	-	X	-	-	-	-	-	-	-	-	-	-	-
180	-	X	-	-	X	X	-	-	N	-	-	-	-
175	X	X	-	-	X	-	X	-	X	X	-	-	-
170	X	X	X	-	X	X	-	X	X	X	-	-	-
165	X	X	-	-	X	X	-	-	X	-	-	-	X
160	-	-	X	-	X	X	X	X	X	X	-	-	X
155	-	-	X	-	X	-	-	-	X	-	-	-	X
150	X	X	X	-	X	X	X	X	X	X	-	X	-
145	X	X	X	-	X	X	X	X	X	X	-	-	X
140	X	-	X	X	X	X	X	X	X	X	-	-	X
135	X	X	X	X	X	X	X	X	X	X	X	-	X
130	X	-	X	X	X	X	X	X	-	-	X	X	X
125	X	X	X	X	X	X	X	-	X	-	X	-	X
120	X	X	X	X	X	X	X	X	X	X	X	X	X
115	X	X	X	X	X	X	X	X	-	-	X	X	X
110	X	-	X	X	X	X	X	X	X	-	X	X	X
105	X	X	X	X	X	X	X	X	X	X	-	X	X
100	X	X	X	X	X	X	X	X	X	X	X	X	X
90	X	X	X	X	X	X	X	X	X	X	X	-	X
80	X	X	X	X	X	X	X	X	X	X	X	X	X
70	X	X	X	X	X	X	X	X	X	X	X	X	X
60	X	X	X	X	X	X	X	X	X	X	X	X	X
50	X	X	X	X	X	X	X	X	X	X	X	X	X
35	X	X	X	X	X	X	X	X	X	X	X	X	X
	1 to 1 8 deg	1 to 1 20 deg	3 to 1 8 deg	3 to 1 20 deg	1 to 1 8 deg	1 to 1 20 deg	3 to 1 8 deg	3 to 1 20 deg	1 to 1 8 deg	1 to 1 20 deg	3 to 1 8 deg	3 to 1 20 deg	1 to 1 8 deg
		NACA 0012				SC1095				VR12			Base
	20	19	20	15	23	21	19	18	20	16	13	12	19
	0.8	0.76	0.8	0.6	0.92	0.84	0.76	0.72	0.8	0.64	0.52	0.48	0.76
		0.74				0.81				0.61			0.76

Figure 32. Forward Airspeed Airfoil Selection Chart

The SC1095 was the best forward flight performer by a significant margin, followed by the NACA 0012, then the VR-12. Difficulty was found in trying to evenly compare the hover data with the forward flight data. Attempts were made to add the percent increase in FM at 10,000 feet to the percent increase in total forward airspeed convergence for each airfoil. This proved unsuccessful, because the range of increase in FM is approximately 9%, while the range of increase in forward airspeed is approximately 15%, giving a significant weight to the airspeed simulations. An attempt was made at weighting the hover and airspeed values so that hover was given more importance. This proved inconclusive, as arbitrarily chosen values could drive any of the airfoils to

selection. Finally, the base model forward airspeed information was used to set the standard, and the determination was made that the airspeed portion of this investigation should be validated on a pass-fail basis. The problem statement of this thesis is concerned with the low end of the airspeed spectrum; hence, the relative merits of maximum forward airspeed are irrelevant, provided the selected airfoil meets or beats the current maximum airspeed. The chart bears out that each of the airfoils surpassed the base model in similar configuration, i.e. at -8 degrees of twist and a 1:1 taper ratio. Since all three airfoil options were validated in forward flight, their hover performance became the basis of selection, and the VR-12 was picked as the best performer.

Twist

The hover figure of merit for the base airfoil was tested at four different values of washout: 8, 12, 16 and 20, as discussed in the previous section. Analytical results were also gained regarding twist from the forward flight validation. In the same manner that airfoil results were summed and normalized by the maximum number of convergences, so the twist data was added for both -8 degrees and -20 degrees and normalized by the same forward airspeed convergence. By making a double y-axis plot versus twist, the hover FM and the normalized forward airspeed convergence factor can be graphed together, and the crossing point represents the most advantageous combination.

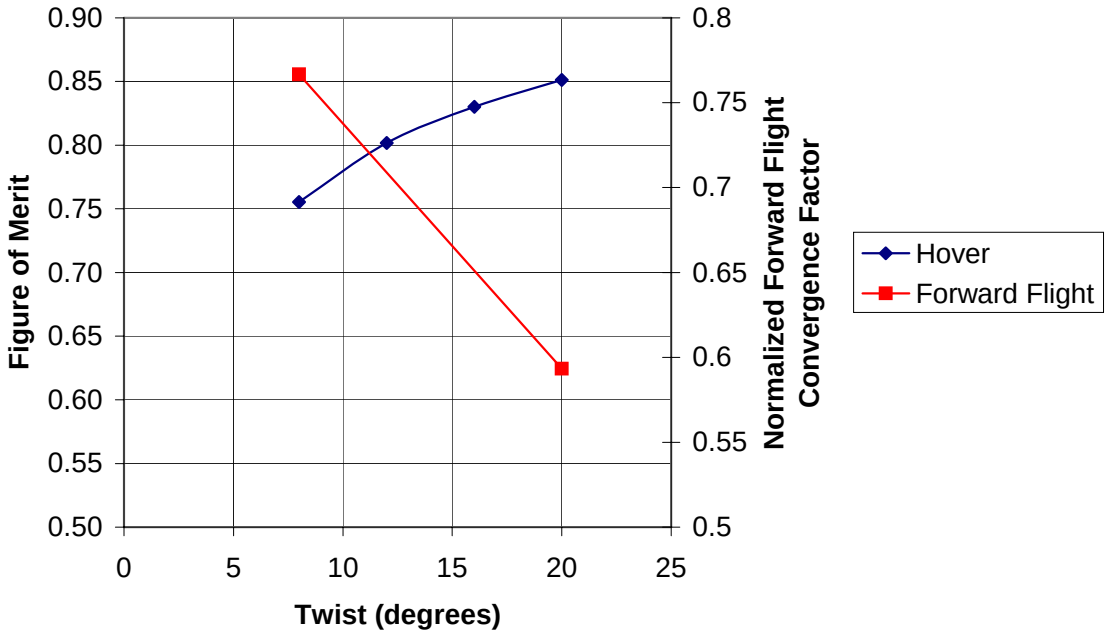

Figure 33. Hover and Forward Flight Results for Twist Determination

The hover curve, Figure 33, shows how the figure of merit of the hovering rotor improves as the twist is increased from -8 to -20 degrees, while the forward flight curve shows the decrease in forward flight for the same variation in twist. Only two different twist values were used in the forward flight simulations; therefore, the curve represents a linear relationship. The two curves cross at approximately -11.3 degrees twist. Since the accuracy of the chart is about 1 degree, it was decided to use the previously studied twist of -12 degrees.

Taper

Like twist, taper is turned into a double y-axis plot so that the hover and forward flight results can be compared. Taper was simulated at 1:1 and 3:1 ratios in the forward flight regime thus these two values render a linear distribution of taper. The forward

flight factor for taper decreases with increasing taper ratio, while the hover FM increases with increasing taper, and they cross at a taper ratio of 1.6.

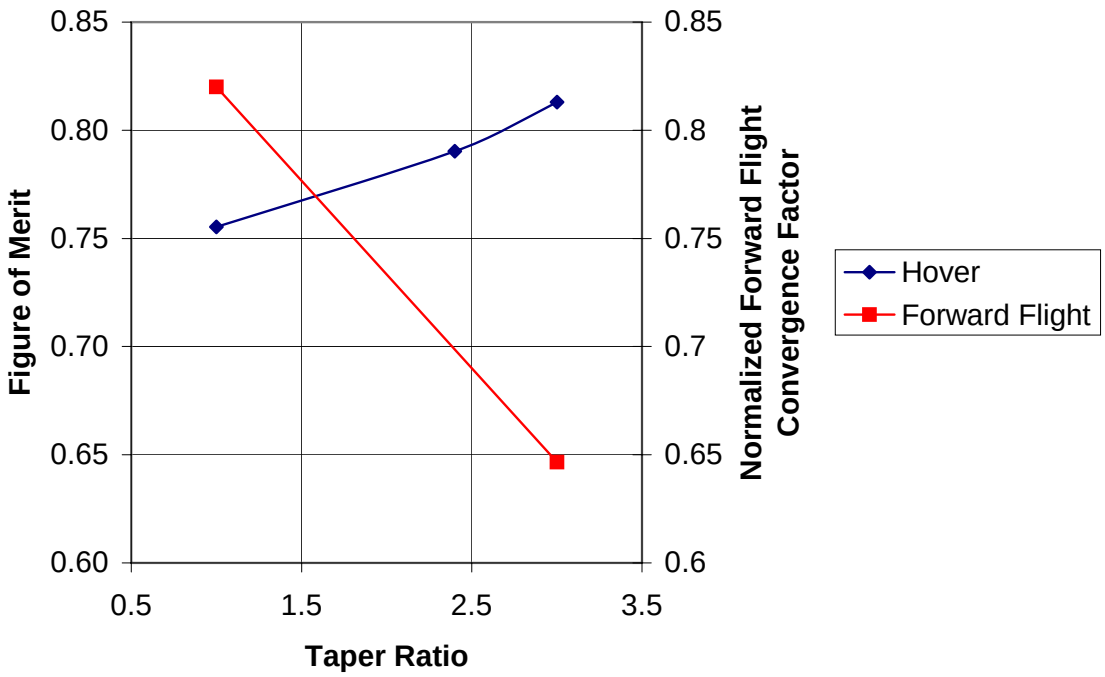

Figure 34. Hover and Forward Flight Results for Taper Determination

To summarize the changes, the new blade design was originally to be comprised of the VR-12 airfoil with -12 degrees twist and a taper ratio of 1.6:1. It was shown that those design changes were inadequate and needed to be modified In anticipation of the upcoming results, Leishman states that, "It is common for linear blade twist and taper planform variations to be employed on helicopter rotor blades, and this is found sufficiently close to the optimum values defined on the basis of BEMT [blade element momentum theory]." (4:98)

Running simulations on the new blade found the following. The hover results were excellent, and the new design had a better FM than any of the other options. However, this new design did not meet the forward flight threshold set by the base model. Therefore, it was decided to decrease the twist by 1 degree and re run the forward flight simulation. This process was to be repeated until the proper forward flight convergence was met. Bracketing the solution was not attempted because it was thought that the forward flight convergence was very close, and it was desired to maintain as much twist as possible for better hover performance.

Simulations were run while decreasing the twist from -12 degrees to -9 degrees in 1-degree increments without meeting the required number of successful convergences. This turned attention to the taper ratio. Information from Figure 32, indicated that the VR-12 airfoil was more tolerant of increasing twist angle than it was of increasing taper ratio. However, it was thought that the 1.6:1 taper ratio was sufficiently small to allow its integration without complication. This notion proved fallacious. In a second wave of attempted airspeed convergences, zero taper was applied while the twist was again decreased from -12-degrees in 1-degree increments. This proved a much better technique as the required airspeed convergence number was hit at -11 degrees of twist.

New Tail Rotor Performance

Following a lengthy iterative process with the new rotor blade, the airspeed convergence requirement was met, and the new blade design solidified. The new tail rotor was made up of the VR-12 with -11 degrees of twist and no taper. Hover, airspeed and hover slide simulations were run with the following results.

Hover

The new tail rotor blade performed with substantial improvements over the base model. The target improvement was a 10% decrease in tail rotor power in a 10,000 foot HOGE, and the results yield an 11.47% decrease. The three degrees of extra twist over the original VR-12 model took the percent savings from 9% to the current yield. This is consistent with the twist investigation on the base model previously mentioned. With the base model, the increase in twist from -8 degrees to -12 degrees provided a 3.4% savings, which is nearly the same represented here between the VR-12 at -8 degrees and -11 degrees. Figure 35 shows how the combination of a new airfoil and added twist results in significant improvements in HOGE power reduction. The figure of merit for the airfoil comparison yields a 13% increase over the base model as shown by Figure 36.

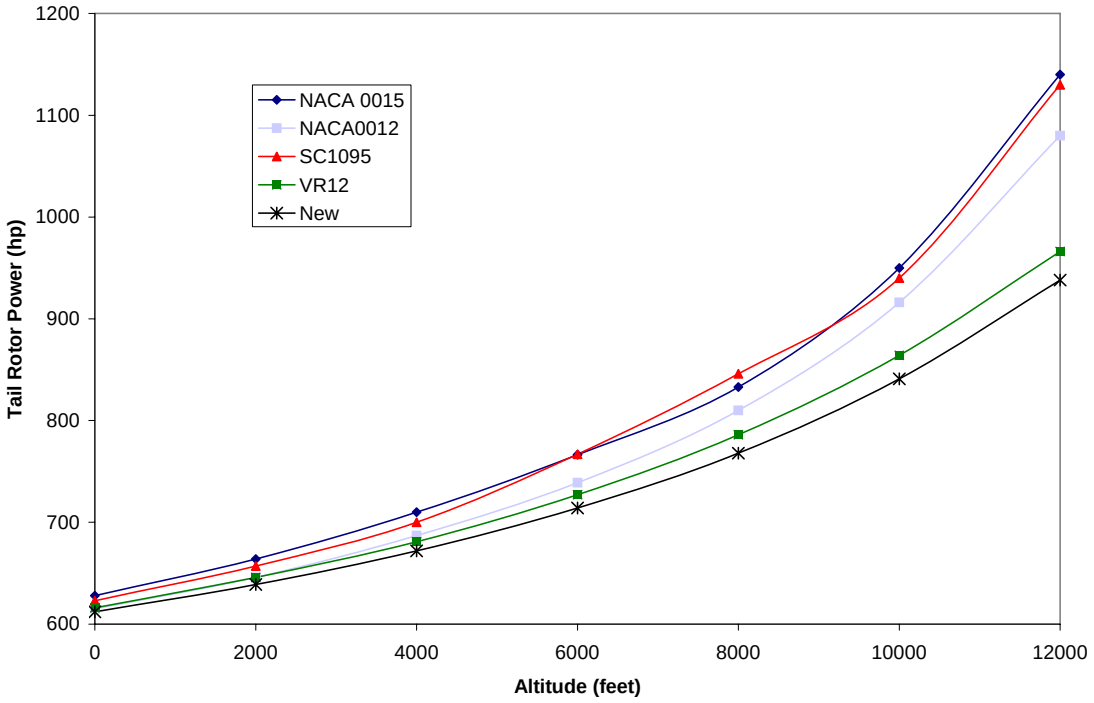

Figure 35. New Tail Rotor Blade Power Required vs. Other Airfoils

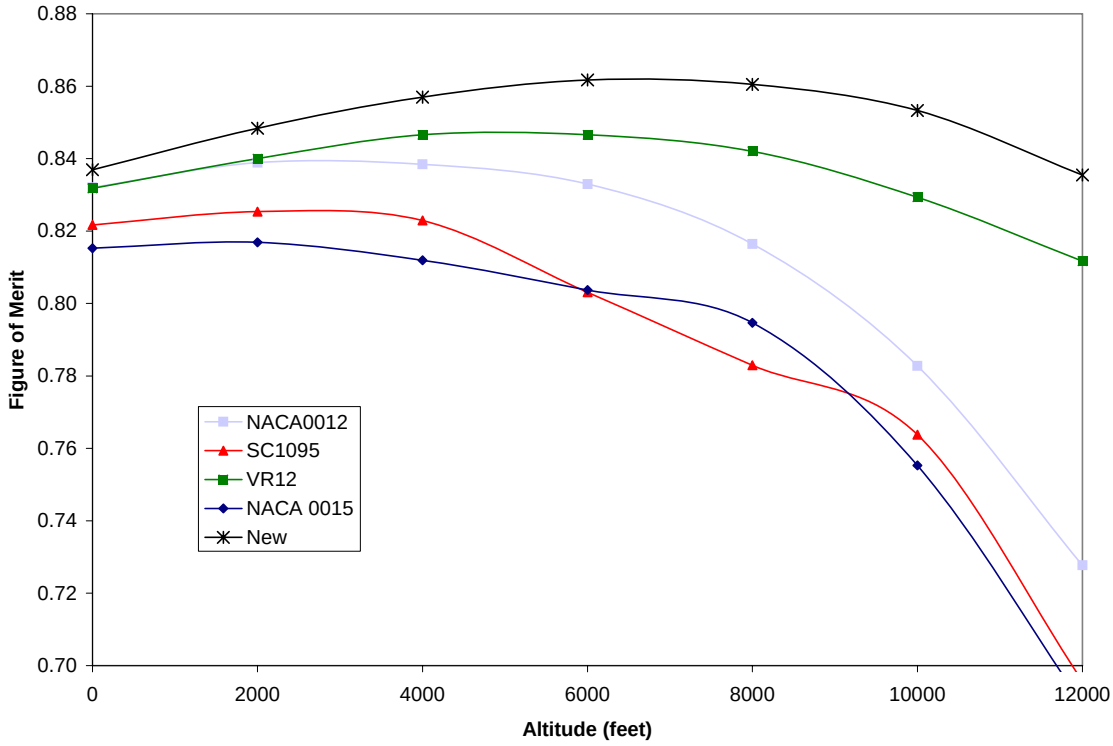

Figure 36. New Tail Rotor Blade Figure of Merit vs. Other Airfoils

Figure 37 shows the power required savings of the new blade over the base model twist variations. The power required savings is less than one percent but recall that Prouty stated that -20 degrees of twist was the closest linear approximation to the ideally twisted blade. Note that the new blade design registers less power required and a higher figure of merit in HOGE than even the -20 degrees of twist. The benefits of this will be seen in forward flight; while the new design was able to validate the forward airspeed convergence, the -20 degree twist airfoil will suffer from vibratory loads and may not successfully converge. The interesting part here is that hover performance may be increased without excessive twist, which will allow for a greater forward flight window.

Figure 38 is the figure of merit and shows an increase over the -20 degrees of twist of nearly 3%.

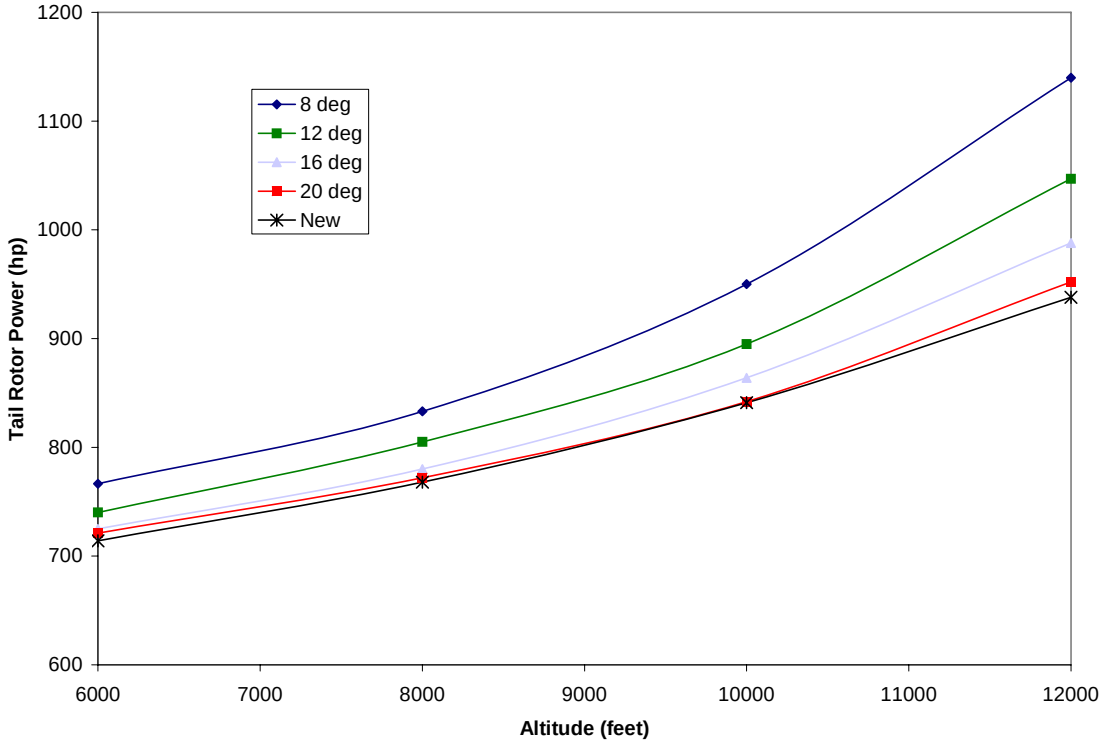

Figure 37. New Tail Rotor Blade Power Required vs. Base Model Twist Variations

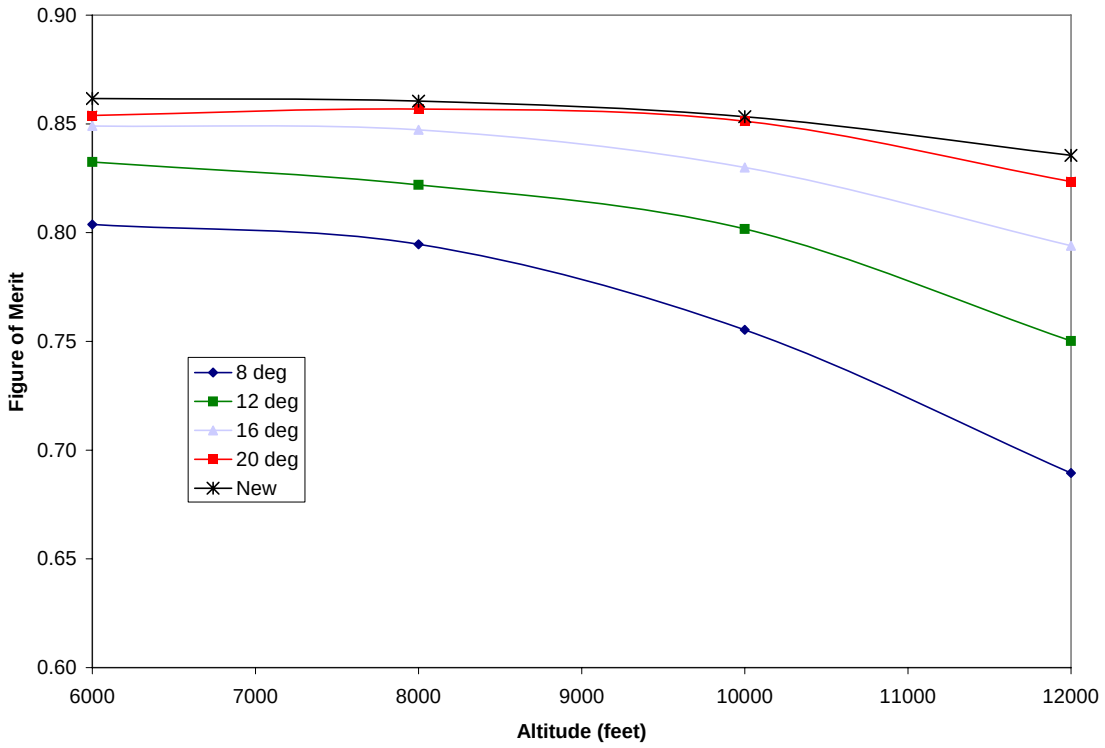

Figure 38. New Tail Rotor Blade Figure of Merit vs Base Model Twist Variations

The taper ratio of the new blade was set at 1:1 as the VR-12 exhibited a lack of forgiveness for this technique of operating at the maximum L/D across the entire rotor disk. Figure 39 shows a decrease in power required of 4.6% from the 3:1 tapered base model to the new blade. This same trend is represented in Figure 40 as a 4.9% increase in figure of merit.

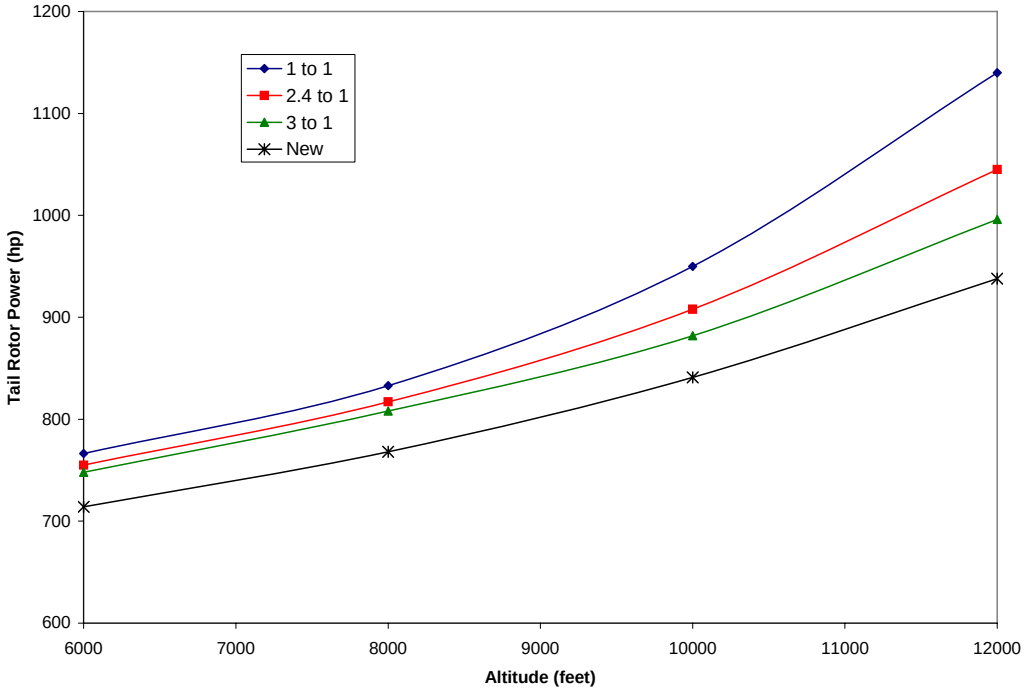

Figure 39. New Tail Rotor Blade Power Required vs Base Model Taper Ratio Options

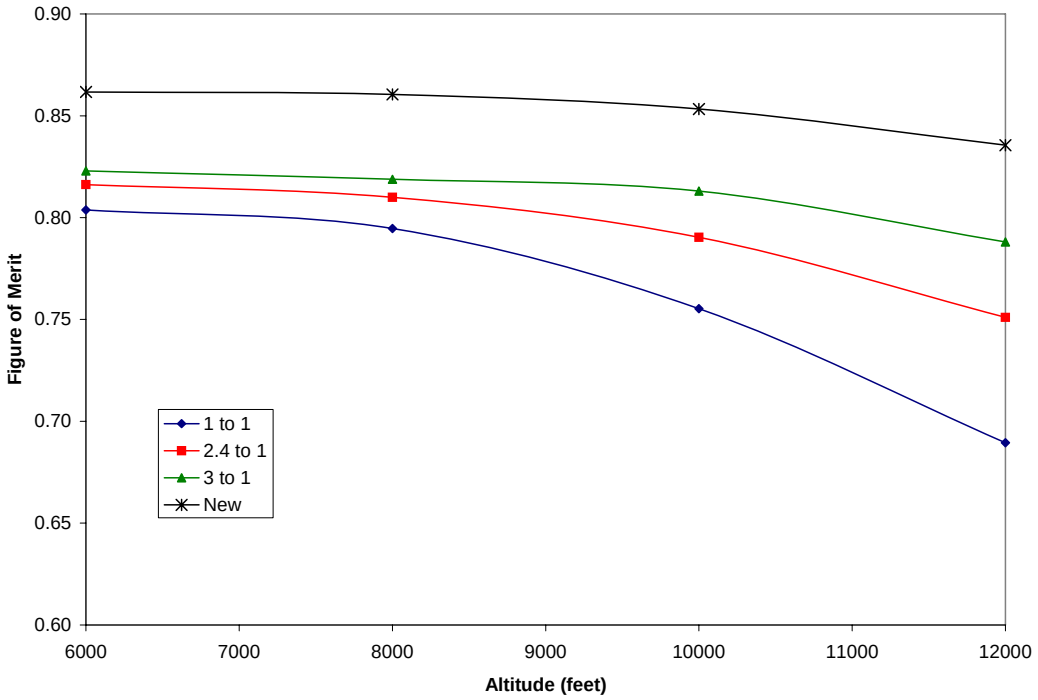

Figure 40. New Tail Rotor Blade Figure of Merit vs Base Model Taper Ratio Options

Forward Flight

The new tail rotor blade successfully demonstrated verification of the forward flight airspeed requirement. This shows that, while designed for improved hover performance, the new tail rotor blade did not negatively affect the operational flight envelope of the current design.

190	X	-
185	-	-
180	X	-
175	X	-
170	X	-
165	X	X
160	X	X
155	X	X
150	-	-
145	X	X
140	X	X
135	X	X
130	-	X
125	X	X
120	X	X
115	-	X
110	X	X
105	X	X
100	X	X
90	X	X
80	X	X
70	X	X
60	X	X
50	X	X
35	X	X
	1 to 1 11 deg VR12	1 to 1 8 deg Base
	21	19
	0.84	0.76

Figure 41. Forward Airspeed Verification Chart

Hover Slide

The hover slide, Figure 42 and Figure 43, shows that the new tail rotor blade performs with less power required and less tail rotor collective pitch than does the base

model. The two figures indicate that the greatest power and collective are required at the 300 degree position. The new tail rotor blade has a 5.5% decrease in power at that critical point. The maximum collective pitch occurs thirty degrees prior to that at 270 degrees, where the new blade uses nearly 9% less pitch. The handling qualities are satisfied because the control rigging is capable of handling a blade that requires less pitch in all wind positions.

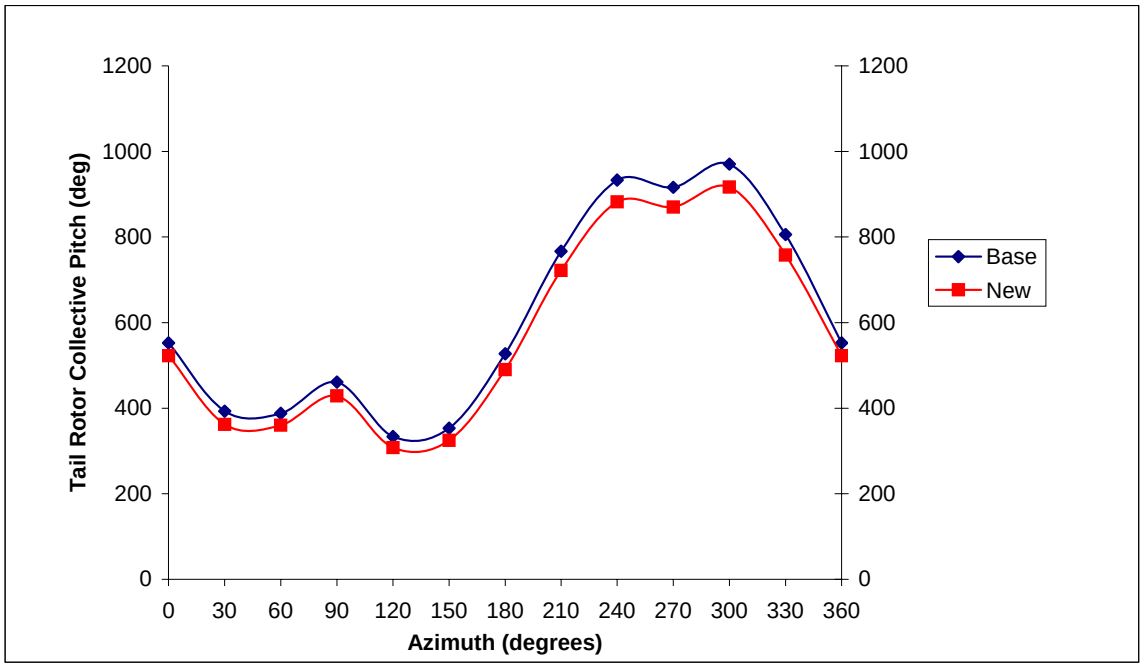

Figure 42. Tail Rotor Power Required in Azimuthally Varying Winds

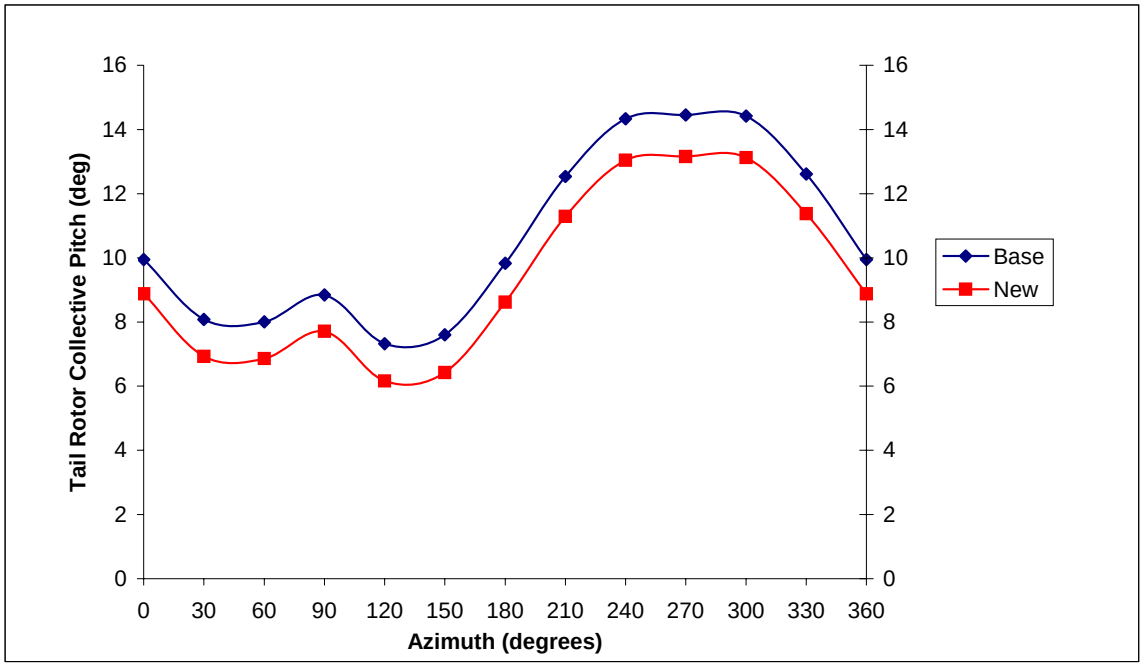

Figure 43. Tail Rotor Collective Pitch vs Azimuth in 35 kt Winds

IV. Conclusions and Recommendations

Conclusions

The first conclusions deal with the performance of the individual design modifications. The -20 degree twist was the winner for having the greatest reduction of required power compared to the base model. That kind of hover performance comes with the price of a lower forward flight airspeed maximum. The -16 and -12 degree twists also made significant contributions to reducing power required, so much so that the -12 degrees became the model for the new tail rotor. The next best grouping was a toss up between the airfoils and taper. At 9% power savings, the VR-12 easily claimed the best airfoil prize. But not too far behind at 7% savings was the 5 blades without maintaining rotor solidity. The 5^{th} identical blade added significant solidity; a requirement for heavy lift operations. Finally, radius came in last as the least effective change for increasing hover performance due to the fact that omega was not reduced for the larger diameter rotor disks.

The second set of conclusions deals with the combinations of several design options. Once the airfoil was chosen it was a matter of give and take as to which changes to incorporate into the new design. Twist was obviously the most effective form of increasing efficiency in the hover, but it also had a big draw back in poor forward flight performance. To strike a balance between twist and airfoil was quite time consuming, and to balance three changes simultaneously proved too difficult for solution. The forward flight convergence chart proved quite helpful in seeing trends and relationships

in the different options. All the airfoils more readily accepted the higher twist values than the high taper values. This may be because the twist values increased no more than 2.5 times whereas the taper was increased up to 3 times the original value.

The third set of conclusions deals with the effectiveness of the modeling and testing process. The model built for this study was rudimentary, yet it had all the required fidelity to produce a similar helicopter to which certain modifications could be made. Certainly there was not one to one correlation between actual power numbers and FM numbers, but the relationship was close enough so as to draw correct inferences. The testing of this model was conclusive regarding the relative merits of certain design criteria. The checks and balances put into place ensured that all portions of the flight envelop would be upgraded or stay the same.

The final conclusion from this thesis refers back to the original scenario. Recall that the high altitude single engine failure resulted in the helicopter being 4000 pounds over its ability to maintain a climb rate of 250 feet per minute. The newly designed tail rotor results in an overall helicopter power savings of 109 horse power, which translates into 3955 pounds of thrust. While not covering the entire 4000 pound weight overage, the new tail rotor design would have sufficiently mitigated the single engine loss and allowed a much different outcome. While no analysis can change the results of a mishap, it can assist in preventing future mishaps by asking the right questions and providing workable solutions.

Suggestions for Further Study

The RCAS model for this thesis could be upgraded in order to produce more accurate numbers during simulation. While this thesis is accurate in relative numbers, a model with more fidelity could produce numbers, which are much closer to reality. A method for this would be to take the rotor systems as they are and add the body, engines and transmission systems. Greater accuracy in results would also result from defining more accurate geometry, inertia properties, flexible blades, free wake, dynamic stall, interference modeling and a horizontal tail.

As a continuation of the forward flight validation process further investigation should include the vibratory loads of the new tail rotor blade in forward flight.

For the aerodynamicist, other airfoils may provide better performance than the VR-12. Even combinations of different types of blades, varying with span, could produce airfoils with even greater flexibility than currently employed.

Appendix A: RCAS Input File

```
! Initialize RDB - use menu 2GCROOT
MENU RCASROOT
11
E

1

! <carriage return> and return to command mode
COMMAND

!====================================================================
!============================ MODEL =================================
!====================================================================

S SUBSYSIDS
!  List subsystem IDs in the model
!  Subsystem Name(s)
A       FUSE
A      MROTOR
A      TROTOR

S GFRAMEORIG
! G frame origin of the  node to which the G frame is attached.
!                     Primitive             Active Degrees of Freedom
!   Subsystem         Structure     Node    Translational  Rotational
!     Name              Name         ID        X  Y  Z       X  Y  Z
a     FUSE             FUSEPS         2        1  1  1       1  1  1

N
! Define properties for trim springs and dampers
! Type       ------- Translational -----      -------- Rotational -----
----
! SPR/DMP    KX1         KX2         KX3       KThetax     KThetay
KThetaz
!a SPR    3.200e+06  3.200e+06  3.200e+06  2.800e+07  2.800e+08
2.800e+08
!a DMP    7.240e+04  7.240e+04  7.240e+04  1.360e+06  6.960e+06
6.960e+06
a DMP    3.240e+04  3.240e+04  3.240e+04  1.360e+06  4.960e+07
5.660e+07
a SPR    2.200e+05  2.200e+05  2.200e+05  1.500e+07  3.500e+08
4.000e+08

S SSORIGIN
!  Subsystem             Origin Coordinates WRT G frame
!    Name          x            y            z
a   FUSE           0            0            0
A   MROTOR         3            0           -6
A   TROTOR       -44           -9          -10

s ssorient
!  Subsystem     rotation 1 WRT G  rotation 2        rotation 3
!    Name      axis angle(deg)   axis angle(deg)   axis angle(deg)
```

```
A   FUSE         2       0         1       0         0       0
A   MROTOR       2     175         1       0         0       0
A   TROTOR       2     180         1     -70         0       0


S CONTROLMIXER
! Control Value at zero   ------ Coefficients for Pilot Control -------
-
!  ID     pilot control    Coll.     Lat.     Long.      Pedal    Throt
A  1           0         .017453      0        0          0         0
A  2           0             0    .017453      0          0         0
A  3           0             0        0     .017453       0         0
A  4           0             0        0        0      .017453       0

S ROTNONCONST
!Cnstr.  Subsys.  Primit.  Node  Subsys.  Primit.   Node
!  ID     Name     Name     ID    Name     Name      ID
A  1      FUSE    FUSEPS    1    MROTOR   BLADE1    20
A  2      FUSE    FUSEPS    4    TROTOR   TBLADE1   50

!====================================================================
!============================ SUBSYSTEM ==============================
!                               FUSE

S SELSUBSYS
! Select a subsystem. Note that all the following data will pertain
! to this subsystem until another subsystem is selected.
a FUSE

S SUBSYSTYP
! Select subsystem type.
! 1=rotor, 2=fuselage, 3=control
a    2

S SUBSYSCOMP
! List the names of the primitive structures for the subsystem.
! primitive structure name
a    FUSEPS
a    VFINPS

s psorigin
!   Primitive       Primitive Origin Offset
!   Name          x            y            z
a   FUSEPS        0            0            0
a   VFINPS     -39.0           0            0

s psorient
!   Primitive     rotation 1        rotation 2        rotation 3
!     Name      axis angle(deg)   axis angle(deg)   axis angle(deg)
A    FUSEPS       3       0         2       0         0       0
A    VFINPS       3     -90         2      70         0       0

S CONNCONST
!  Constr.       Primitive    Node ID          Primitive    Node ID
!    ID         Name (DOFL)   (DOFL)          Name (DOFR)   (DOFR)
```

```
a    11          VFINPS          1               FUSEPS         3


!========================================================================
!======================== PRIMITIVE STRUCTURE ===========================
!                              FUSEPS

S PRIMITIVEID
! Select a primitive structure
! Primitive structure_id
A FUSEPS

S ELDATASETID
! Select an element property data set.
! Data set_id
A ELPROPF

S FENODE
! Specify the node ID and its coordinates wrt PS
!   Node              Node Coordinates (feet)
!    ID            x            y            z
A     1            3            0           -6     ! Hub
A     2            0            0            0     ! C.g.
A     3          -39            0            0     ! V-tail
A     4          -44           -9          -10     ! Tail rotor

S RBMELE
! Generate rigid body mass element.
! ELID,  node ID, prop ID
a   1      2        1

S RIGIDBAR
!  Element  Node1  Node2        Center of gravity offset
!    ID      ID     ID         X            Y            Z
a     2       2      1         0            0            0
a     3       2      3         0            0            0
a     4       3      4         0            0            0

!======================== PRIMITIVE STRUCTURE ===========================
!                              VFINPS

S PRIMITIVEID
! Select a primitive structure
! Primitive structure_id
A VFINPS

S ELDATASETID
! Select an element property data set.
! Data set_id
A ELPROPF

S FENODE
! Specify the node ID and its coordinates wrt PS
!   Node              Node Coordinates (feet)
!    ID            x            y            z
```

```
A     1            0            0            0
A     2           10           -5            0

S RIGIDBAR
!  Element  Node1  Node2        Center of gravity offset
!    ID      ID     ID         X            Y            Z
a     1       1      2         0            0            0

S RBMELE
! Generate rigid body mass element.
! ELID,  node ID, prop ID
a   2      1        2  !dummy mass


!====================================================================
!============================ SUBSYSTEM ==============================
!                               ROTOR

S SELSUBSYS
! Select a subsystem. Note that all the following data will pertain
! to this subsystem until another subsystem is selected.
! Subsystem Name
A MROTOR

S SUBSYSTYP
! Select subsystem type:  1=rotor, 2=fuselage, 3=control
! Subsystem Type
A    1

S SUBSYSCOMP
! List the names of the primitive structures for the subsystem.
! primitive structure name
!          Primitive Structure
!               Name
A               BLADE1
A               BLADE2
A               BLADE3
A               BLADE4
A               BLADE5
A               BLADE6
A               BLADE7

S CORNODE
! Identify current rotor center of rotation
! Prim_str_ID     Node_ID
A   BLADE1         20

S BLADECOMP
! Blade                  Primitive Structure Name(s)
! Index       1         2        3          4         5         6
7
A  1        BLADE1     --        --        --         --        --
--
A  2        BLADE2     --        --        --         --        --
--
```

```
A  3        BLADE3     --        --        --         --        --
--
A  4        BLADE4     --        --        --         --        --
--
A  5        BLADE5     --        --        --         --        --
--
A  6        BLADE6     --        --        --         --        --
--
A  7        BLADE7     --        --        --         --        --
--

S PSORIGIN
! Primitive Structure frame origin offset WRT sub-system
!      Primitive         Primitive Origin Offset
!        Name          x            y            z
A        BLADE1        0            0            0
A        BLADE2        0            0            0
A        BLADE3        0            0            0
A        BLADE4        0            0            0
A        BLADE5        0            0            0
A        BLADE6        0            0            0
A        BLADE7        0            0            0

S PSORIENT
! Primitive Structure frame orientation WRT sub-system
!   Primitive     rotation 1        rotation 2        rotation 3
!     Name      axis angle(deg)   axis angle(deg)   axis angle(deg)
A    BLADE1       3       0         2      -3.         0       0
A    BLADE2       3     -51.4285    2      -3.         0       0
A    BLADE3       3    -102.8571    2      -3.         0       0
A    BLADE4       3    -154.2857    2      -3.         0       0
A    BLADE5       3    -205.7142    2      -3.         0       0
A    BLADE6       3    -257.1429    2      -3.         0       0
A    BLADE7       3    -308.5714    2      -3.         0       0

S CONNCONST
!  Constr.       Primitive    Node ID          Primitive    Node ID
!    ID         Name (DOFL)   (DOFL)          Name (DOFR)   (DOFR)
a     1           BLADE2        20              BLADE1        20
a     2           BLADE3        20              BLADE1        20
a     3           BLADE4        20              BLADE1        20
a     4           BLADE5        20              BLADE1        20
a     5           BLADE6        20              BLADE1        20
a     6           BLADE7        20              BLADE1        20
S ROTORPARAM
!          Rotor Rotational
!          Speed (rad/sec)
A             18.745

!=========================================================================
!======================== PRIMITIVE STRUCTURE ============================
!                              BLADE1

S PRIMITIVEID
! Select a primitive structure
```

```
! Primitive Structure Name(s)
A          BLADE1

S ELDATASETID
! Select an element property data set.
!   Element Data Table Name
A           ELPROPB

S FENODE
! Specify the node IDs and their coordinates WRT Primitive Structure
!   Node              Node Coordinates (feet)
!    ID             x       y     z
A    20             0       0     0   ! Blade root Node
A     8          39.5       0     0   ! blade tip node

S RIGIDBLADE
!   Element   Node   Prop       Hinge Sequence number (0-3)
!    ID        ID     ID      Lead-Lag     Flap     Pitch Bearing
a     1        20      1         1           2           0

S CONTROLCONNECT
! Control   Swashplate   Swashplate   Element Type         Element
!   ID      or Direct    Phase(deg)  (HIN/AUX/ENG ...)    or ACP ID
a    1       SPCOLL         0.0           RBE                 1
a    2       SPLATR         0.0           RBE                 1
a    3       SPLONG         0.0           RBE                 1

!========================================================================
!======================== Copy Primitives ===========================
!    blade1 to blade2, blade3, blade4, blade5, blade6 and blade7

S PRIMIT
! Row_id  Source_Prim_Str_id     Dest_Prim_Str_id
A    1       BLADE1              BLADE2
A    2       BLADE2              BLADE3
A    3       BLADE3              BLADE4
A    4       BLADE4              BLADE5
A    5       BLADE5              BLADE6
A    6       BLADE6              BLADE7


!========================================================================
!======================== STRUCTURAL PROPERTIES =========================
!

S ELEPROPID
! List the names of element property data sets.
! element_prop_id
A ELPROPB

S RBEPRP
!             ------------------ Lead-lag Hinge ----------------------
! Prop_id     Hinge_Offset       Mass        Damping        Stiffness
!                 (ft)          (slugs)    (lbs-sec/rad)   (ft-lbs/rad)
a    1            2.15            0         4400           150000
```

```
N
!             ---------------------- Flap Hinge ----------------------
! Prop_id     Hinge_Offset       Mass        Damping        Stiffness
!                 (ft)          (slugs)    (lbs-sec/rad)   (ft-lbs/rad)
a    1            2.15            0             0           15000

N
!             --------------------- Pitch Bearing -------------------
! Prop_id     Hinge_Offset       Mass        Damping        Stiffness
!                 (ft)          (slugs)    (lbs-sec/rad)   (ft-lbs/rad)
a    1            0               0             0               0

N
! Prop_id     Blade_Mass      Blade-CG          Ixx           Iyy
!              (slugs)          (ft)        (slug-ft**2)   (slug-ft**2)
a    1          11.53           15.0           0.200         4800


S ELEPROPID
! List the names of element property data sets.
! element_prop_id
A ELPROPF

S RBMPRP
! Prop    Mass     ----- C.G. Offset (ft) --       Inertia Tensor
(slug-ft**2)
!  ID    (slug)    x_1^E     x_2^E     x_3^E       |Ixx       Ixy
Ixz|
!                                                  |Iyy       Iyz
Izz|
a  1     1958.1      0       0         0.0      1.0E+5  0    0 3.5E+6
0  4*e+6
a  2      1.e-6      0       0          0         0   0    0     0    0
0

!====================================================================
!============================ SUBSYSTEM ==============================
!                               TROTOR

S SELSUBSYS
! Select a subsystem. Note that all the following data will pertain
! to this subsystem until another subsystem is selected.
! Subsystem Name
A TROTOR

S SUBSYSTYP
! Select subsystem type:  1=rotor, 2=fuselage, 3=control
! Subsystem Type
A    1

S SUBSYSCOMP
! List the names of the primitive structures for the subsystem.
! primitive structure name
!          Primitive Structure
```

```
!                Name
A                TBLADE1
A                TBLADE2
A                TBLADE3
A                TBLADE4

S CORNODE
! Identify current rotor center of rotation
! Prim_str_ID     Node_ID
A  TBLADE1         50

S BLADECOMP
! Blade                  Primitive Structure Name(s)
! Index       1         2        3          4         5         6
7
A  1       TBLADE1     --        --        --         --        --
--
A  2       TBLADE2     --        --        --         --        --
--
A  3       TBLADE3     --        --        --         --        --
--
A  4       TBLADE4     --        --        --         --        --
--

S PSORIGIN
! Primitive Structure frame origin offset WRT sub-system
!      Primitive         Primitive Origin Offset
!        Name          x            y            z
A       TBLADE1        0            0            0
A       TBLADE2        0            0            0
A       TBLADE3        0            0            0
A       TBLADE4        0            0            0

S PSORIENT
! Primitive Structure frame orientation WRT sub-system
!   Primitive     rotation 1        rotation 2        rotation 3
!     Name      axis angle(deg)   axis angle(deg)   axis angle(deg)
A   TBLADE1       3       0         2      0          0       0
A   TBLADE2       3     -90         2      0          0       0
A   TBLADE3       3    -180         2      0          0       0
A   TBLADE4       3    -270         2      0          0       0

S CONNCONST
!  Constr.       Primitive    Node ID          Primitive    Node ID
!    ID         Name (DOFL)   (DOFL)          Name (DOFR)   (DOFR)
a     7          TBLADE2       50             TBLADE1       50
a     8          TBLADE3       50             TBLADE1       50
a     9          TBLADE4       50             TBLADE1       50

S ROTORPARAM
!          Rotor Rotational
!          Speed (rad/sec)
A             73.2

!====================================================================
```

```
!======================== PRIMITIVE STRUCTURE ========================
!                              TBLADE1

S PRIMITIVEID
! Select a primitive structure
! Primitive Structure Name(s)
A          TBLADE1

S ELDATASETID
! Select an element property data set.
!   Element Data Table Name
A           TELPROPB

S FENODE
! Specify the node IDs and their coordinates WRT Primitive Structure
!   Node              Node Coordinates (feet)
!    ID             x       y     z
A      50           0       0     0   ! Blade root Node
A      70          10       0     0   ! blade tip node

S RIGIDBLADE
!   Element   Node   Prop       Hinge Sequence number (0-3)
!    ID        ID     ID      Lead-Lag     Flap     Pitch Bearing
a    1         50      2         0           1           0

S CONTROLCONNECT
! Control   Swashplate   Swashplate   Element Type         Element
!   ID      or Direct    Phase(deg)  (HIN/AUX/ENG ...)    or ACP ID
a    4       SPCOLL         0.0           RBE                 1

!=========================================================================
!======================== Copy Primitives ============================
!                 blade1 to blade2, blade3, blade4

S PRIMIT
! Row_id  Source_Prim_Str_id     Dest_Prim_Str_id
A    7        TBLADE1             TBLADE2
A    8        TBLADE2             TBLADE3
A    9        TBLADE3             TBLADE4

EXIT

COMMAND

COPYPRIMSTRUCT

COMMAND

!=========================================================================
!======================== STRUCTURAL PROPERTIES ======================
!

S ELEPROPID
! List the names of element property data sets.
! element_prop_id
```

```
A TELPROPB

S RBEPRP
!             ------------------ Lead-lag Hinge ----------------------
! Prop_id     Hinge_Offset       Mass        Damping        Stiffness
!                 (ft)          (slugs)    (lbs-sec/rad)   (ft-lbs/rad)
a    2             0               0             0              0

N
!             ---------------------- Flap Hinge ----------------------
! Prop_id     Hinge_Offset       Mass        Damping        Stiffness
!                 (ft)          (slugs)    (lbs-sec/rad)   (ft-lbs/rad)
a    2             1.0             0             0              0

N
!             --------------------- Pitch Bearing --------------------
! Prop_id     Hinge_Offset       Mass        Damping        Stiffness
!                 (ft)          (slugs)    (lbs-sec/rad)   (ft-lbs/rad)
a    2             0               0             0              0

N
! Prop_id     Blade_Mass      Blade-CG          Ixx           Iyy
!              (slugs)          (ft)        (slug-ft**2)   (slug-ft**2)
a    2          1.55             4.5           0.02           13.5


S ELEPROPID
! List the names of element property data sets.
! element_prop_id
A TELPROPF

!====================================================================
!======================== AERODYNAMIC MODEL ==========================
!====================================================================

S AEROMODCOMP
! List of Supercomponent of the system
a ADROTOR
a TAROTOR
a BODYSC
a VFINSC

S SCORIGIN
!  Supercomponent          Origin Coordinates
!       Name          x            y            z
a      ADROTOR        3            0           -6
a      TAROTOR      -44           -9          -10
a      BODYSC         0            0            0
a      VFINSC       -39            0            0

S SCORIENT
! Supercomponent   rotation 1        rotation 2        rotation 3
!       Name      axis angle(deg)   axis angle(deg)   axis angle(deg)
A     ADROTOR       2     175         1       0         2       0
A     TAROTOR       2     180         1     -70         2       0
```

```
A     BODYSC        3       0         1       0         2       0
A     VFINSC        3     -90         1       0         2      70

S AIRFOIL
!   Airfoil              Quasi Steady Airloads
!     ID                  2D Table File Name
a  bladeaf                    SC1095.C81
a tbladeaf                    NACA0012.C81

N
!  Airfoil   -- Linear Airfoil Coefficients --     Zero Lift Angle
!    ID      C_radial    CL_a      CD       CM     of Attack (deg)
!a   bladeaf      0       6.28     0.01      0.0        0.0
!a  tbladeaf      0       6.28     0.01      0.0        0.0
a   FW0013        0       6.28     0.15      0.0        0.0

N
!   Airfoil           Nonlinear UnSteady and Dynamic Stall
!     ID            Airfoil Data File Name (Leishman-Beddos)
!a  bladeaf                       NACA0012.LEI

!=========================================================================
!====================== AERODYNAMIC SUPERCOMPONENT ======================
!                              ADROTOR

S AEROSUPCOMPID
! Supercomponent name to be define or modified
a       ADROTOR

S SUPCMPTYP
! 1 => rotor, 2 => wing, 3 => body
a   1

S COMPID
! List the Components which comprise the Supercomponent
! Component     Primitive   CP Root   Blade tip
!  Name(s)      Structure    El_id     node_id
a  ADBLADE1      BLADE1        0          8
a  ADBLADE2      BLADE2        0          8
a  ADBLADE3      BLADE3        0          8
a  ADBLADE4      BLADE4        0          8
a  ADBLADE5      BLADE5        0          8
a  ADBLADE6      BLADE6        0          8
a  ADBLADE7      BLADE7        0          8

S CPORIGIN
! Component         Component Origin Offset
!   Name          x            y            z
A ADBLADE1        0            0            0
A ADBLADE2        0            0            0
A ADBLADE3        0            0            0
A ADBLADE4        0            0            0
A ADBLADE5        0            0            0
A ADBLADE6        0            0            0
A ADBLADE7        0            0            0
```

```
S CPORIENT
! Component     rotation 1        rotation 2        rotation 3
!    Name      axis angle(deg)   axis angle(deg)   axis angle(deg)
A ADBLADE1       3       0         2      -3.         0       0
A ADBLADE2       3     -51.4285    2      -3.         0       0
A ADBLADE3       3    -102.8571    2      -3.         0       0
A ADBLADE4       3    -154.2857    2      -3.         0       0
A ADBLADE5       3    -205.7142    2      -3.         0       0
A ADBLADE6       3    -257.1429    2      -3.         0       0
A ADBLADE7       3    -308.5714    2      -3.         0       0

S INFLOW
! 0. No inflow (wings).
! 1. Uniform momentum inflow (half wings and rotors)
! 2. Uniform momentum inflow (full wings)
! 3  Peters and He inflow model (rotors only).
! 5. Alternate Prescribed vortex wake ( only rotors).
! 6. Free vortex Wake (Only Rotor)
a        1

S AEROPTION
!   Yawed     Tip     Unsteady   Dynamic  Linear Afoil   Compress.
!   Flow      Loss     Flow      Stall    coefficient    effects
!  (0:1)     (0:1)    (0:1)      (0:3)      (0:1)         (0:1)
a    1         0        1          0          0             1

S THRUSTAVE
! Thrust Average      # Time Steps         Prescribed     # of
Revolutions
!     Option         in Thrust Ave.          Thrust        to Average
TPP
a       2                 36                1.0e-07               1

S SUPCMPTOSS
! Subsystem name for the current supercomponent
a        MROTOR

!========================================================================
!====================== AERODYNAMIC COMPONENT ======================
!                            ADBLADE1

S AEROCOMPID
! Component name to be defined or modified
a  ADBLADE1

S COMPTYPE
! 1 => lifting surface,  2 => body,  3 => Aux/tail rotor
a       1

S AERONODE
! Aerodynamic node ids and their coordinate wrt component
! Node           ------- Coordinates -------
!  ID            x            y            z
a  1           5.0           0            0
```

```
a  2           10.0           0            0
a  3           15.0           0            0
a  4           20.0           0            0
a  5           25.0           0            0
a  6           30.0           0            0
a  7           32.0           0            0
a  8           34.0           0            0
a  9           36.0           0            0
a 10           38.0           0            0
a 11           39.5           0            0

S AEROSEG
! Seg.   Aerodyn Node IDs    Chord     Airfoil  Element Twist
! ID   (Inboard)(Outboard)   (ft)        ID      ID     (rad)
a  1        1       2       2.44       bladeaf    0   .195521
a  2        2       3       2.44       bladeaf    0   .151335
a  3        3       4       2.44       bladeaf    0   .017150
a  4        4       5       2.44       bladeaf    0   .062964
a  5        5       6       2.44       bladeaf    0   .018779
a  6        6       7       2.44       bladeaf    0  -.012151
a  7        7       8       2.44       bladeaf    0  -.029825
a  8        8       9       2.44       bladeaf    0  -.047499
a  9        9      10       2.44       bladeaf    0  -.065174
a 10       10      11       2.44       bladeaf    0  -.080639

!========================================================================
!            Define Aerodynamic Component ADBLADE2, ADBLADE3, ...
!                      Using COPY option
!========================================================================

S AEROCO
! Copy ID,    source component, destination component
a    1             ADBLADE1           ADBLADE2
a    2             ADBLADE2           ADBLADE3
a    3             ADBLADE3           ADBLADE4
a    4             ADBLADE4           ADBLADE5
a    5             ADBLADE5           ADBLADE6
a    6             ADBLADE6           ADBLADE7

!========================================================================
!====================== AERODYNAMIC SUPERCOMPONENT ======================
!                             TAROTOR

S AEROSUPCOMPID
! Supercomponent name to be define or modified
a      TAROTOR

S SUPCMPTYP
! 1 => rotor, 2 => wing, 3 => body
a   1

S COMPID
! List the Components which comprise the Supercomponent
! Component     Primitive   CP Root   Blade tip
!  Name(s)      Structure    El_id     node_id
```

```
a  TABLADE1     TBLADE1        0          70
a  TABLADE2     TBLADE2        0          70
a  TABLADE3     TBLADE3        0          70
a  TABLADE4     TBLADE4        0          70

S CPORIGIN
! Component         Component Origin Offset
!   Name          x            y            z
A TABLADE1        0            0            0
A TABLADE2        0            0            0
A TABLADE3        0            0            0
A TABLADE4        0            0            0

S CPORIENT
! Component     rotation 1        rotation 2        rotation 3
!    Name      axis angle(deg)   axis angle(deg)   axis angle(deg)
A TABLADE1       3       0         2     0           0       0
A TABLADE2       3     -90         2     0           0       0
A TABLADE3       3    -180         2     0           0       0
A TABLADE4       3    -270         2     0           0       0

S INFLOW
! 0. No inflow (wings).
! 1. Uniform momentum inflow (half wings and rotors)
! 2. Uniform momentum inflow (full wings)
! 3  Peters and He inflow model (rotors only).
! 5. Alternate Prescribed vortex wake ( only rotors).
! 6. Free vortex Wake (Only Rotor)
a        1

S AEROPTION
!   Yawed     Tip     Unsteady   Dynamic  Linear Afoil   Compress.
!   Flow      Loss     Flow      Stall    coefficient    effects
!  (0:1)     (0:1)    (0:1)      (0:3)      (0:1)         (0:1)
a    1         0        1          0          0             1

S THRUSTAVE
! Thrust Average      # Time Steps         Prescribed     # of
Revolutions
!     Option         in Thrust Ave.          Thrust        to Average
TPP
a       2                 36               1.0e-07               1

S SUPCMPTOSS
! Subsystem name for the current supercomponent
a        TROTOR

!====================================================================
!======================= AERODYNAMIC COMPONENT =======================
!                              TABLADE1

S AEROCOMPID
! Component name to be defined or modified
a  TABLADE1
```

```
S COMPTYPE
! 1 => lifting surface,  2 => body,  3 => Aux/tail rotor
a       1

S AERONODE
! Aerodynamic node ids and their coordinate wrt component
! Node           ------- Coordinates -------
!  ID            x            y            z
a  21            2.0           0            0
a  22            3.0           0            0
a  23            4.0           0            0
a  24            5.0           0            0
a  25            6.0           0            0
a  26            7.0           0            0
a  27            8.0           0            0
a  28            8.5           0            0
a  29            9.0           0            0
a  30            9.5           0            0
a  31           10.0           0            0

S AEROSEG
! Seg.   Aerodyn Node IDs    Chord     Airfoil  Element Twist
! ID   (Inboard)(Outboard)   (ft)        ID      ID     (rad)
a  21       21      22       2.05      tbladeaf    0   .069813
a  22       22      23       1.91      tbladeaf    0   .055850
a  23       23      24       1.77      tbladeaf    0   .041888
a  24       24      25       1.63      tbladeaf    0   .027925
a  25       25      26       1.49      tbladeaf    0   .013963
a  26       26      27       1.35      tbladeaf    0         0
a  27       27      28       1.25      tbladeaf    0  -.010472
a  28       28      29       1.18      tbladeaf    0  -.017453
a  29       29      30       1.11      tbladeaf    0  -.024435
a  30       30      31       1.04      tbladeaf    0  -.031416

!====================================================================
!            Define Aerodynamic Component ADBLADE2, ADBLADE3, ...
!                      Using COPY option
!====================================================================

S AEROCO
! Copy ID,    source component, destination component
a   21             TABLADE1           TABLADE2
a   22             TABLADE2           TABLADE3
a   23             TABLADE3           TABLADE4

EXIT

COMMAND

COPYAEROCOMP

COMMAND

!====================================================================
!====================== AERODYNAMIC SUPERCOMPONENT ==================
```

```
!                               BODYSC
S AEROSUPCOMPID
! Supercomponent name to be define or modified
a          BODYSC

S SUPCMPTOSS
! Subsystem name for the current supercomponent
a         FUSE

S SUPCMPTYP
! 1 => rotor, 2 => wing, 3 => body  4 => AUX ROT
a     3

S COMPID
! List the Components which comprise the Supercomponent
! Component     Primitive   CP Root   Blade tip
!  Name(s)      Structure    El_id     node_id
a  BODYCP        FUSEPS        1           0

S CPORIGIN
! Component         Component Origin Offset
!   Name          x            y            z
a  BODYCP         0            0            0

S CPORIENT
! Component     rotation 1        rotation 2        rotation 3
!    Name      axis angle(deg)   axis angle(deg)   axis angle(deg)
A  BODYCP        0      0         0       0         0       0

S INFLOW
! inflow option
! 0 => no inflow 1 => Uniform, 2 => uniform for full wing, 3 => dynamic
inflow,
! 4 => Classical wake, 5 => prescribed generalized wake, 6 => free wake
a        0

S AEROPTION
! aerodynamic options (tip loss, airfoil tables)
! yawed flow, tip loss, u/s aero, dynamic stall, linear coefficients
a     0           0        0           0                1

!=========================================================================
!======================== AERODYNAMIC COMPONENT ==========================
!                              BODYCP

S AEROCOMPID
! Component name for defining or modifying
a BODYCP

S COMPTYPE
! 1 => lifting surface,  2 => body  3 => AUX ROT
a 2

s BODYAEROTAB
!       DEFINE AERODYNAMIC COEFFICIENTS FOR THE CURRENT BODY COMPONENT
```

```
!  Option  External    -------- Parameters for closed form expressions
--------
!       File      L_o/q    L_1/q    D_o/q    D_1/q    D_2/q    M_o/q
M_1/q
a 2    ----       0.0       0.0     20.00     0.0      0.0      0.0
0.0

!=====================================================================
!====================== AERODYNAMIC SUPERCOMPONENT ====================
!                              VFINSC

S AEROSUPCOMPID
! Supercomponent name to be define or modified
a  VFINSC

S SUPCMPTYP
! 1 => rotor, 2 => wing, 3 => body
a   2

S COMPID
! List the Components which comprise the Supercomponent
! Component     Primitive   CP Root   Blade tip
!  Name(s)      Structure    El_id     node_id
a  VFINCP       VFINPS         2           0

S CPORIGIN
! Component         Component Origin Offset
!   Name          x            y            z
a  VFINCP         0            0            0

S CPORIENT
! Component     rotation 1        rotation 2        rotation 3
!    Name      axis angle(deg)   axis angle(deg)   axis angle(deg)
a  VFINCP         0      0         0       0         0       0

S INFLOW
! 0. No inflow (wings).
! 1. Uniform momentum inflow (half wings and rotors)
! 2. Uniform momentum inflow (full wings)
! 3  Peters and He inflow model (rotors only).
! 5. Alternate Prescribed vortex wake ( only rotors).
! 6. Free vortex Wake (Only Rotor)
a        0

S AEROPTION
!   Yawed     Tip     Unsteady   Dynamic  Linear Afoil   Compress.
!   Flow      Loss     Flow      Stall    coefficient    effects
!  (0:1)     (0:1)    (0:1)      (0:3)      (0:1)         (0:1)
a    0         0        0          0          1             0

S THRUSTAVE
! Thrust Average      # Time Steps         Prescribed     # of
Revolutions
!     Option         in Thrust Ave.          Thrust        to Average
TPP
```

```
a       0                 36                1.0E-07               1

S SUPCMPTOSS
! Subsystem name for the current supercomponent
a        FUSE

!=====================================================================
!======================= AERODYNAMIC COMPONENT ========================
!                             VFINCP

S AEROCOMPID
! Component name to be defined or modified
a  VFINCP

S COMPTYPE
! 1 => lifting surface,  2 => body,  3 => Aux/tail rotor
a       1

S AERONODE
! Aerodynamic node ids and their coordinate wrt component
! Node           ------- Coordinates -------
!  ID            x           y           z
a  1             0           0.0         0
a  2            10           -5          0

S AEROSEG
! Seg.   Aerodyn Node IDs    Chord     Airfoil  Element Twist
! ID   (Inboard)(Outboard)   (ft)        ID      ID     (rad)
a  1        1       2          5     FW0013      1        0


!=====================================================================
!========================== ANALYSIS DATA ============================
!=====================================================================

S SELANALYSIS
! Case      Trim   Mane   Stab   Init      ----- Scope Script -----
!  ID       (0:3)  (0:1)  (0:1)  Cond             File Name
A  01         1      0      0      D                NO

N
! Case_id               Case_Title
a  01                   example7

S INITCOND
! screen #1 - initial pilot control positions
! collective    lateral     longitudinal   pedal    throttle
A    9.68       2.25         -4.166         10.7      0.0

N
! G frame position Frame wrt I
!    X    Y    Z      Roll          Pitch      Yaw
a    0    0    0       0             0         0

N
```

```
!  vehicle (G frame) position and attitude angles
!   x0    y0      z0            roll          pitch       yaw
!   ft    ft      ft            rad            rad        rad
A   0      0       0             0              0          0

N
!  Acceleration wrt I frame in I coord.    Omegad wrt I frame in G
coord.
!    Axi          Ayi          Azi       OmegaXD      OmegaYD
OmegaZD

S SYSTEMFLAGS
! Global element formulation flags (1=Yes, 0=No)
!   Gravity        Aero
!   Effects       Effects
A      1             1

S AEROSTATCONST
! Define aerostatic conditions for standard sea level
! Spec_type    Altitude    Temperature      Density     Vel_of_sound
!  (0:4)        (ft)        (Deg F)      (slugs/ft**3)    (ft/sec)
a    1          10000            0               0             0

!=============================================================================
!============================ TRIM DATA ======================================
!=============================================================================

S CONVERGETOL
!# of  # of  # of   -Displacement Tolerance-    --Velocity Tolerance-
Min.
!Trim  PSol  Time    translation   rotation     translation rotation
# of
!Iter  Iter  Step      (ft)         (rad)        (ft/sec)   (rad/sec)
PS Rev
A 25    22    36      0.005       0.002           .1          .2
15

S INTEGPARAM
!No. of| Newmark Constants|  HHT    | Displace.  | Velocity  | Relax.
!Iter. | Alpha  |  Delta  | Param   |   Tol      |   Tol     | Facbor
A 30      .25       .5      -.00      1.0E-5        1.0E-4      1.0

S REASSEMBLE
! Row    Periodic Solution     Period Number    Number of Time
!  ID      From      TO        From      TO    Steps Per Assemble
a   1       1         1          1        1           6


S TRIMVAR
! Trim   TrimVar      TrimVar   Target  TargetValue   TargetTol
! VarID  PertValue    DampFact    ID
a   1     1.0           0.5        3        0.0           20
a   2     1.0           0.5        4        0.0           20
a   3     1.0           0.5        5        0.0           20
a   4     1.0           0.5        6        0.0           20
```

```
a   6     2.E-02        0.5        2        0.0          20
a   7     3.E-02        0.5        1        0.0          20

S COMMPERIOD
!DEFINE THE COMMON PERIOD OF ALL ROTORS FOR TRIM
!   Name       Rotor Period Ratio    Tolerance
a  mrotor            1                .1

!=====================================================================
!========================== OUTPUT DATA ==============================
!=====================================================================

S PERIODICOUTPUT
!  Row   Subsystem   Prim. Struc.            output
!  ID      Name        Name                category
A   1      all         all                 Internal.Loads

S SAVESC
!     Form of SC Data             Directory and File Name
!      (RDB or FILES)                  for SC Data
a       RDB                          e7.sav

EXIT

M  RUNANALYSIS
```

Bibliography

1. Department of the Navy, Naval Air Training and Operating Procedures Standardization (NATOPS), Chief of Naval Operations, Pentagon, 2001.
2. Newman, S., The Foundations of Helicopter Flight, St. Edmundsbury Press Ltd., Suffolk, 1994.
3. Cook, C.V., A Review of Tail Rotor Design and Performance, *Vertica*, 2:163-181, 1979.
4. Leishman, J.G., Principles of Helicopter Aerodynamics, Press Syndicate of the University of Cambridge, United Kingdom, 2001.
5. Byham, G.M., "An Overview of Conventional Tail Rotors," Helicopter Yaw Control Concepts, The Royal Aeronautical Society, 1990.
6. Prouty, R.W., Helicopter Performance, Stability, and Control, Krieger Publishing Company, Malabar, Florida, 1995.
7. USAAMCOM/AFDD, "RCAS Theory Manual, Rotorcraft Comprehensive Analysis System, Version 2.0," TR 02-A-005, Moffett Field, CA, May 2003.
8. Lynn, R.R., Robinson, F.D., Batra, N.N., Duhon, J.M., "Tail Rotor Design Part I – Aerodynamics," 25th American Helicopter Society annual National Forum, May 1969.
9. Wiesner W, Kohler G. "Tail Rotor Design Guide," *DefenseTechnical Information Center*, AD-775 391, January 1974.
10. Byham, G.M. "An Overview of Conventional Tail Rotors", The Royal Aeronautical Society, Helicopter Yaw Control Concepts, Two Day Conference, 28 January – 1 March 1990
11. Ellin, A.D.S. Lieutenant, Royal Navy "Flight Measurement Illustrating Key Features of Tail Rotor Loading Distribution" The Royal Aeronautical Society, Helicopter Yaw Control Concepts, Two Day Conference, 28 January – 1 March 1990.
12. Hodgkinson, J. Aircraft Handling Qualities, American Institute of Aeronautics and Astronautics, Inc., United Kingdom 1999.
13. Jones K.D., Panel Code V2, Steady, 2-D, Incompressible, Inviscid Flow Solver http://www.aa.nps.navy.mil/~jones/ January 2005.
14. SP-3300 Flight Research at Ames, 1940-1997, Flying Qualities, Stability and Control, and Performance Evaluations, http://history.nasa.gov/SP-3300/ch4.htm
15. Raymer D.P., Aircraft Design: A Conceptual Approach, American Institute of Aeronautics and Astronautics, Inc., Virginia, 1999.

Vita

Following two Mediterranean deployments as a Marine Corps CH-53E pilot assigned to Marine Medium Helicopter Squadron 266 attached to the 24th Marine Expeditionary Unit, James A. Pritchard became an instructor at Marine Helicopter Training Squadron 302. Several months prior to Operation Iraqi Freedom, he was transferred to Marine Heavy Helicopter Squadron 464, where he served as an augment pilot for the duration of the war. In July of 2003 he moved from Jacksonville, NC to his present duty station at the Air Force Institute of Technology in Dayton, OH in order to study Aeronautical Engineering. Following this assignment, he will move to Pensacola, FL and serve as the Rotary Wing Aeronautical Engineering Instructor at the Naval Aviation Safety Officer School.

REPORT DOCUMENTATION PAGE

Form Approved
OMB No. 074-0188

PLEASE DO NOT RETURN YOUR FORM TO THE ABOVE ADDRESS.

1. REPORT DATE *(DD-MM-YYYY)* 10 Mar 05	**2. REPORT TYPE** **Master's Thesis**	**3. DATES COVERED** *(From – To)* Aug 03 – Mar 05

4. TITLE AND SUBTITLE

A REDESIGNED TAIL ROTOR FOR IMPROVEMENT OF CH-53E HIGH-ALTITUDE PERFORMANCE

5a. CONTRACT NUMBER

5b. GRANT NUMBER

5c. PROGRAM ELEMENT NUMBER

6. AUTHOR(S)

Pritchard, James, A., Major, USMC

5d. PROJECT NUMBER

5e. TASK NUMBER

5f. WORK UNIT NUMBER

7. PERFORMING ORGANIZATION NAMES(S) AND ADDRESS(S)

Air Force Institute of Technology
Graduate School of Engineering and Management (AFIT/EN)
2950 Hobson Way Building 641
WPAFB OH 45433-7765

8. PERFORMING ORGANIZATION REPORT NUMBER

AFIT/GAE/ENY/05-M27

9. SPONSORING/MONITORING AGENCY NAME(S) AND ADDRESS(ES)

Commander, Naval Air Systems Command
Attn: PMA 261, Class Desk, Maj Mike McGhee
47123 Buse Rd, B2272 Unit IPT
Patuxtent River, MD 20670-1547

10. SPONSOR/MONITOR'S ACRONYM(S)

11. SPONSOR/MONITOR'S REPORT NUMBER(S)

12. DISTRIBUTION/AVAILABILITY STATEMENT

APPROVED FOR PUBLIC RELEASE; DISTRIBUTION UNLIMITED.

13. SUPPLEMENTARY NOTES

14. ABSTRACT

The Global War on Terror with specific emphasis on the recent military operation in Afghanistan has shown the invaluable contribution that heavy lift helicopters bring to the combatant commander. However, the flight range, altitudes and lift capability required to operate effectively in such an austere environment are pushing the limits of these helicopters. In an attempt to increase the operational capability of the CH-53E, this study will investigate methods for maximizing tail rotor effectiveness at high gross weights and high altitudes. This thesis records an analytical study designed to investigate the intricacies of tail rotor design and, by the computational simulation afforded through the Rotorcraft Comprehensive Analysis System (RCAS), define a tail rotor at high altitude that will reduce the tail rotor power required in hover by 10%. The versatility required of the tail rotor is seen due to the nature of the flow regime, which requires the tail rotor to effectively operate with inflow velocity from any direction, with a spanwise distribution of flow that produces Reynolds numbers up to 5.6e7 and with pilot commanded pitch changes from -10 to 24 degrees. With little to no assistance from the vertical fin, the tail rotor is most heavily relied on for antitorque response in hover; therefore, focus will be placed on hovering efficiencies tempered by solid forward flight and hover slide performance.

15. SUBJECT TERMS

CH-53E, Helicopter, Tail Rotor, Design

16. SECURITY CLASSIFICATION OF:			**17. LIMITATION OF ABSTRACT**	**18. NUMBER OF PAGES**	**19a. NAME OF RESPONSIBLE PERSON**
REPORT	**ABSTRACT**	**c. THIS PAGE**			**Donald L. Kunz**
U	**U**	**U**	**UU**	135	**19b. TELEPHONE NUMBER** *(Include area code)* (937) 255-3636, ext 4548